

## CHAPTER 4

### Results and discussion

This chapter contains the results of electric field induced-strain and polarization behavior measurement by modified Michelson interferometer, for ferroelectric materials. First, an aging behavior, time dependence of ferroelectric materials, of PLZT ceramics was explained. Second, the PMN-PZT induced-strain results which measured at frequency of 1 to 0.01 Hz, frequency dependence of ferroelectric materials in induced-strain measurement, were explained. Third, the PMN-PZT, PMN-PT and PLZT induced-strain results which measured at various temperatures, temperature dependence of ferroelectric materials, were explained. Finally, the PMN-PZT, PMN-PT and PLZT induced-strain results which measured under different magnetic field condition, magnetic field effect to induced-strain measurement of ferroelectric materials, were explained. The results were calculated and plotted the induced-strain and polarization as a function of electric field relation ( $s$ - $P$ - $E$ ), induced-strain as a function of polarization relation ( $s$ - $P$ ), and analyzed the behavior.

#### 4.1 Electrostrictive properties using modified Michelson interferometer

##### 4.1.1 Frequency dependence in induced-strain PMN-PZT

Frequency dependence of piezoelectric/electrostrictive properties is the important character where the shape and size of ferroelectric materials changes in response to frequency when piezoelectric/ electrostriction materials are selected in the commercial electronic equipment such as electroceramic, electrooptic and sensor/actuator applications. To observe frequency dependence behavior of ferroelectric samples, the attractive actuator ferroelectric ceramic material  $\text{Pb}(\text{Mg}_{1/3}\text{Nb}_{2/3})\text{O}_3$ - $0.3\text{Pb}(\text{Zr}_{0.52}\text{Ti}_{0.48})\text{O}_3$  PMN and  $x\text{Pb}(\text{Mg}_{1/3}\text{Nb}_{2/3})\text{O}_3$ - $(1-x)\text{Pb}(\text{Zr}_{0.52}\text{Ti}_{0.48})\text{O}_3$  or  $x\text{PMN}$ - $(1-x)\text{PZT}$  samples, where  $x = 0.9, 0.7, 0.5$  and  $0.3$ , were chosen and fabricated by solid mixing oxide

method. To investigate the electric field induced strain and polarization behavior modified Michelson interferometer technique was used at various frequencies.

Figure 4.1 shows dielectric constant and dielectric loss as a function of temperature at various frequencies of PMN and  $x\text{Pb}(\text{Mg}_{1/3}\text{Nb}_{2/3})\text{O}_3-(1-x)\text{Pb}(\text{Zr}_{0.52}\text{Ti}_{0.48})\text{O}_3$  or  $x\text{PMN}-(1-x)\text{PZT}$  samples where  $x = 0.9, 0.7, 0.5$  and  $0.3$ . In Figure 4.1(a) and (b), it can be seen that dielectric property of each sample is different where PMN and 0.1PMN-0.9PZT were paraelectric phase at room temperature. The maximum peak of dielectric constant  $T_m$ , phase transition temperature, was lower than room temperature which was agreed with previous result that shows the maximum peak of dielectric constant  $T_m$  at  $-20^\circ\text{C}$  and  $20^\circ\text{C}$  of PMN and 0.1PMN-0.9PZT respectively as shown in Figure 4.1(f) [43]. And the dielectric loss demonstrated higher values at lower frequency due to the electrical loss of lower spontaneous polarization ferroelectric materials [44]. In Figure 4.1(c-e), 0.7PMN-0.3PZT, 0.5PMN-0.5PZT and 0.3PMN-0.7PZT samples show relaxor ferroelectric properties. The broad peak of maximum dielectric constant decreased and shifted to higher temperature when frequency was increased, the maximum dielectric constant was around  $70, 90$  and  $110^\circ\text{C}$  respectively. And the dielectric loss demonstrated higher values at higher frequency due to the higher hysteresis spontaneous polarization inside ferroelectric materials [44].

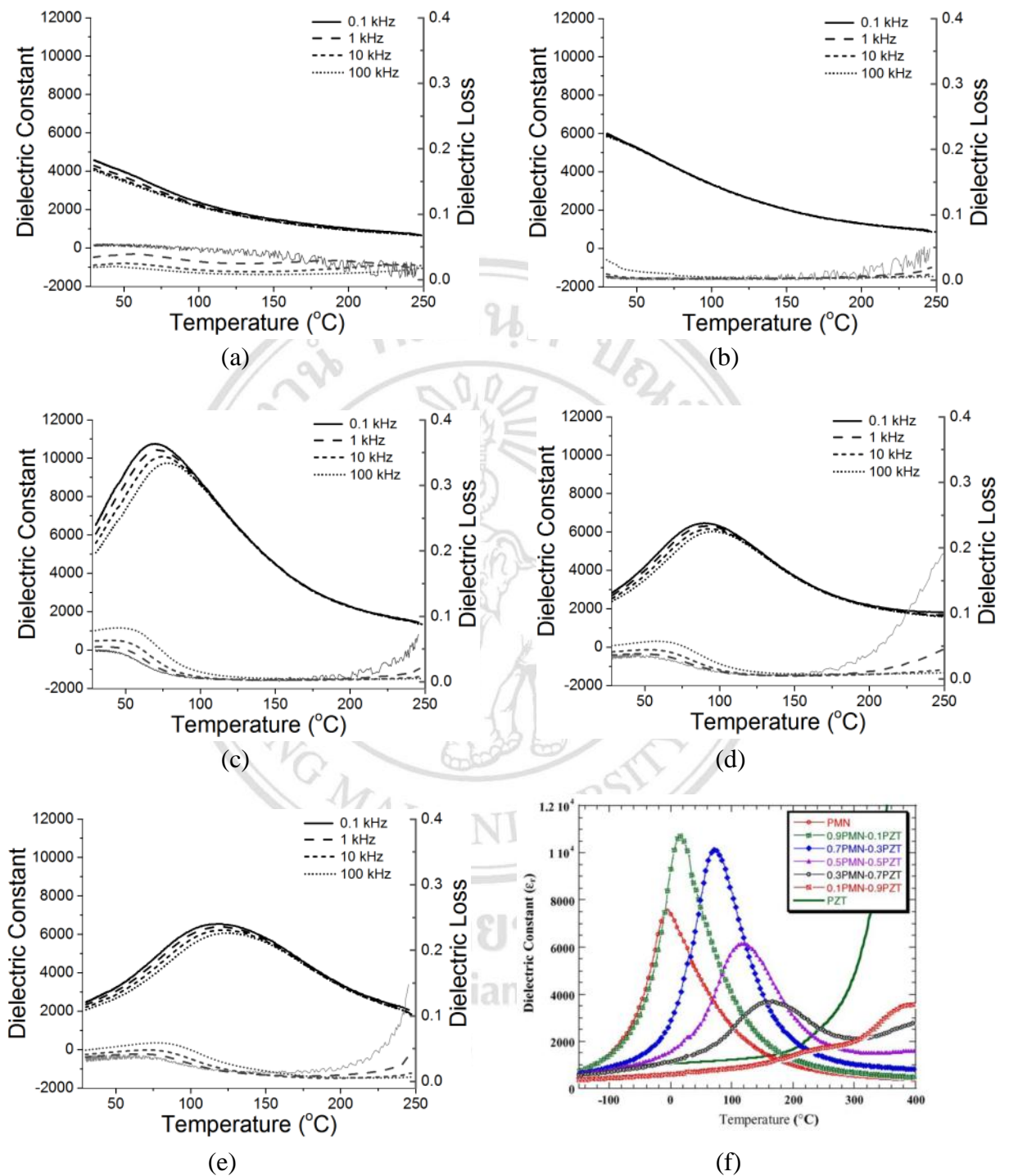


Figure 4.1 The temperature dependence of the dielectric constant ( $\epsilon_r$ ) of (a) PMN and  $x$ PMN-(1- $x$ )PZT samples where (b)  $x=0.9$ , (c)  $x=0.7$ , (d)  $x=0.5$ , (e)  $x=0.3$  and (f) temperature dependence at the temperature range of -150°C to 400°C from Yimmirun et al. [43]

Figures 4.2 and 4.3 show electric field induced-strain and polarization at various frequencies of PMN and 0.1PMN-0.9PZT samples, respectively. Both samples show slim loop of polarization and quadratic shape curve of induced strain as a function of applied electric field indicating non spontaneous polarization inside in paraelectric phase. In Figure 4.2, PMN sample demonstrated less hysteresis of polarization from 1 to 0.2 Hz of applied electric field frequency, but shows increase of hysteresis loss of polarization as a function of decreased frequency from 0.1 to 0.02 Hz of applied electric field frequency caused by frequency dependence of the electrical loss. Electrical charge can pass through the sample of low impedance due to lower frequency and less spontaneous polarization [44]. The maximum polarization decreased and the remnant polarization increased when the frequency decreased from 0.1 to 0.02 Hz, resulting from charge accumulated at the layer inside the PMN sample. The induced strain shows less change and quadratic shape curve for all applied electric field frequency. In Figure 4.3, 0.1PMN-0.9PZT sample demonstrated less hysteresis of polarization at 1 Hz of applied electric field frequency, and shows increase of hysteresis loss of polarization when the frequency was decreased to 0.02 Hz. This is due to frequency dependence of the electrical loss like PMN samples [44]. The maximum polarization increased when the frequency was decreased from 0.1 to 0.02 Hz but shows less change in maximum induced strain, which shows quadratic shape curve for all applied electric field frequency, resulting from fewer layers inside the 0.1PMN-0.9PZT sample.

Figures 4.4 and 4.5 show induced-strain as a function of polarization at various frequencies of PMN and 0.1PMN-0.9PZT samples, respectively. Both samples show polarization dependence of induced strain which is the quadratic relation to applied electric field frequency. It also shows hysteresis of induced strain as a function of polarization when electrical loss was increased.

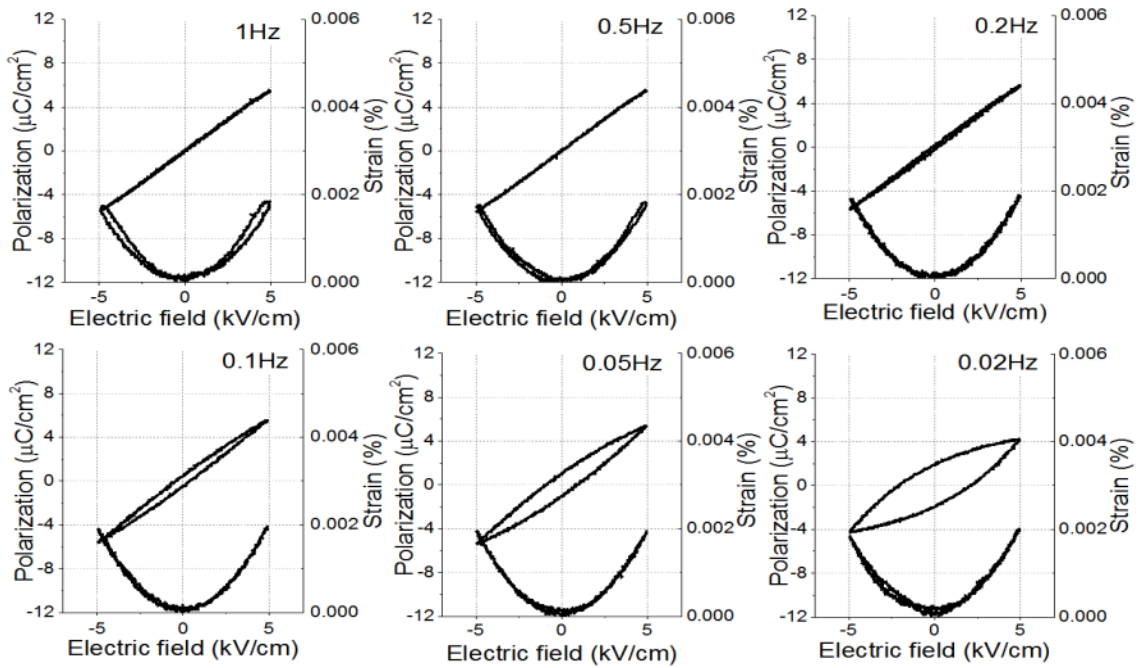


Figure 4.2 The frequency dependence of electric field induced strain and polarization of PMN

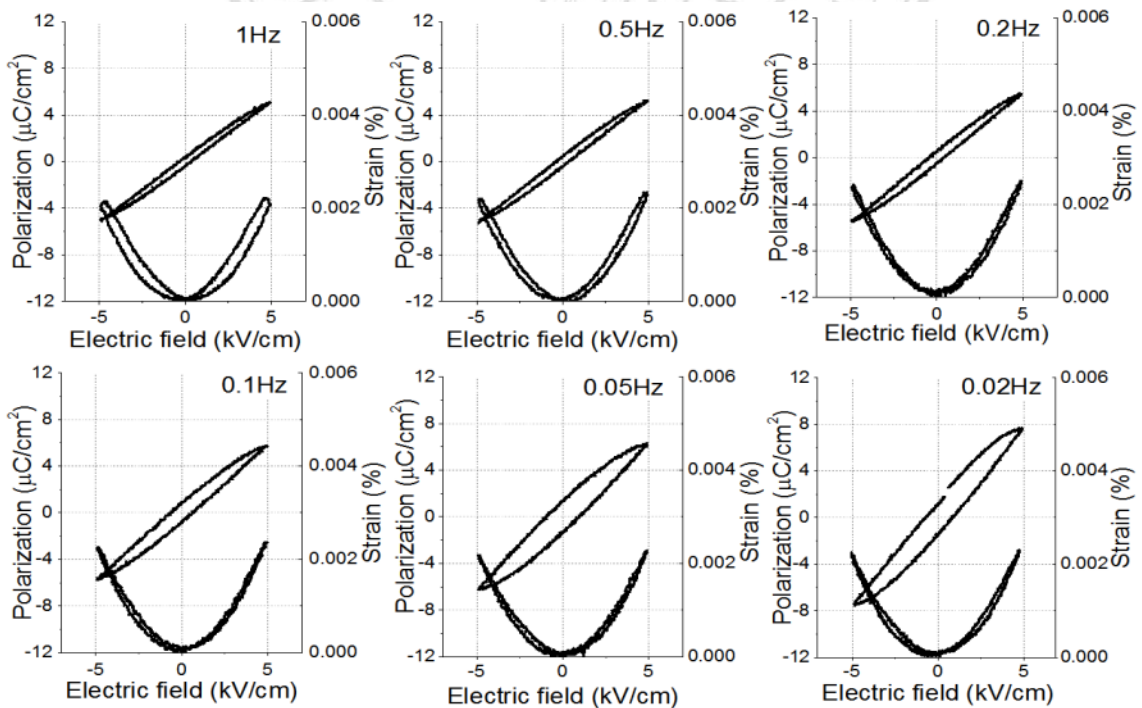


Figure 4.3 The frequency dependence of electric field induced strain and polarization of 0.9PMN-0.1PZT

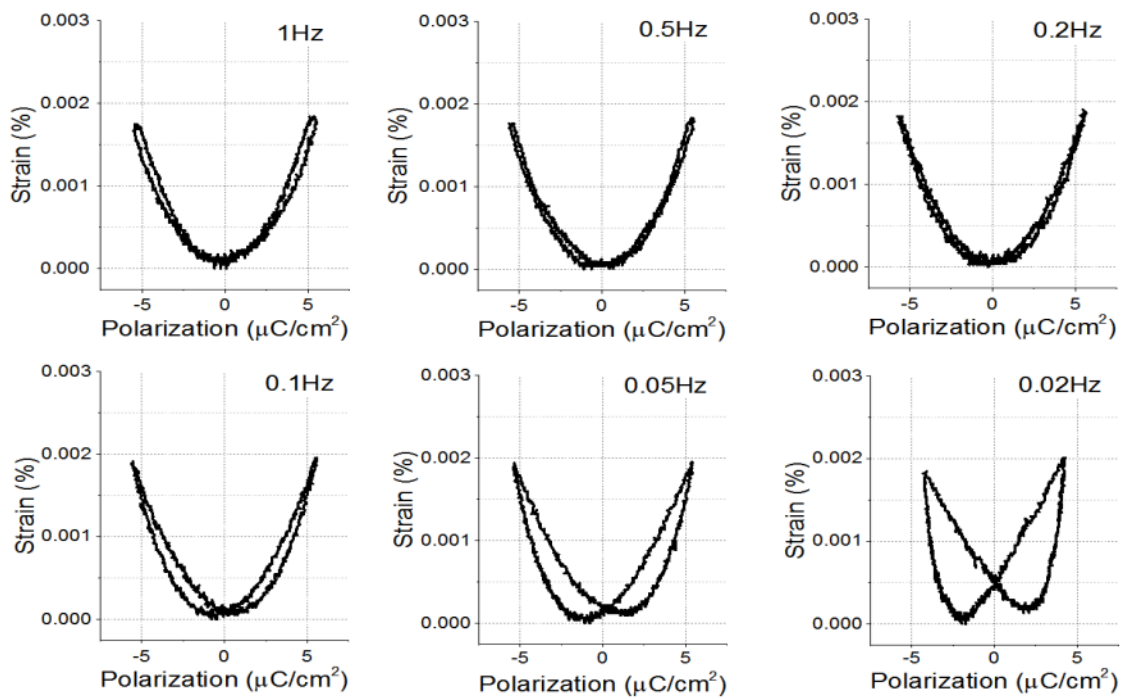


Figure 4.4 The frequency dependence of induced strain as a function of polarization of PMN

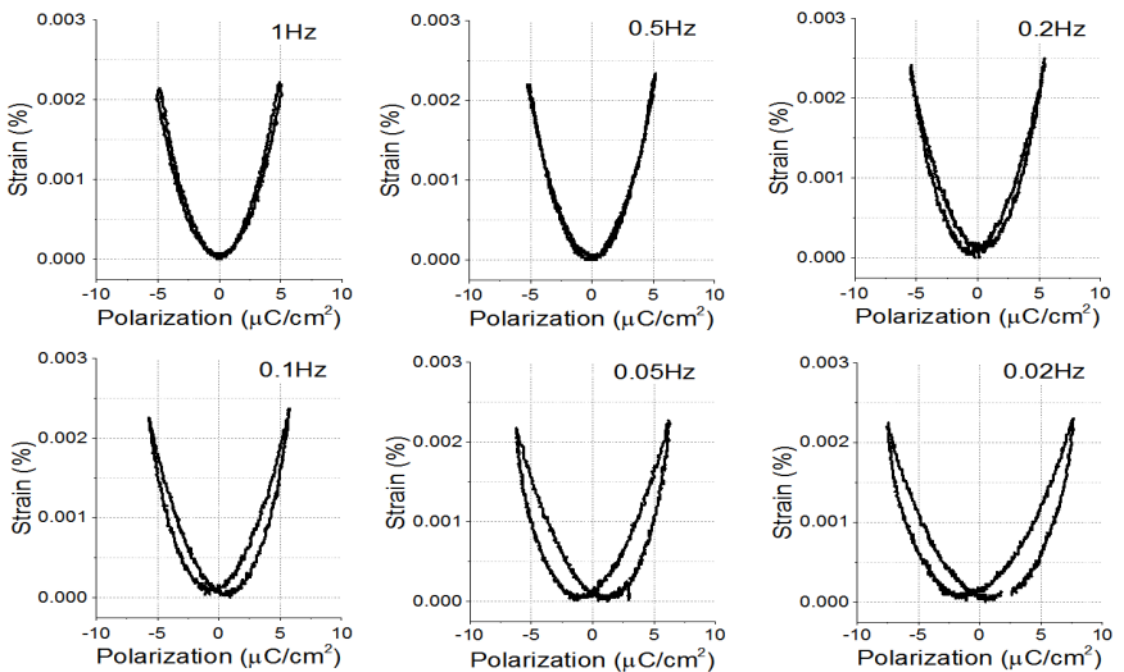


Figure 4.5 The frequency dependence of induced strain as a function of polarization of 0.9PMN-0.1PZT

Figures 4.6, 4.7 and 4.8 show electric field induced-strain and polarization at various frequencies of 0.7PMN–0.3PZT, 0.5PMN-0.5PZT and 0.3PMN-0.7PZT samples, respectively. All samples show hysteresis loop of polarization and butterfly shape curve of induced strain as a function of applied electric field indicating spontaneous polarization in ferroelectric phase. In Figure 4.6, 0.7PMN–0.3PZT sample demonstrated changes of hysteresis polarization when the applied electric field frequency was decreased from 1 to 0.01 Hz. Especially from 0.2 to 0.01 Hz, the hysteresis polarization changed from hysteresis of anti-clockwise direction at 0.2 and 0.1 Hz to non-hysteresis slimmer loop polarization at 0.05 Hz then shows clockwise hysteresis polarization at 0.02 and 0.01 Hz, caused by frequency dependence of the electrical loss. Electrical charge can pass through the sample of lowering impedance due to lower frequency. And the maximum polarization was decreased when the frequency decreased from 0.2 to 0.01 Hz resulting from charge accumulated at the layer inside the PMN sample [44,45]. The induced strain increased when the frequency was decreased and butterfly shape curve for all applied electric field frequency can be observed. In Figure 4.7, 0.5PMN-0.5PZT sample demonstrated increase of hysteresis polarization and the maximum polarization when the applied electric field frequency was decreased from 1 to 0.2 Hz, but showed less change in the induced strain, which shows butterfly shape curve for all applied electric field frequency, resulting from fewer layers inside and frequency dependence of the electrical loss in the 0.5PMN-0.5PZT sample [44]. In Figure 4.8, 0.3PMN-0.7PZT sample demonstrated increase of hysteresis polarization and the maximum polarization when the applied electric field frequency was decreased from 1 to 0.01 Hz, but showed less change in the induced strain, which shows butterfly shape curve for all applied electric field frequency, resulting from fewer layers inside and frequency dependence of the electrical loss like 0.5PMN-0.5PZT sample [44].

Figures 4.9, 4.10 and 4.11 show induced-strain as a function of polarization at various frequencies of 0.7PMN–0.3PZT, 0.5PMN-0.5PZT and 0.3PMN-0.7PZT samples, respectively. All samples show polarization dependence of induced strain which is the quadratic relation curve with less electrical loss at 1 to 0.1 Hz for 0.7PMN–0.3PZT, 1 Hz for 0.5PMN-0.5PZT and 1 to 0.2 Hz for 0.3PMN-0.7PZT. It also shows hysteresis of induced strain as a function of polarization when electrical loss was increased.

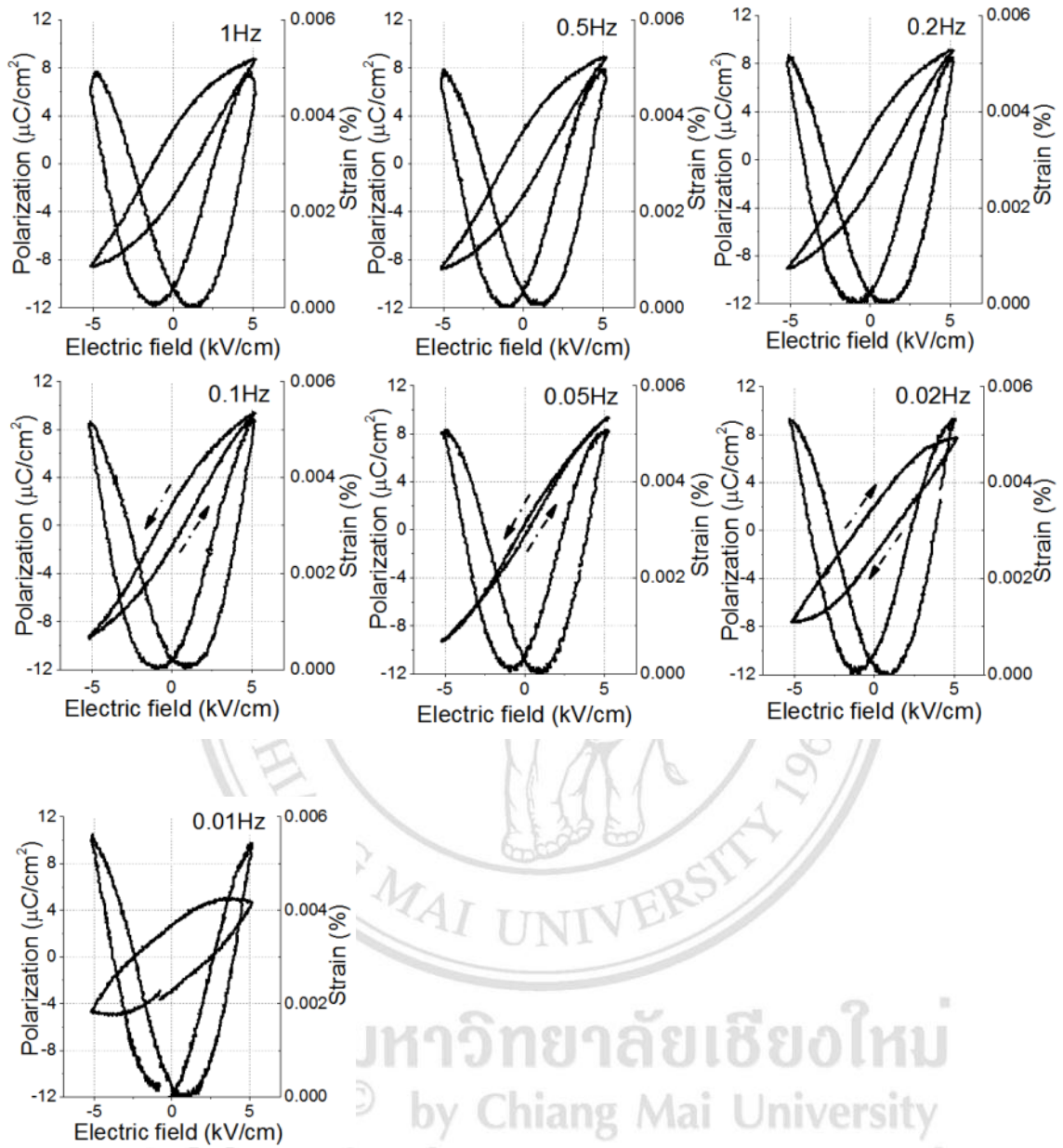


Figure 4.6 The frequency dependence of electric field induced strain and polarization of 0.7PMN-0.3PZT

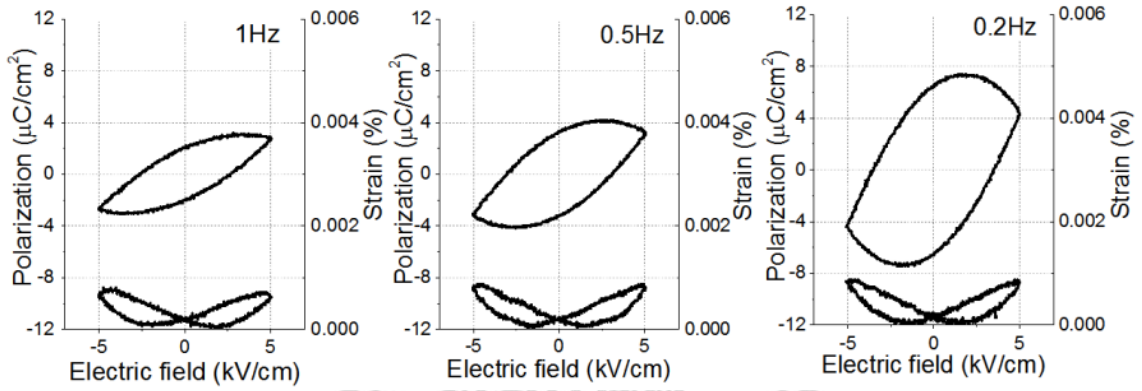


Figure 4.7 The frequency dependence of electric field induced strain and polarization of 0.5PMN-0.5PZT

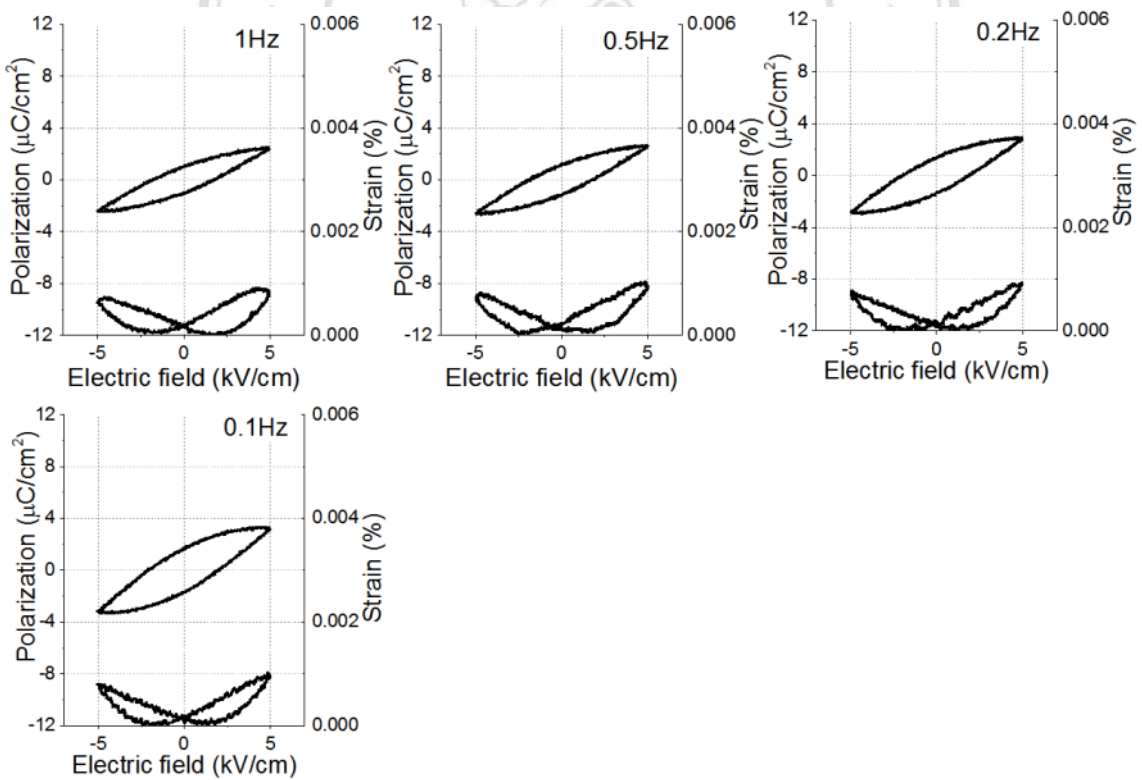


Figure 4.8 The frequency dependence of electric field induced strain and polarization of 0.3PMN-0.7PZT

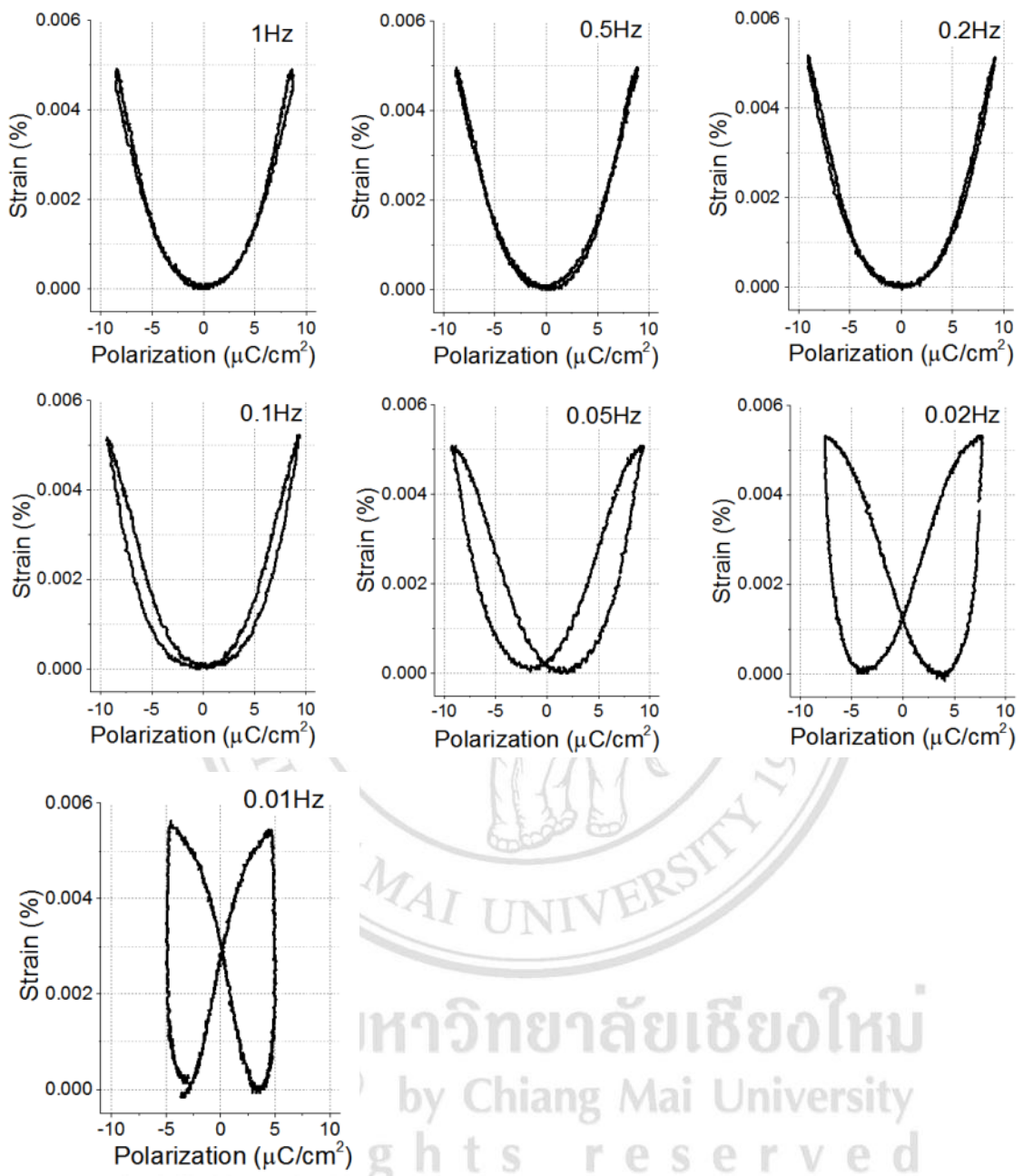


Figure 4.9 The frequency dependence of induced strain as a function of polarization of 0.7PMN-0.3PZT

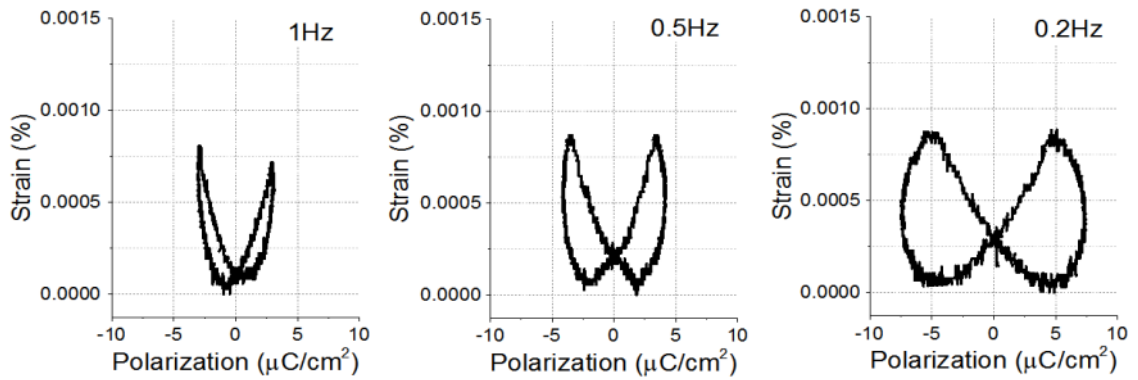


Figure 4.10 The frequency dependence of induced strain as a function of polarization of 0.5PMN-0.5PZT

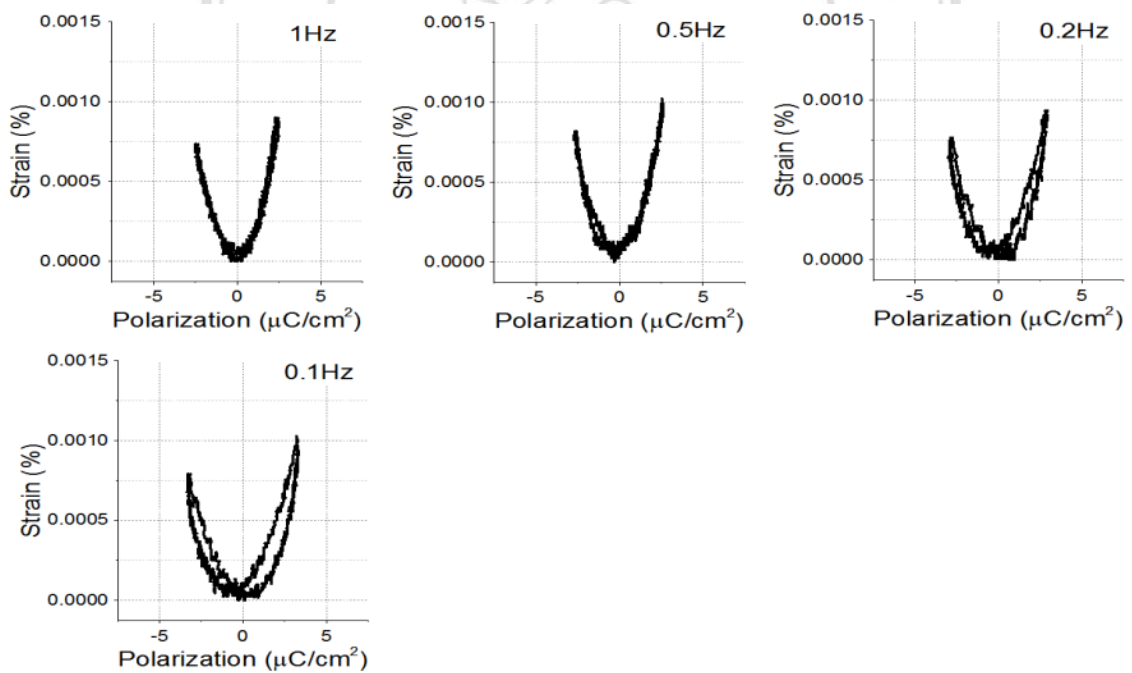


Figure 4.11 The frequency dependence of induced strain as a function of polarization of 0.3PMN-0.7PZT

Figures 4.12 and 4.13 show induced-strain shape as a function of electric field and polarization respectively of the less spontaneous polarization PMN sample at various frequencies. In Figure 4.12, the induced strain shows quadratic shape curve as a function of electric field for all frequency, implying no spontaneous polarization inside the sample corresponding to the dielectric constant in Figure 4.1(a) at room temperature. The maximum induced strain was increased when the frequency of applied electric field was decreased from 1 to 0.05 Hz but decreased at 0.02 Hz corresponding to Figure 4.2 that the polarization was dropped at 0.02 Hz according to the charges accumulated at the layer inside the ferroelectric materials. In Figure 4.13, the maximum induced strain as a function of polarization was increased from 1 to 0.05 Hz as a quadratic shape curve but shows decreases as a hysteresis induced strain shape according to the electrical loss at 0.02 Hz [44]. It can be seen clearly that frequency affected the change in the induced strain behavior related to the change of polarization [42].

Figures 4.14 and 4.15 show induced-strain shape as a function of electric field and polarization respectively of the high spontaneous polarization 0.7PMN-0.3PZT sample at various frequencies. In Figure 4.14, the induced strain shows butterfly shape curve as a function of electric field for all frequency, implying the spontaneous polarization inside the sample corresponding to the dielectric constant in Figure 4.1(c) at room temperature. The maximum induced strain was increased when the frequency of applied electric field was decreased from 1 to 0.01 Hz corresponding to Figure 4.6 that the hysteresis polarization changed to slimmer loop at 0.05 Hz and dropped values at 0.02 and 0.01 Hz according to the charges accumulated at the layer inside the ferroelectric materials but that did not affect to the maximum induced strain of high spontaneous polarization of 0.7PMN-0.3PZT sample, which was different from less spontaneous sample PMN. In Figure 4.15, the induced strain shows quadratic shape curve as a function of polarization as  $90^\circ$  domain rotation [1] and shows hysteresis of induced strain shape curve when the frequency was lower from 0.05 to 0.01 Hz. The maximum induced strain as a function of polarization was increased from 1 to 0.01 Hz. It can be seen clearly that frequency affected the change in the induced strain behavior related to the change of polarization [42].

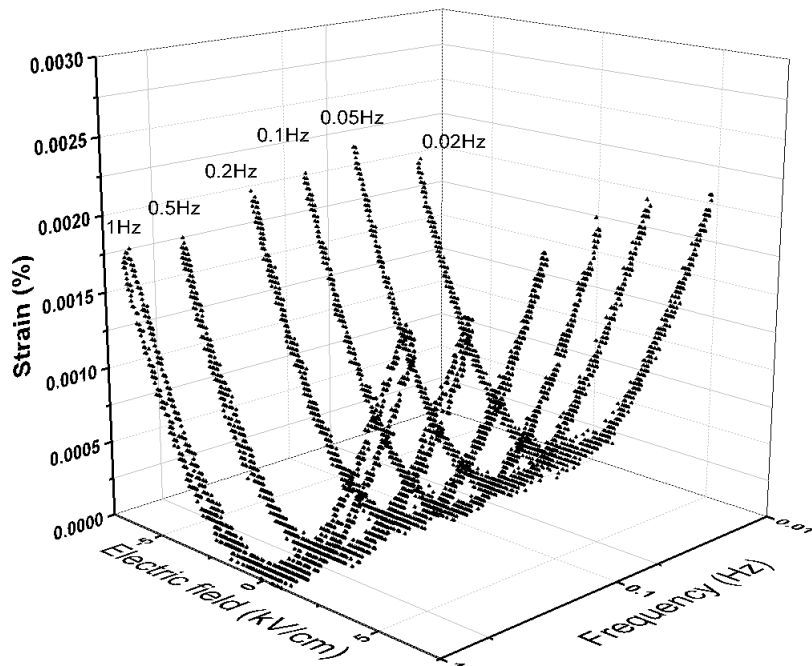


Figure 4.12 The field induced-strain (s-E) of PMN at various frequencies [42]

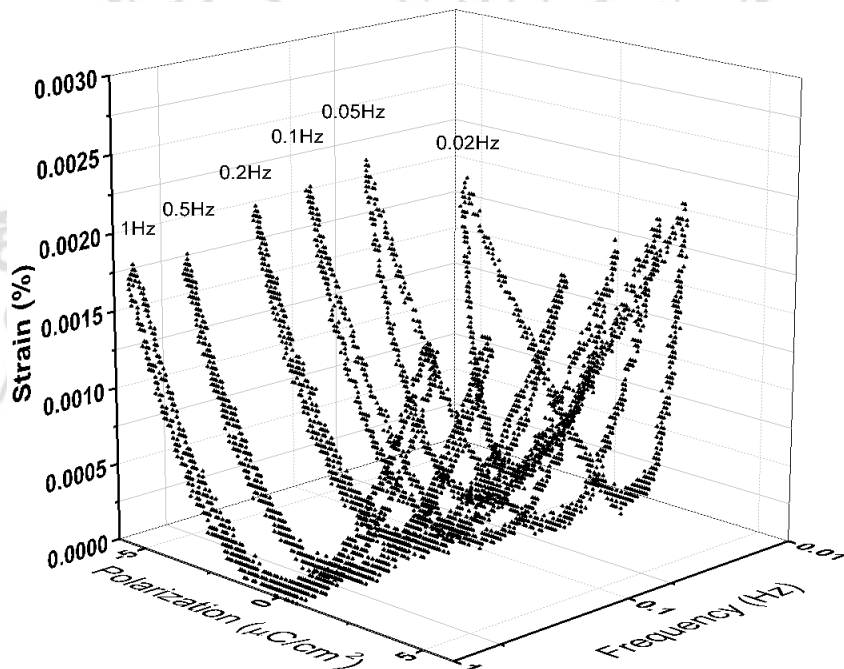


Figure 4.13 The induced-strain as a function of polarization (s-P) curve of PMN at various frequencies [42]

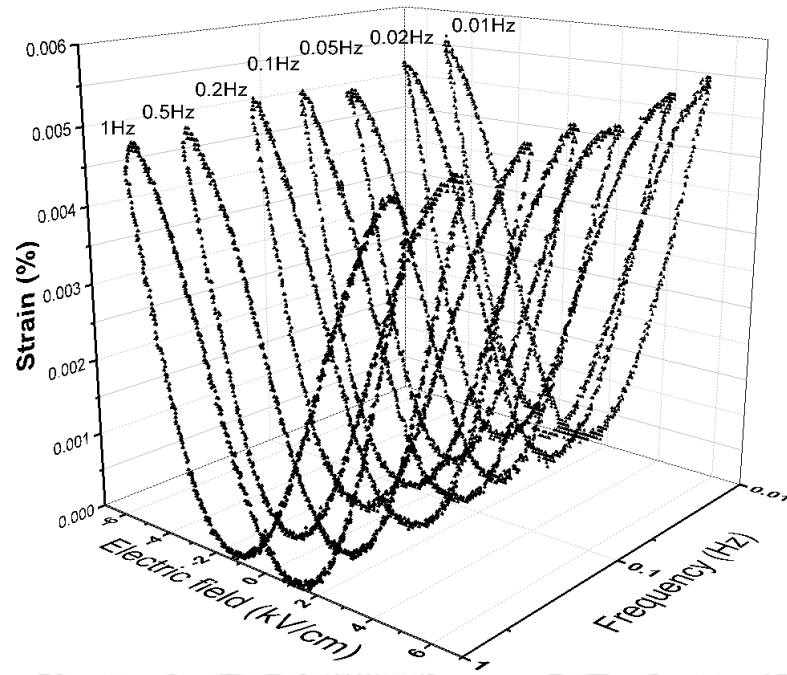


Figure 4.14 The field induced-strain (s-E) of 0.7PMN-0.3PZT at various frequencies [42]

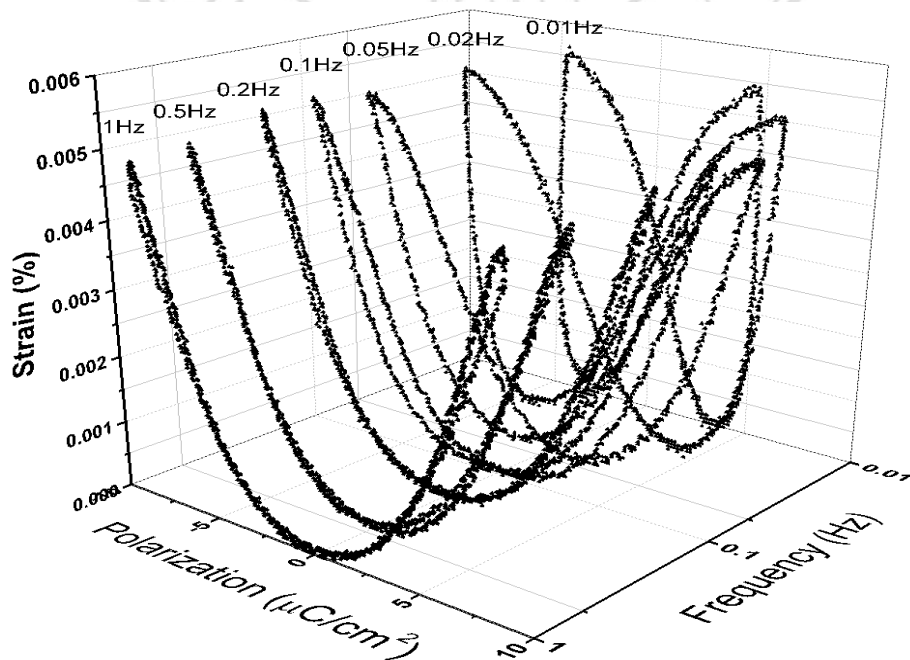


Figure 4.15 The induced-strain as a function of polarization (s-P) curve of 0.7PMN-0.3PZT at various frequencies [42]

The anti-clockwise and clockwise direction of polarization behavior in 0.7PMN-0.3PZT depended on the applied electric field frequency which showed difference resulted to high spontaneous polarization and less spontaneous polarization samples of ferroelectric materials. To observe this behavior of 0.7PMN-0.3PZT sample, the heat was applied when induced strain was measured as shown in Figure 2.16. The 0.7PMN-0.3PZT sample shows increased maximum induced strain and polarization changed from anti-clockwise to slim loop direction when the frequency was decreased from 0.2 to 0.05 Hz due to high spontaneous polarization at 30°C, but 0.7PMN-0.3PZT sample shows decreased maximum induced strain and polarization changed from slim loop to clockwise direction when the frequency was decreased from 0.2 to 0.05 Hz due to less spontaneous polarization at 50°C as shown in Figure 4.17.

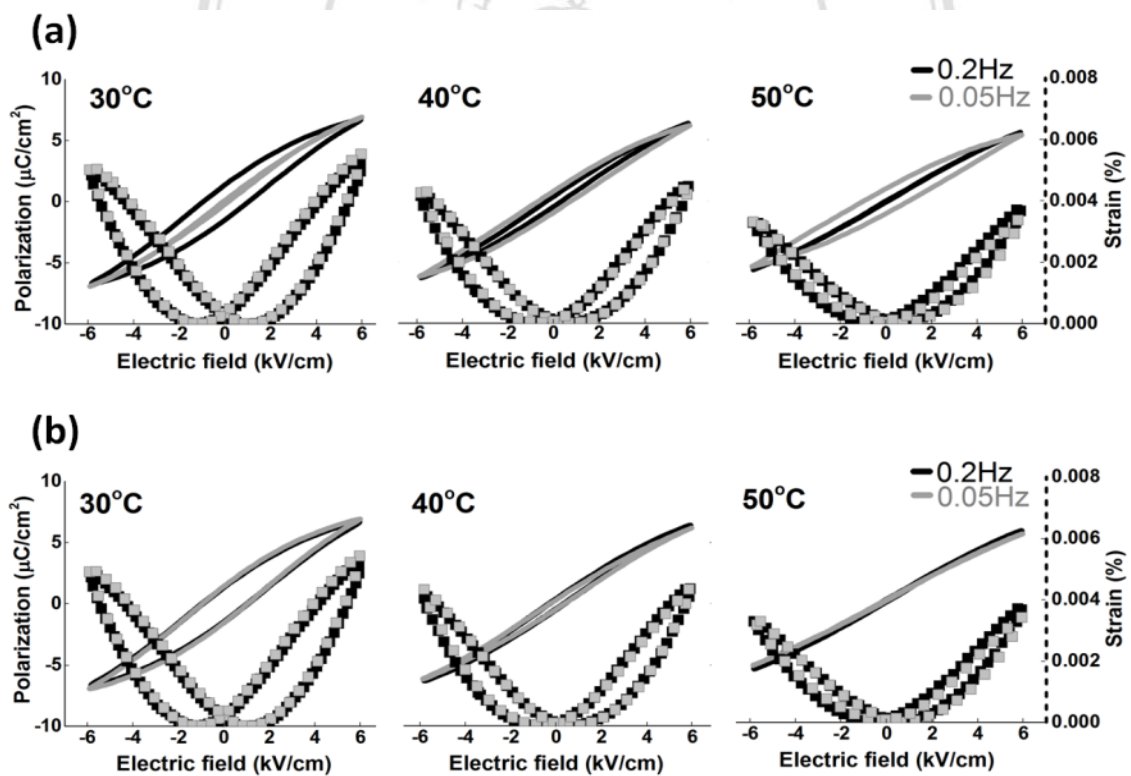


Figure 4.16 Induced strain and polarization of 0.7PMN–0.3PZT at 30°C, 40°C, and 50°C (a) before and (b) after the polarization correction [44]

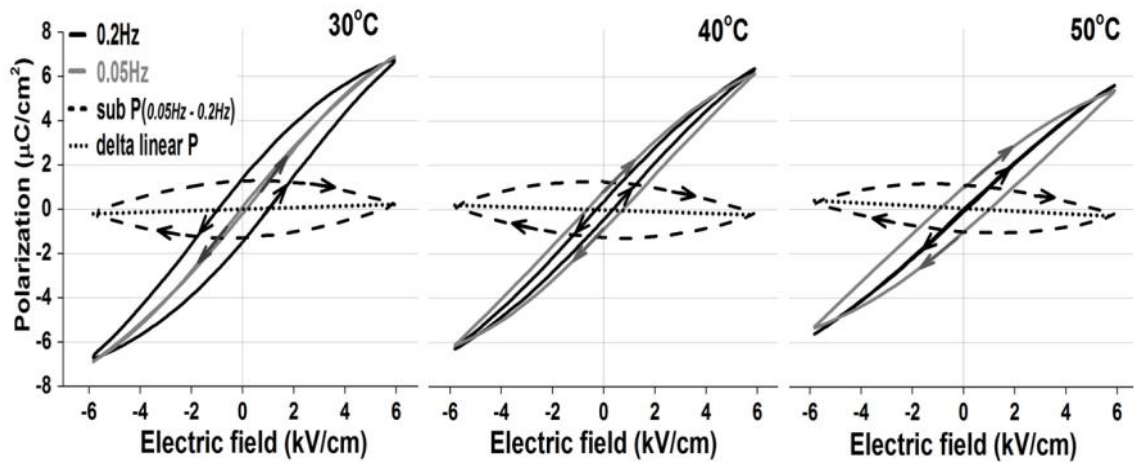


Figure 4.17 The electrical loss (sub P) of 0.7PMN–0.3PZT at 30°C, 40°C, and 50°C [44]

The decrease of induced strain and polarization behavior are according to the electrical loss (subtract of polarization at 0.2 Hz by 0.05 Hz; sub P) as shown in Figure 4.17. When lower frequency was used, the measurement which generated the depolarizing field and minimized the electrical field resulted in decreased maximum induced strain and polarization in less spontaneous polarization sample at 50°C as shown in Figure 4.18.

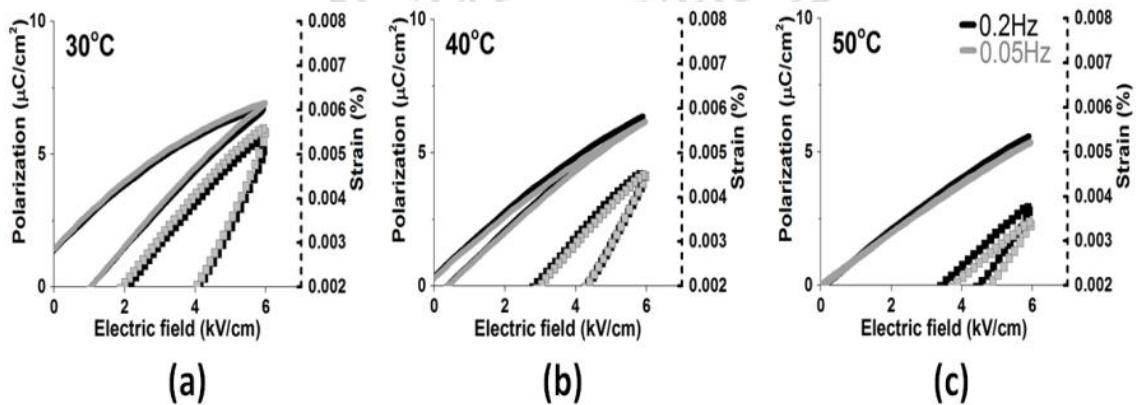


Figure 4.18 The changed of maximum induced strain and polarization of 0.7PMN–0.3PZT at 30°C, 40°C, and 50°C [44]

#### 4.1.2 Aging behavior in induced-strain of 9/70/30 and 9/65/35 PLZT

Time dependence of piezoelectric/electrostrictive properties is the important character, which means the stability changes with time after fabrication and this should be taken into account when piezoelectric/electrostrictive materials are selected in the commercial electronic equipment for electroceramic, electrooptic, and sensor/actuator applications. After fabrication, ferroelectric samples are cooled down from high temperature paraelectric phase to room temperature ferroelectric phase and causes the potential energy inside due to apparent spontaneous polarization in the ferroelectric phase [45-51]. To observe time dependence or aging behavior of ferroelectric sample the attractive transparent ferroelectric ceramic material  $\text{Pb}_{0.91}\text{La}_{0.09}(\text{Zr}_{0.70}\text{Ti}_{0.30})_{0.9775}\text{O}_3$  PLZT (9/70/30) and  $\text{Pb}_{0.91}\text{La}_{0.09}(\text{Zr}_{0.65}\text{Ti}_{0.35})_{0.9775}\text{O}_3$  PLZT (9/65/35), in this work the composition near the morphotropic phase boundary (MPB) between tetragonal and rhombohedral ferroelectric phase was chosen and the ceramic samples were fabricated by solid mixing oxide method and sintering at 1200, 1225, 1250 and 1275°C. The X-ray diffraction pattern and the dielectric constant as a function of temperature of the samples were shown in Figures 4.19 and 4.20 respectively [52].

Figure 4.19 shows X-ray diffraction pattern of PLZT (9/70/30) (gray line) and PLZT (9/65/35) (black line), all samples exhibited perovskite structure where PLZT (9/70/30) samples showed rhombohedral crystal structure but PLZT (9/65/35) samples showed the mixing structure of rhombohedral and tetragonal crystal structure indicating that this composition was near morphotropic phase boundary and free from pyrochlore phase structure [52]. In Figure 4.19(a), the shifted peak position to a higher angle when Zr/Ti contents in PLZT (La/Zr/Ti) composition decrease from PLZT (9/70/30) to PLZT (9/65/35) according to the decrease of lattice parameter when the smaller size of Ti ions were replaced by the bigger size of Zr ions in B-site position of perovskite structure [53]. In Figure 4.19(b), the x-ray diffraction pattern in the angle range from 42.5 to 47.5° of the samples were fitted to separate tetragonal (200) and rhombohedral (020) peak. PLZT (9/70/30) samples shows the (020) rhombohedral peak (dash line) clearly at 1275°C, and PLZT (9/65/35) samples shows the mixing of (020) rhombohedral peak

and (200) tetragonal peaks indicating partial phase transition from rhombohedral to tetragonal at morphotropic phase boundary (MPB) [53,54].

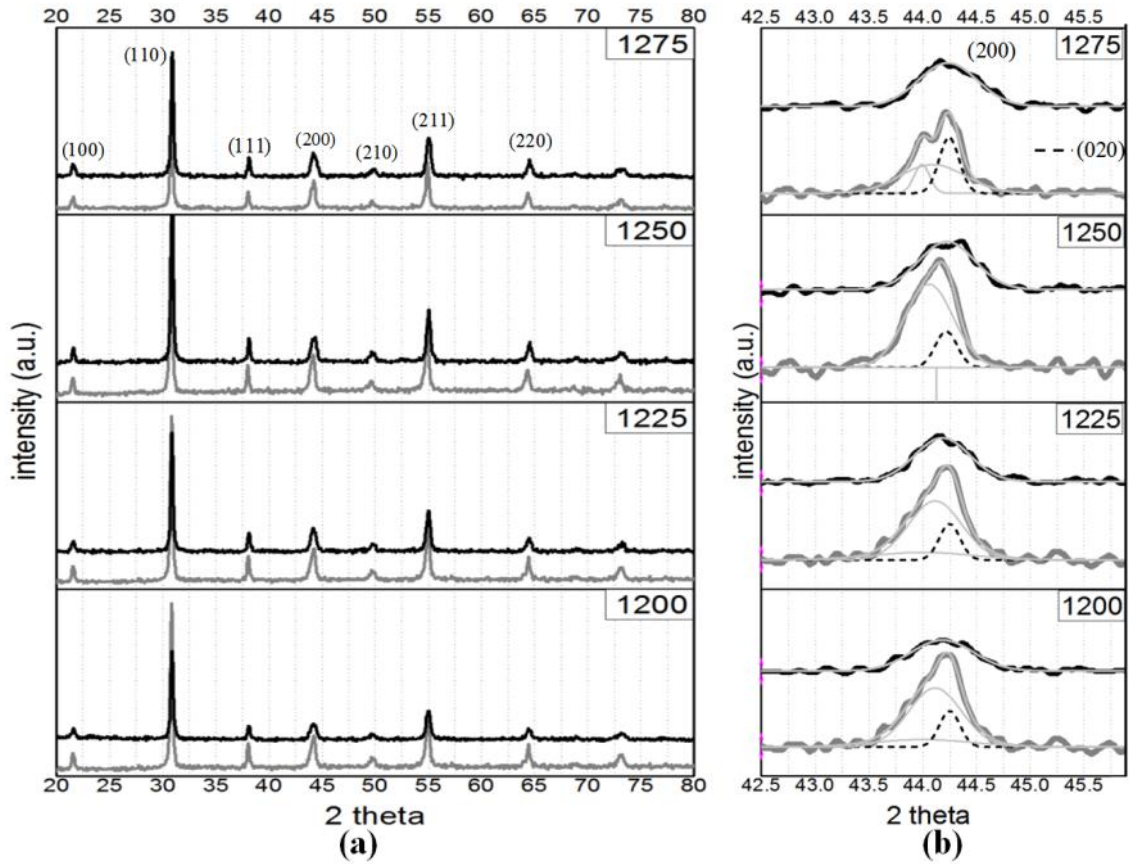


Figure 4.19 (a) X-ray diffraction pattern of PLZT (9/70/30) (gray line) and PLZT (9/65/35) (black line) (b) diffraction pattern between 42.5 and 45.9° [52]

Copyright© by Chiang Mai University  
All rights reserved

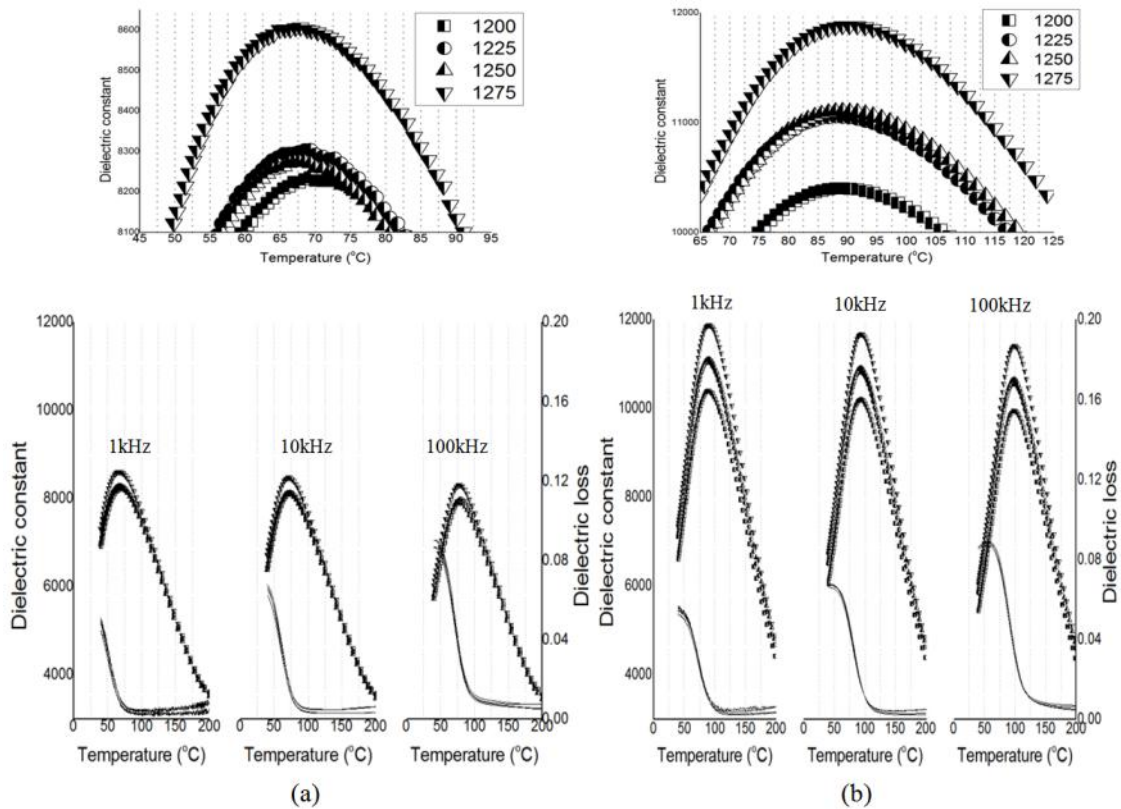


Figure 4.20 The dielectric constant peaks of (a) PLZT (9/70/30) and (b) PLZT (9/65/35) [52]

Figure 4.20 shows the dielectric constant peaks and dielectric loss of PLZT (9/70/30) and PLZT (9/65/35) samples as a function of temperature. The maximum dielectric constant of all samples was broad at a range of temperature, diffuse less and decreased when frequency was increased, which is the relaxation properties of relaxor ferroelectric materials. And dielectric loss increased when frequency was increased. In Figure 4.20(a), PLZT (9/70/30) sample show dielectric constant increases to the maximum when sample was increased sintering temperature from 1200 to 1275°C. It could result from a denser microstructure with fewer pores at higher sintering temperature [52]. The phase transition temperature or the temperature at maximum dielectric constant  $T_m$  of PLZT (9/70/30) samples was decreased from 70 to 67.5°C when increased sintering temperature from 1200 to 1275°C. In Figure 4.20(b), PLZT (9/65/35) samples shows dielectric constant higher than that of PLZT (9/70/30) samples and increases to the maximum when sample was increased sintering temperature from

1200 to 1275°C, which could also result from a denser microstructure. But the phase transition temperature or the temperature at maximum dielectric constant  $T_m$  of PLZT (9/65/35) samples shows sintering-temperature-independent and has phase transition temperature around 90°C [52].

Figures 4.21, 4.22, 4.23 and 4.24 show electric field induced-strain and polarization of PLZT (9/70/30) samples sintered at 1200, 1225, 1250 and 1275°C, respectively. All samples show slim loop of polarization and butterfly shape curve as a function of applied electric field. At zero electric field, all fresh samples demonstrated remnant of polarization and induced strain but that remnants were decreased as a function of time when samples were left to aging for 3, 11 and 19 days. At 19 days of aging, the polarization of all PLZT (9/70/30) samples showed the pinched loop referring to the rearrange of polarization and crystal structure inside to reduce the potential energy in aging phenomena [45-51]. And the remnant of induced strain disappeared too. After 280°C refresh and 600°C annealing, some samples were then showed remnant of polarization and induced strain again.

Figures 4.25, 4.26, 4.27, and 4.28 show induced-strain as a function of polarization of PLZT (9/70/30) samples sintered at 1200, 1225, 1250 and 1275°C, respectively. All fresh and aging samples show polarization dependence of induced strain where the quadratic relation curve demonstrated no remnant strain at zero polarization.

ลิขสิทธิ์มหาวิทยาลัยเชียงใหม่  
Copyright© by Chiang Mai University  
All rights reserved

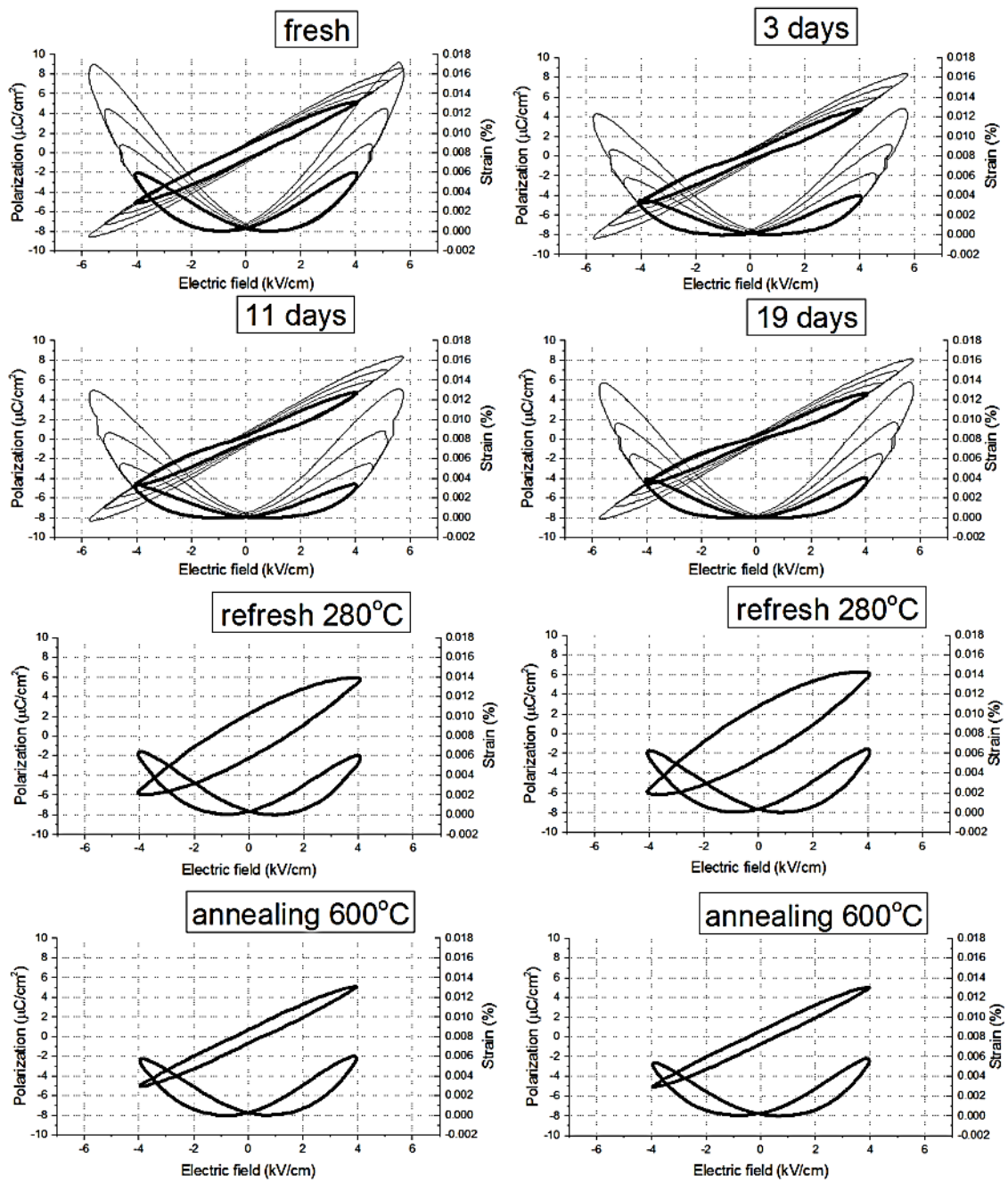


Figure 4.21 The induced-strain and polarization of PLZT (9/70/30) sintered at 1200°C

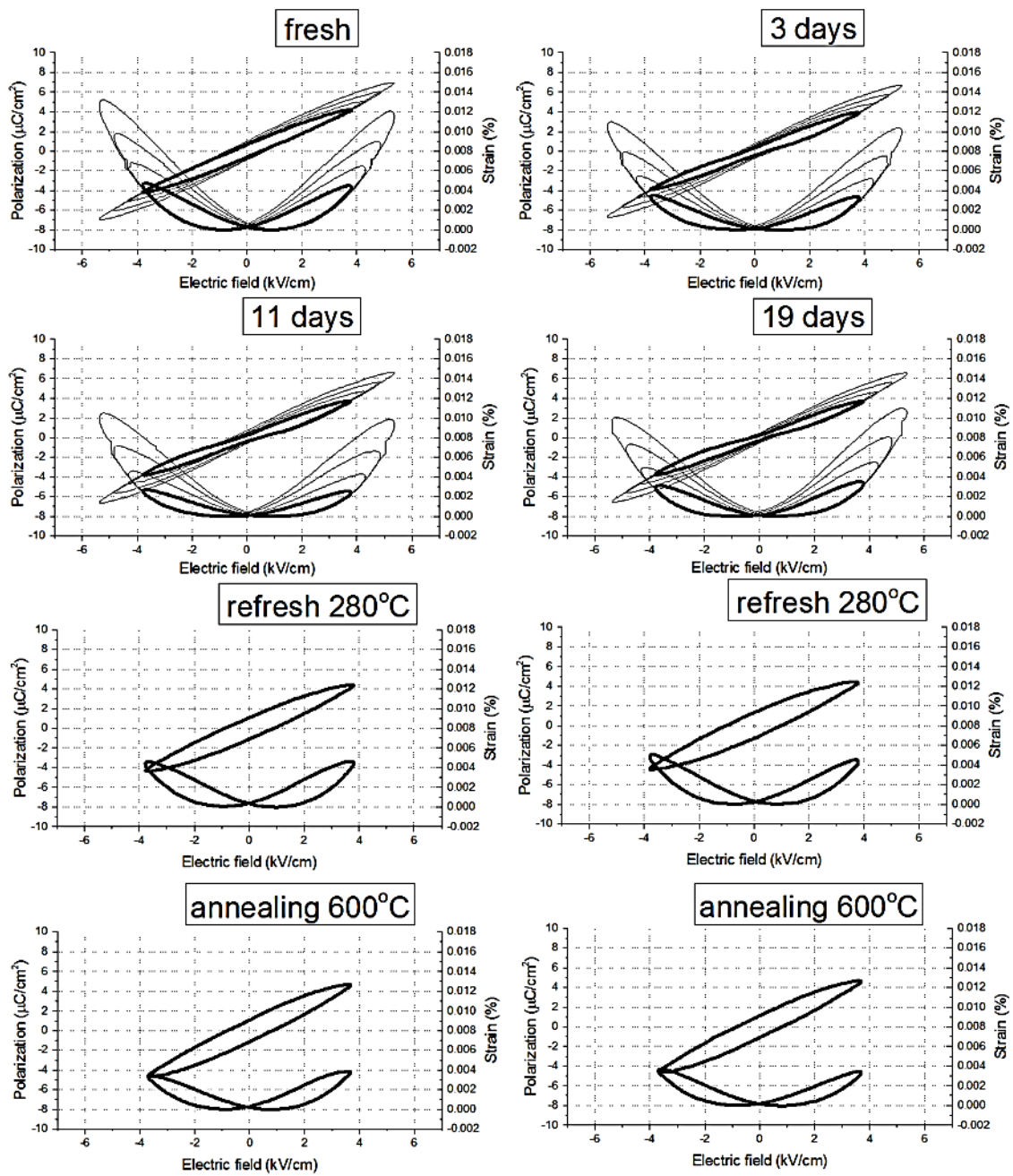


Figure 4.22 The induced-strain and polarization of PLZT (9/70/30) sintered at 1225°C

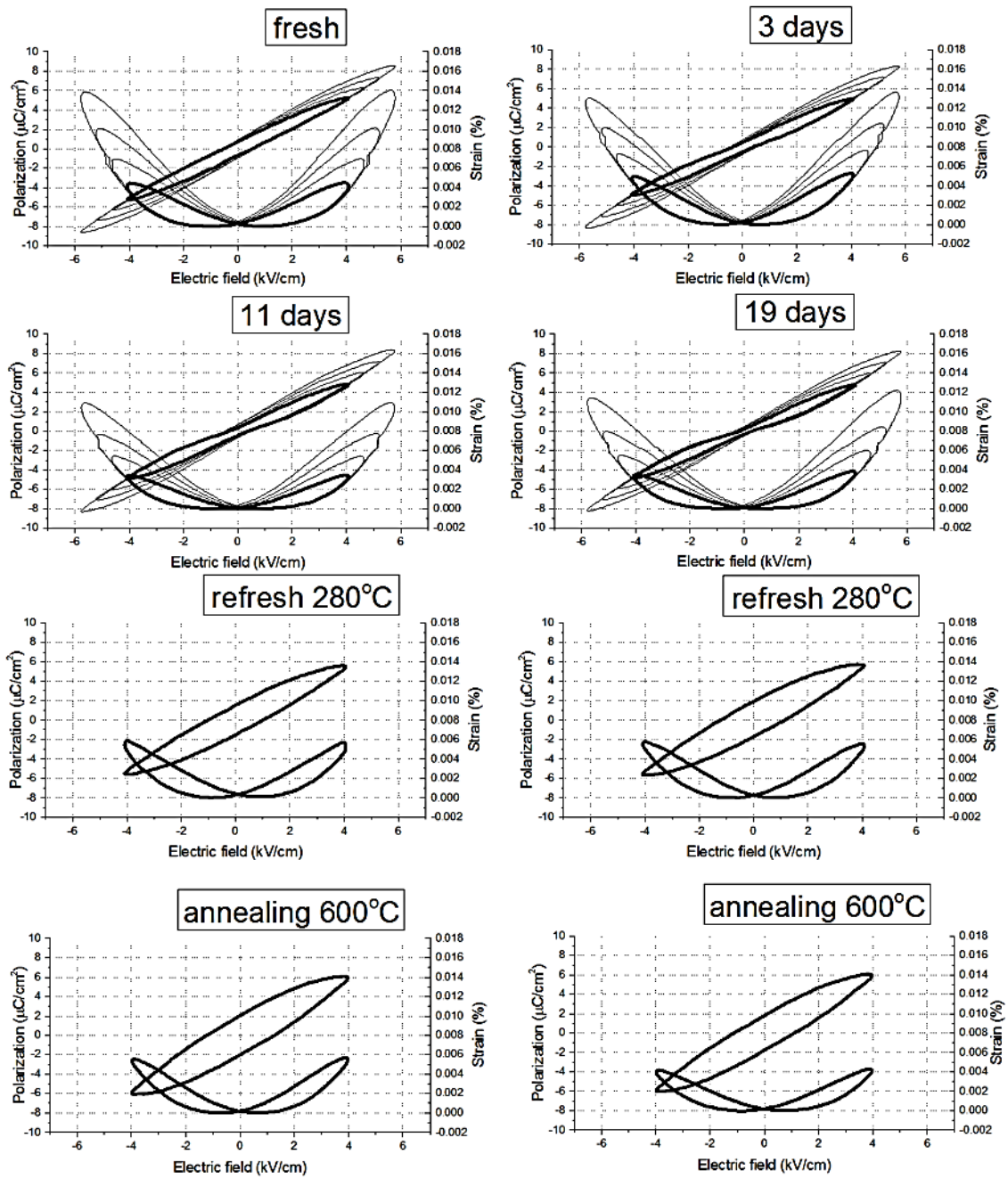


Figure 4.23 The induced-strain and polarization of PLZT (9/70/30) sintered at 1250°C

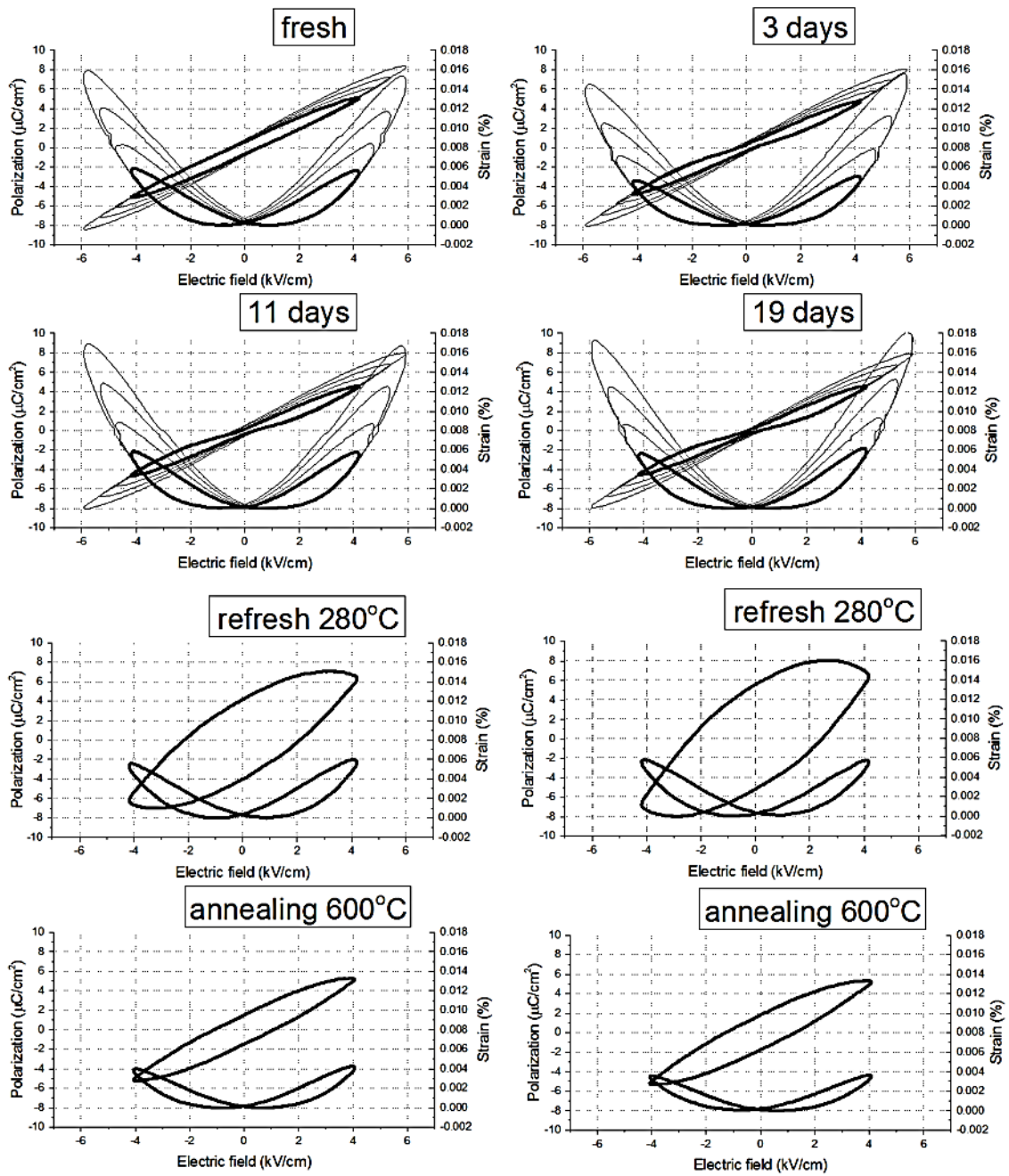


Figure 4.24 The induced-strain and polarization of PLZT (9/70/30) sintered at 1275°C

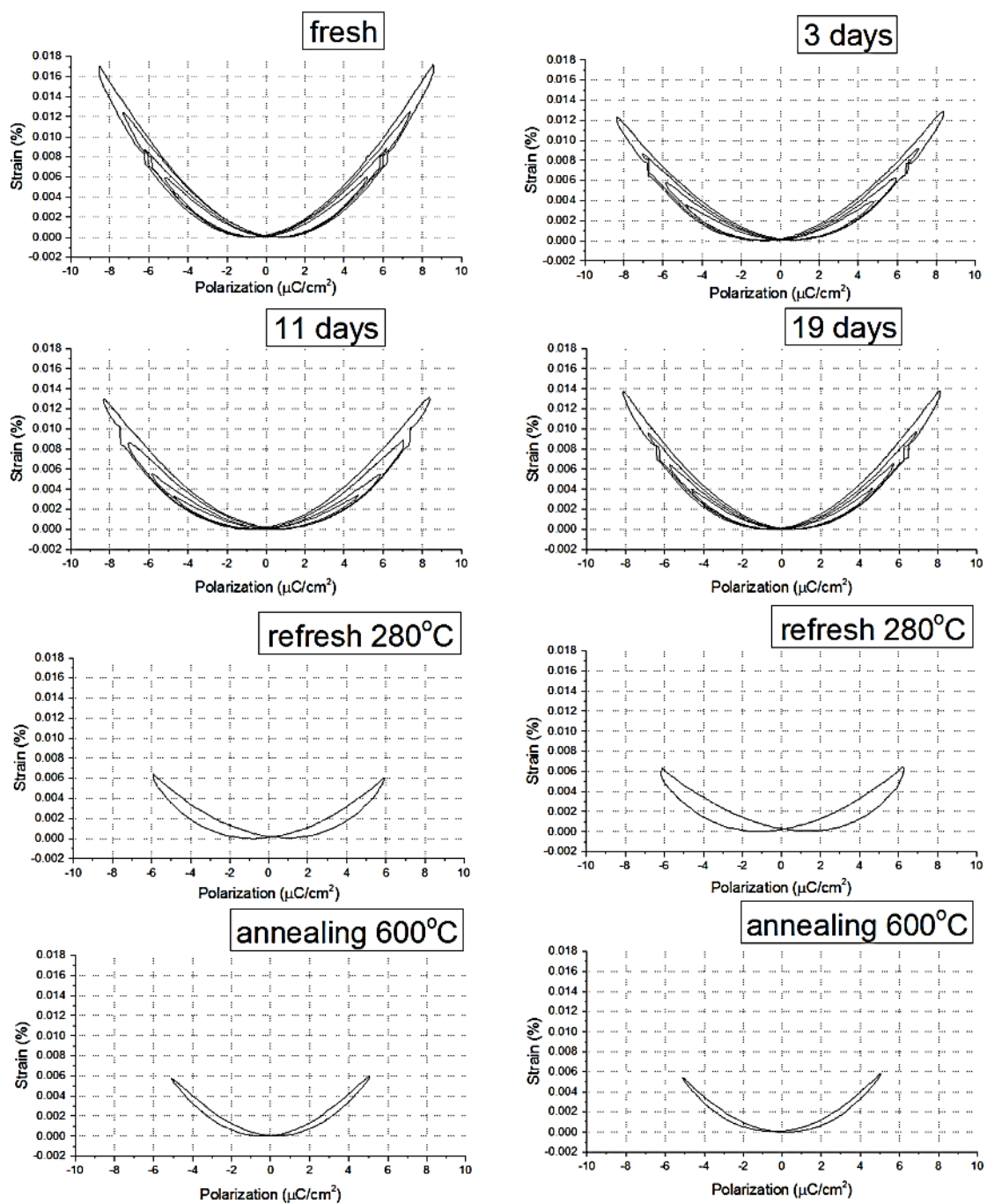


Figure 4.25 The induced-strain as a function of polarization of PLZT (9/70/30) sintered at  $1200^\circ\text{C}$

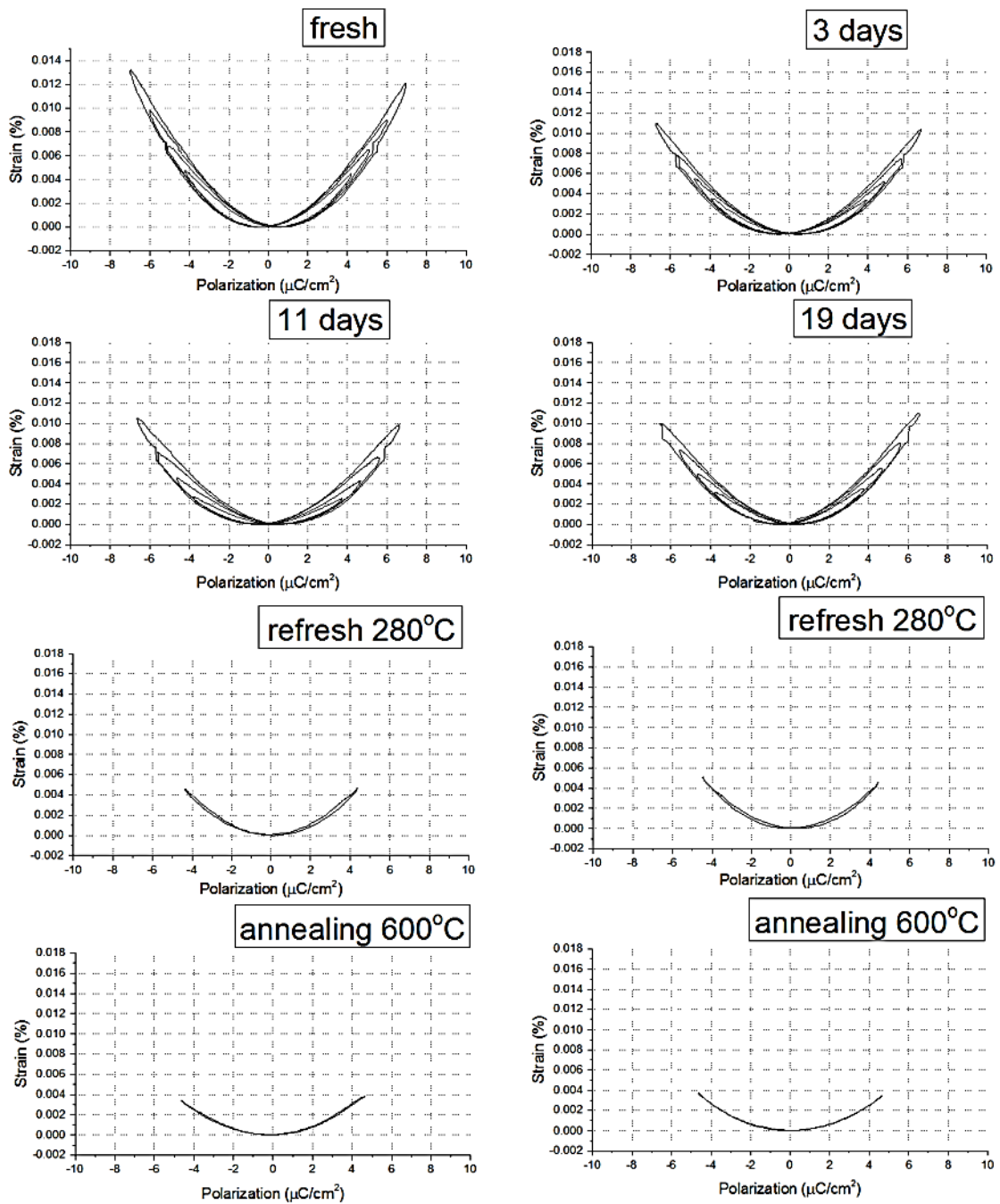


Figure 4.26 The induced-strain as a function of polarization of PLZT (9/70/30) sintered at  $1225^\circ\text{C}$

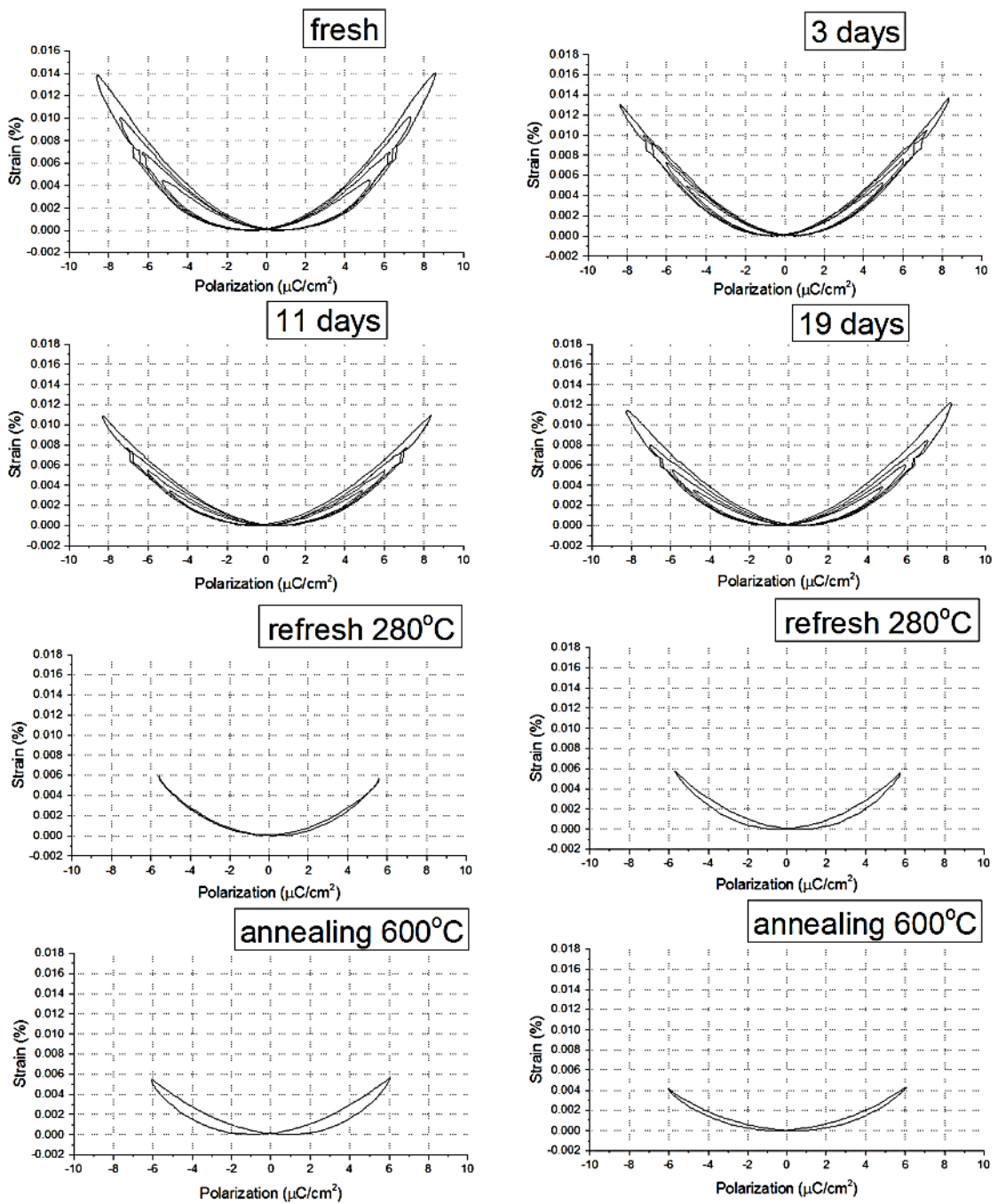


Figure 4.27 The induced-strain as a function of polarization of PLZT (9/70/30) sintered at  $1250^\circ\text{C}$

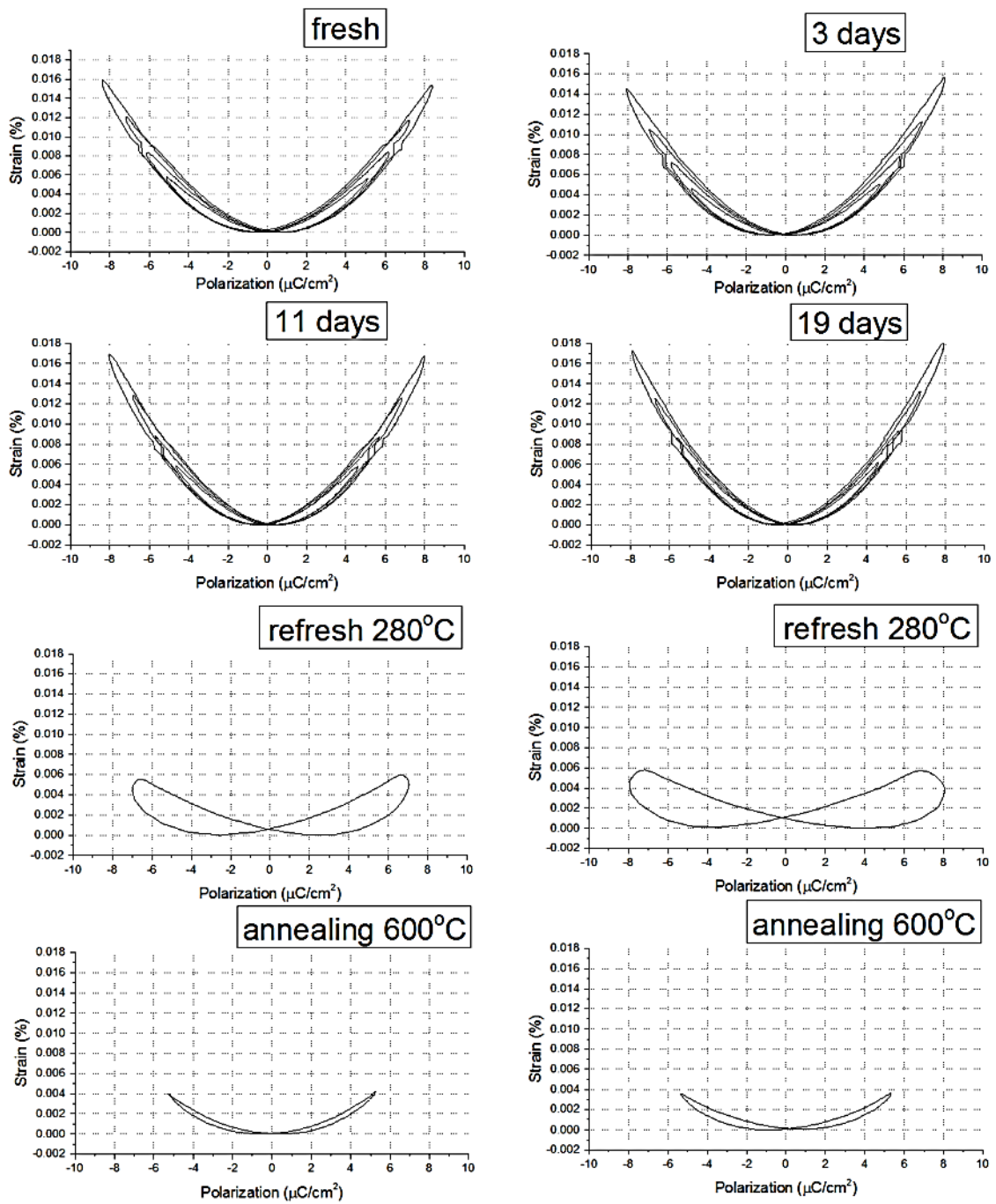


Figure 4.28 The induced-strain as a function of polarization of PLZT (9/70/30) sintered at  $1275^\circ\text{C}$

Figures 4.29, 4.30, 4.31 and 4.32 show electric field induced-strain and polarization of PLZT (9/65/35) samples sintered at 1200, 1225, 1250 and 1275°C, respectively. All samples show loop of polarization and butterfly shape curve as a function of applied electric field. All fresh samples demonstrated higher loop hysteresis polarization than PLZT (9/70/30) samples and balance induced strain and the maximum polarization and induced strain decreased as a function of time when samples was left to aging for 3, 19 and 31 days. At 19 days of aging, the polarization of all PLZT (9/65/35) samples was showed small polarization, the induced strain was decreased and demonstrated asymmetric shape curve due to the rearrangement of spontaneous polarization and crystal structure inside to reduce the elastic energy in aging phenomena [45-51]. After 280°C refresh and 600°C annealing, all samples seem to have a high values of polarization and induced strain again.

Figures 4.33, 4.34, 4.35, and 4.36 show induced-strain as a function of polarization of PLZT (9/65/35) samples sintered at 1200, 1225, 1250 and 1275°C, respectively. All fresh and aging samples show polarization dependence of induced strain where the quadratic relation curve was demonstrated due to 90° domain rotation dominate [1].

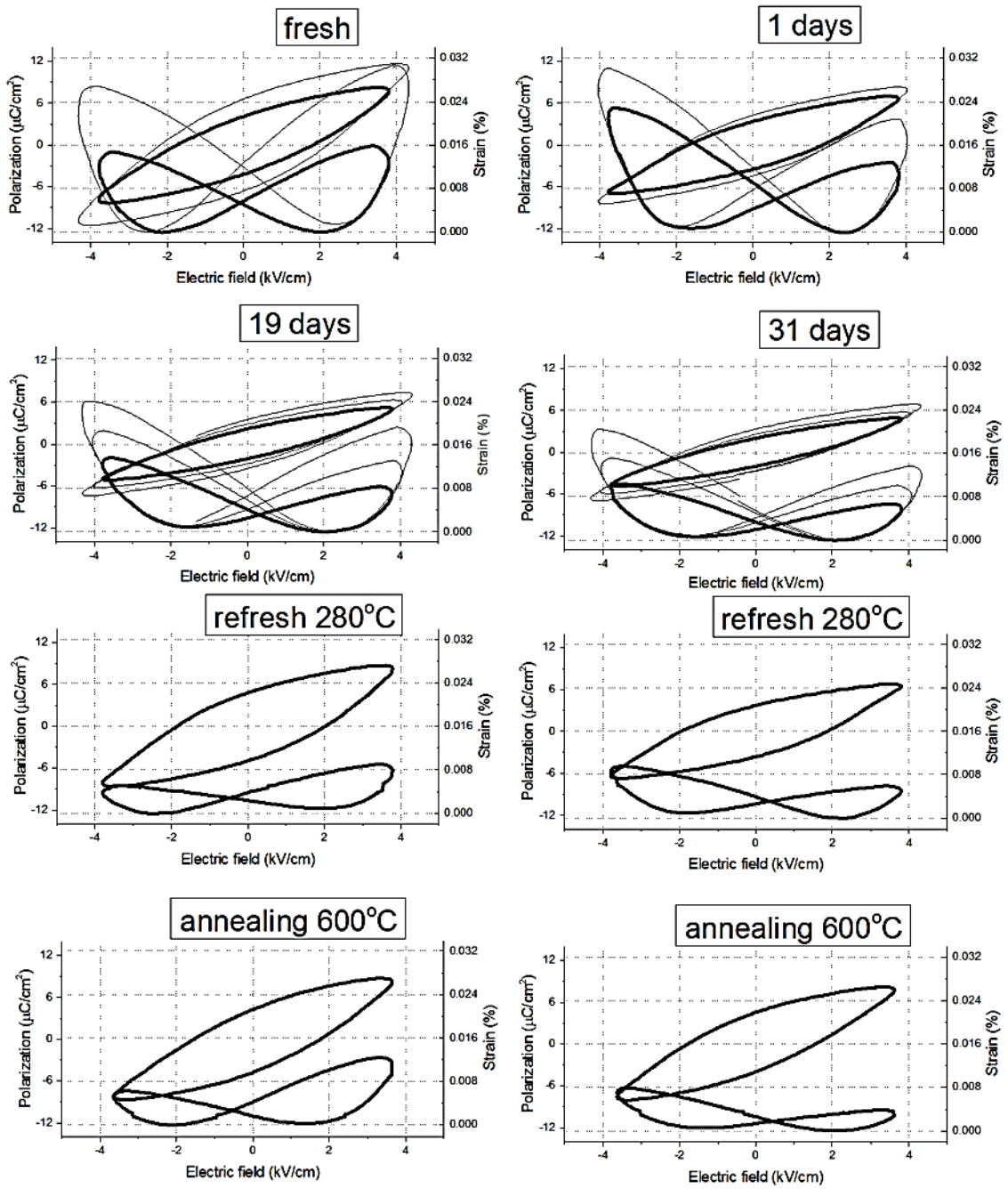


Figure 4.29 The induced-strain and polarization of PLZT (9/65/35) sintered at 1200°C

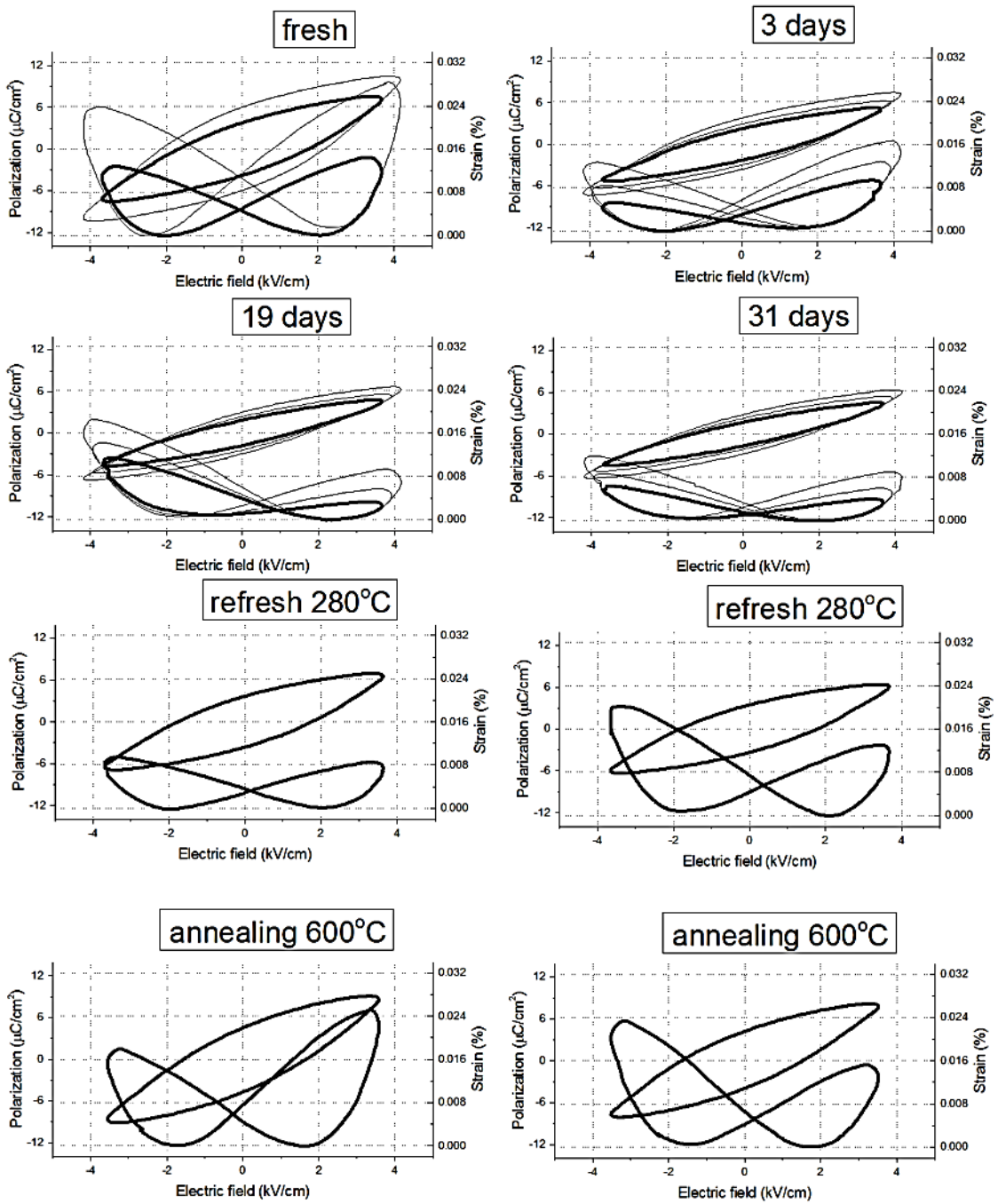


Figure 4.30 The induced-strain and polarization of PLZT (9/65/35) sintered at 1225°C

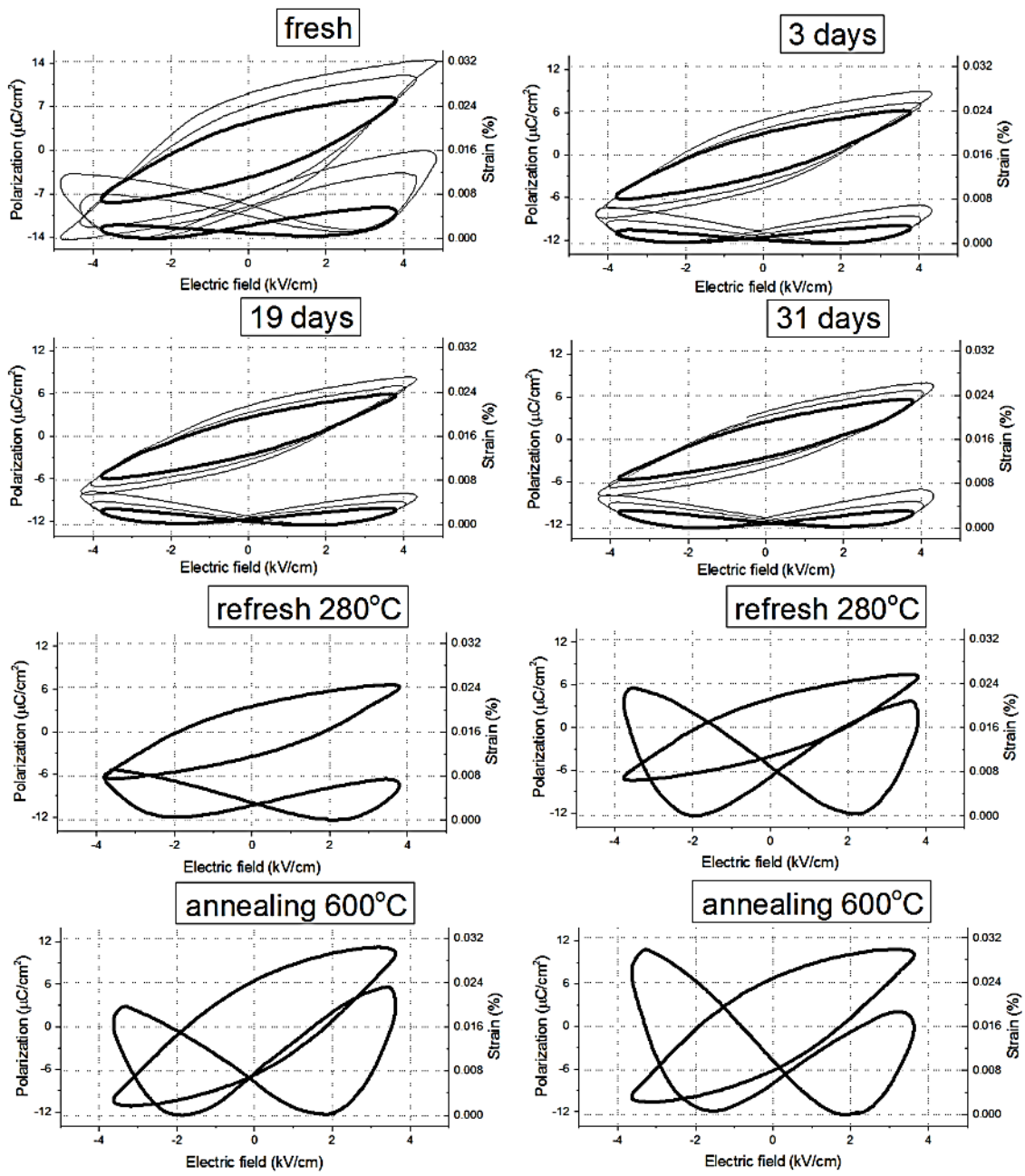


Figure 4.31 The induced-strain and polarization of PLZT (9/65/35) sintered at 1250°C

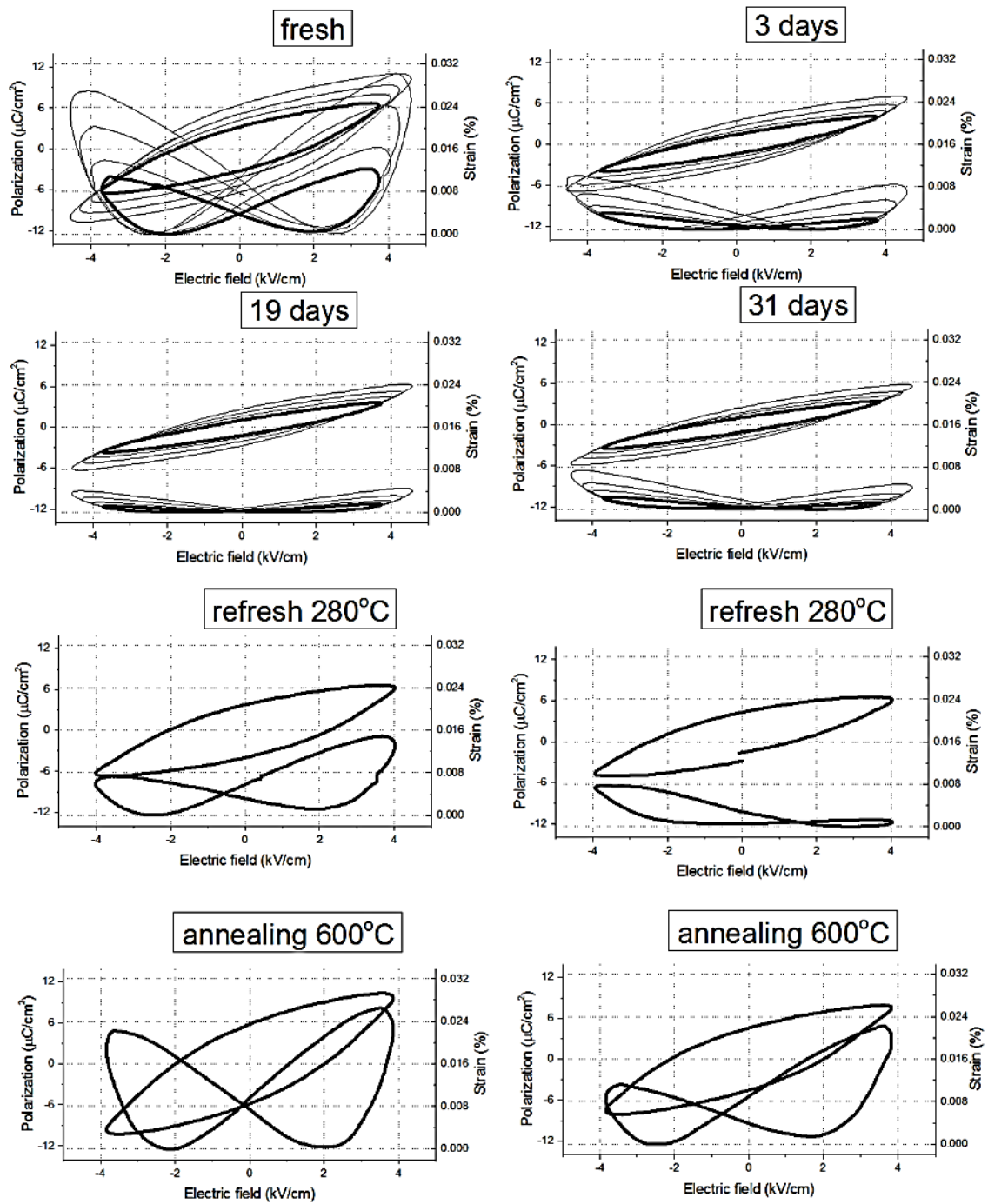


Figure 4.32 The induced-strain and polarization of PLZT (9/65/35) sintered at 1275°C

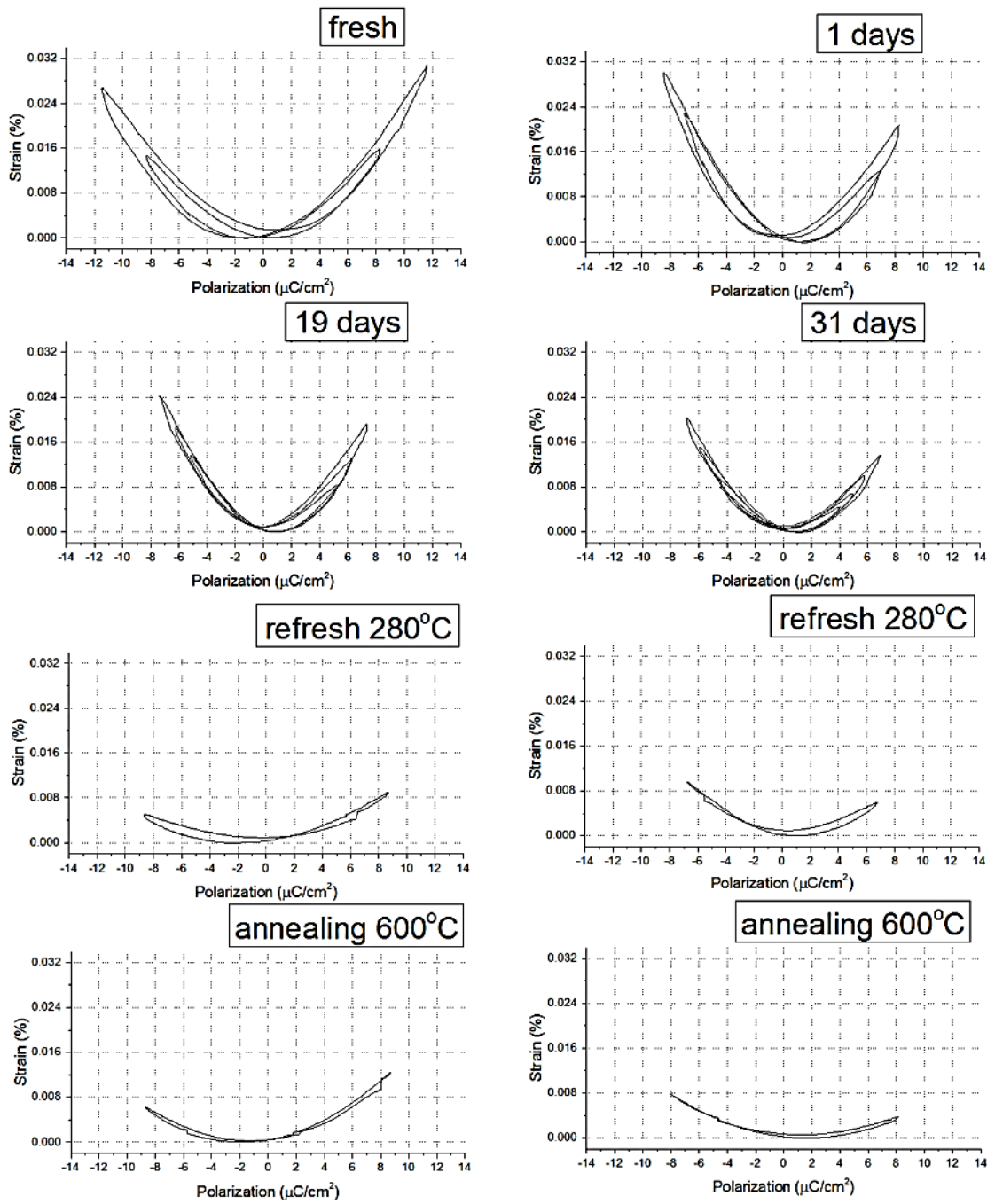


Figure 4.33 The induced-strain as a function of polarization of PLZT (9/65/35) sintered at  $1200^\circ\text{C}$

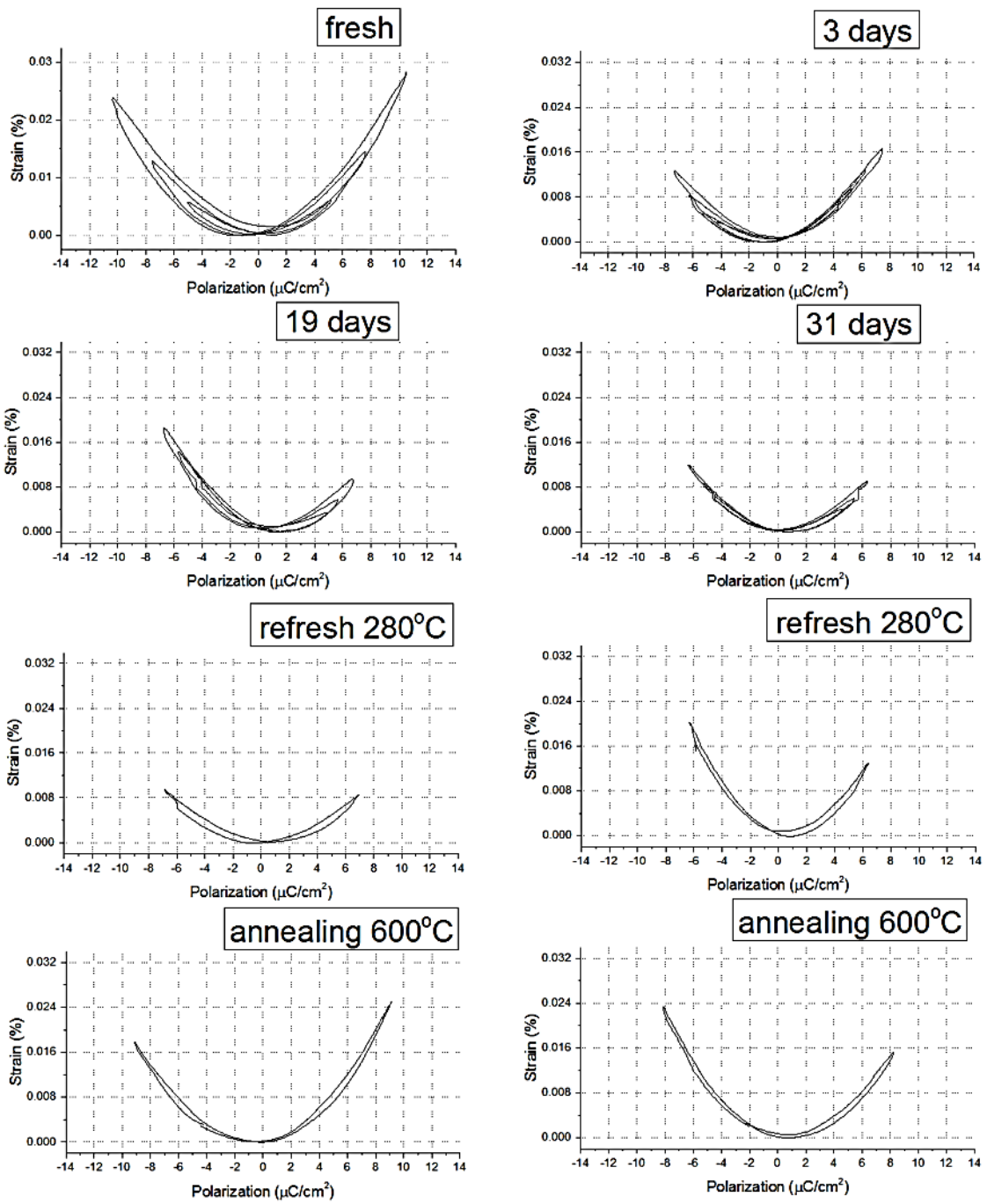


Figure 4.34 The induced-strain as a function of polarization of PLZT (9/65/35) sintered at  $1225^\circ\text{C}$

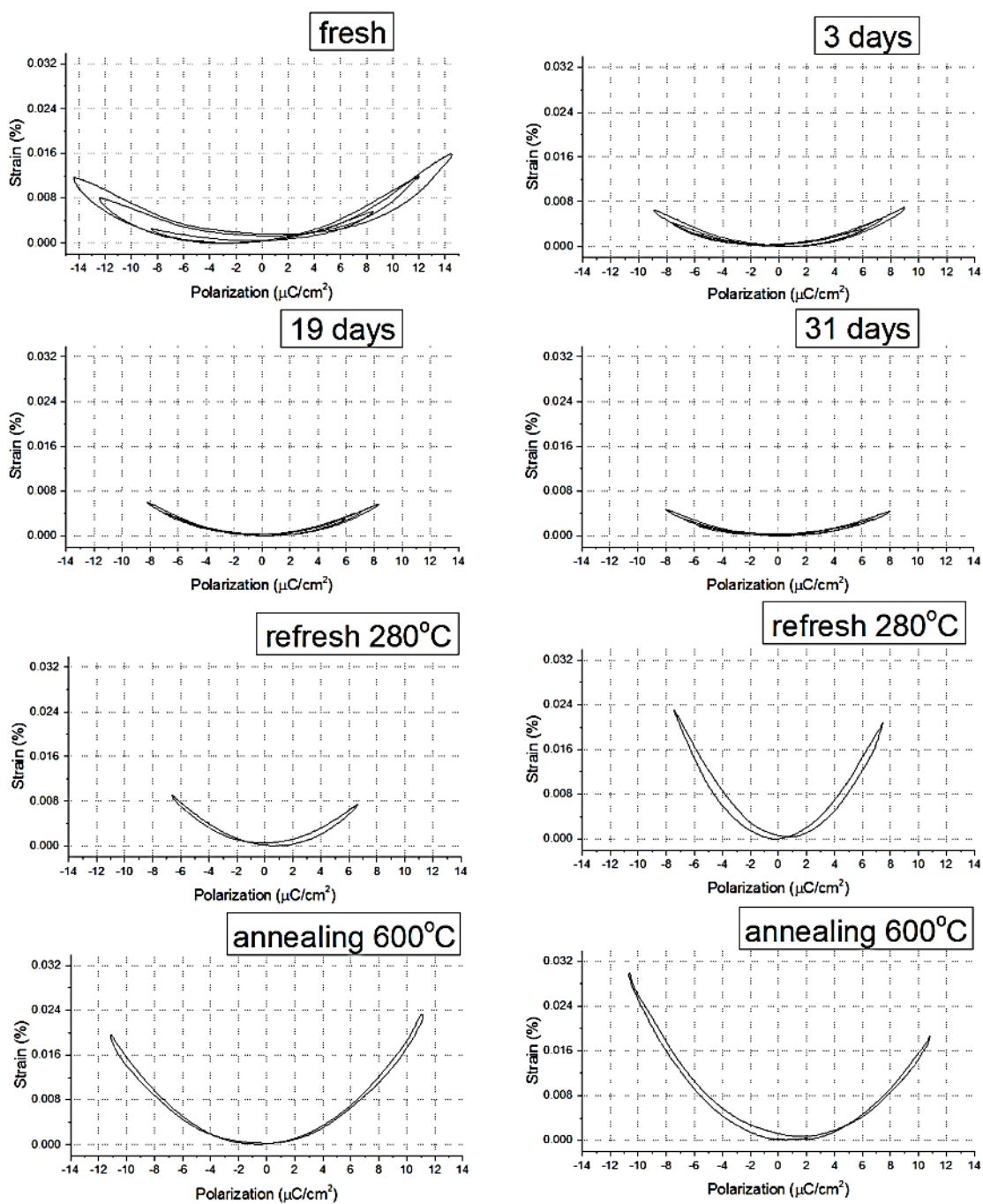


Figure 4.35 The induced-strain as a function of polarization of PLZT (9/65/35) sintered at  $1250^\circ\text{C}$

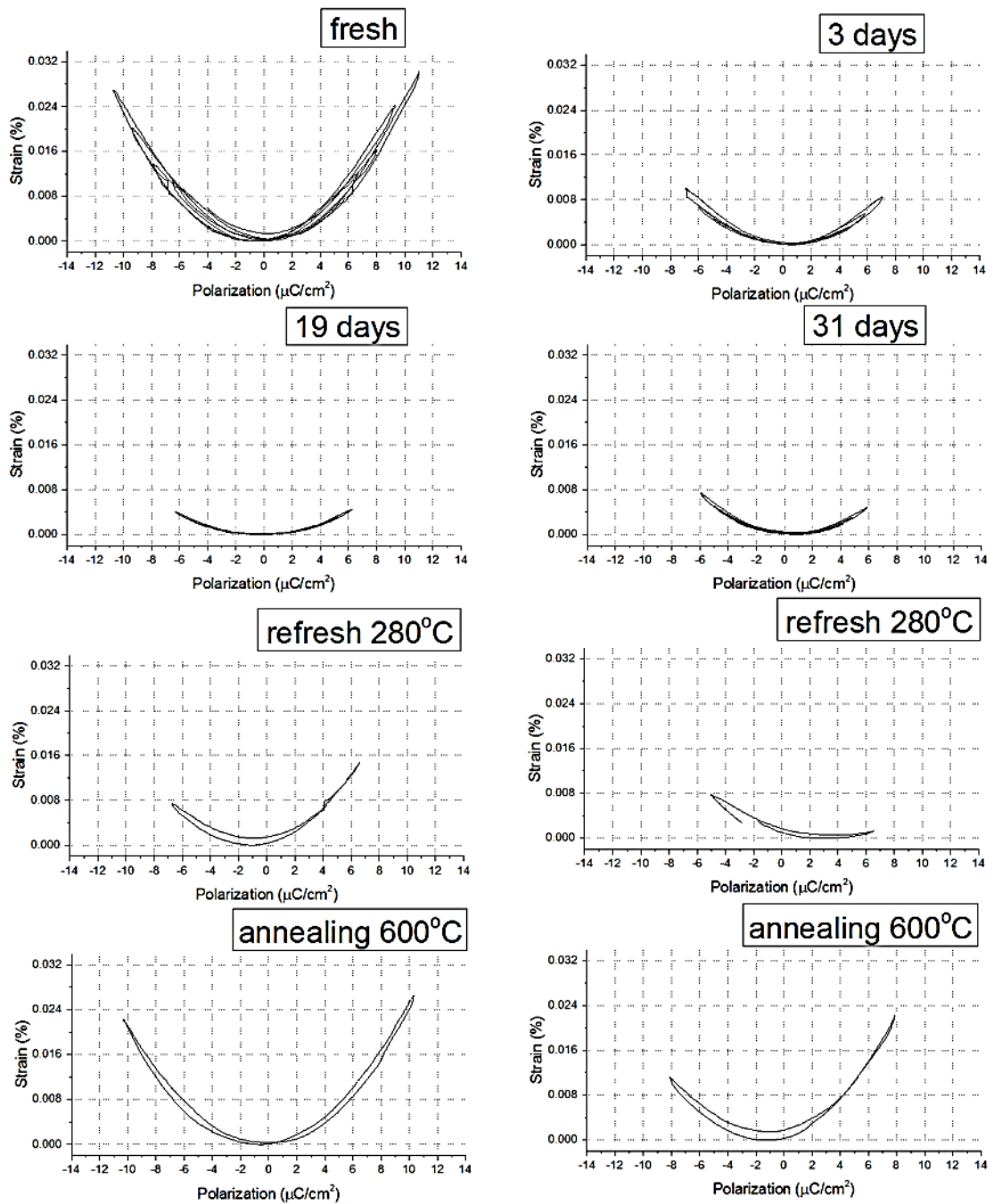


Figure 4.36 The induced-strain as a function of polarization of PLZT (9/65/35) sintered at  $1275^\circ\text{C}$

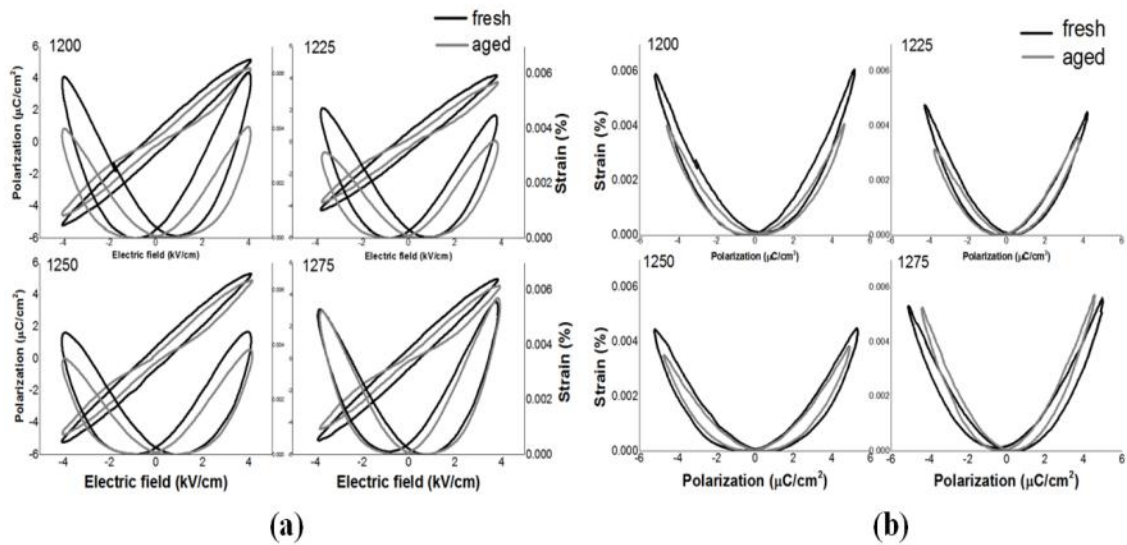


Figure 4.37 The induced-strain and polarization of PLZT (9/70/30) [52]

Figure 4.37 shows the fresh (black line) and 19 days aged (gray line) of induced strain and polarization as a function of applied electric field, and induced strain as a function of polarization of PLZT (9/70/30) samples which were sintered at 1200, 1225, 1250 and 1275°C. In Figure 4.37(a), the remnant polarization and induced strain at zero electric field of fresh samples was disappeared when samples were left to be aged for 19 days, the slim loop hysteresis polarization shape changes to pinched loop hysteresis together with the decrease of maximum polarization in all samples referring to depolarizing field, the orientation of defect dipole to opposite spontaneous polarization inside material to minimize electrostatic energy like domain split into two opposite direction of 180° domain in antiferroelectric materials in the rhombohedral phase of high Zr of PLZT [45-47,55]. The maximum induced strain of PLZT (9/70/30) samples which were sintered at 1200, 1225 and 1250 °C was decreased when samples were aged, the greater decrease can be seen at lower sintering temperature. But it was not affected to PLZT (9/70/30) sample which was sintered at higher temperature 1275°C which caused dense ceramic sample due to fewer pores in microstructure. In Figure 4.37(b), the induced strain was plotted as a function of polarization and demonstrated quadratic relation shape curve, which implies the polarization dependence of induced strain with some hysteresis shape of 180° domain reversal [1].

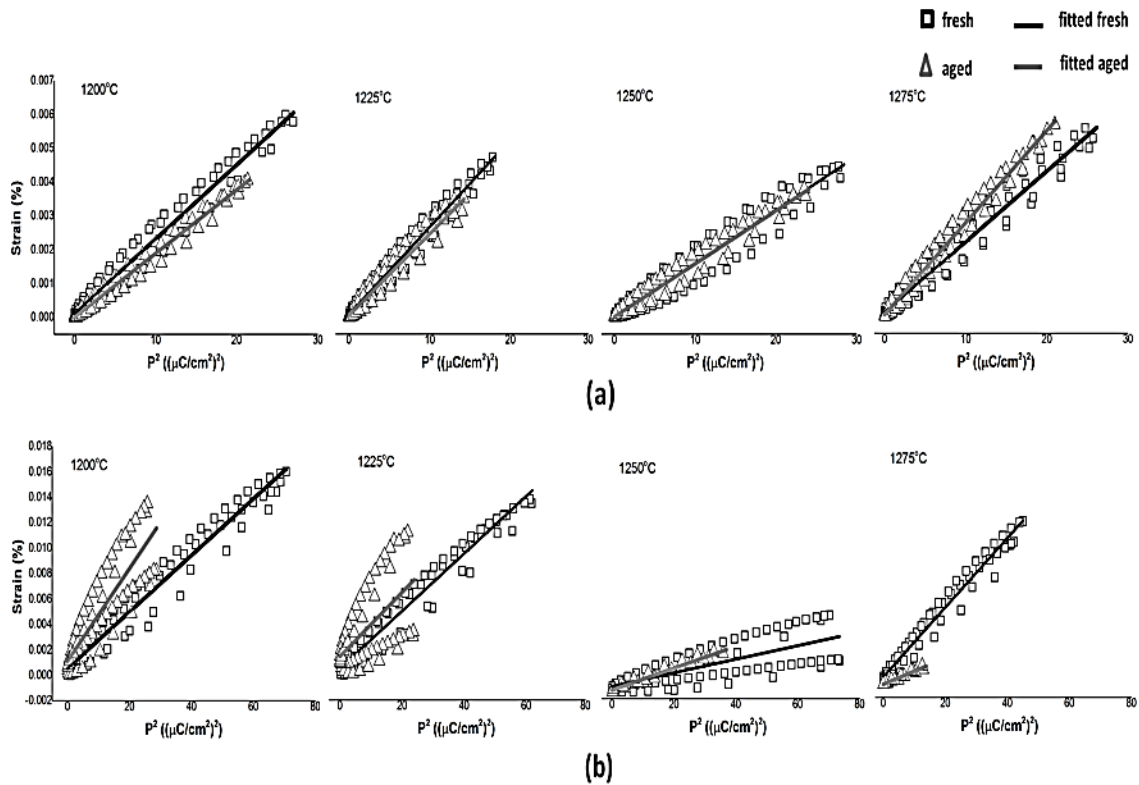


Figure 4.38 The induced strain as function of quadratic polarization ( $s-P^2$ ) of (a) PLZT (9/70/30) and (b) PLZT (9/65/35) [52]

Figure 4.38 shows the graph of induced strain as a function of quadratic polarization ( $s-P^2$ ) to analyze the electrostrictive coefficient  $Q$  (fitted line). In Figure 4.38(a), the fresh samples show higher the electrostrictive coefficient  $Q$  than aging sample at lower sintering temperature but show lower the electrostrictive coefficient  $Q$  when sintering temperature was increased to 1275°C, due to a decrease of polarization in all samples, the internal field biased by vacancies [46-50], more than the decrease of induced strain which fresh induced strain was still close to aging induced strain at 1275°C.

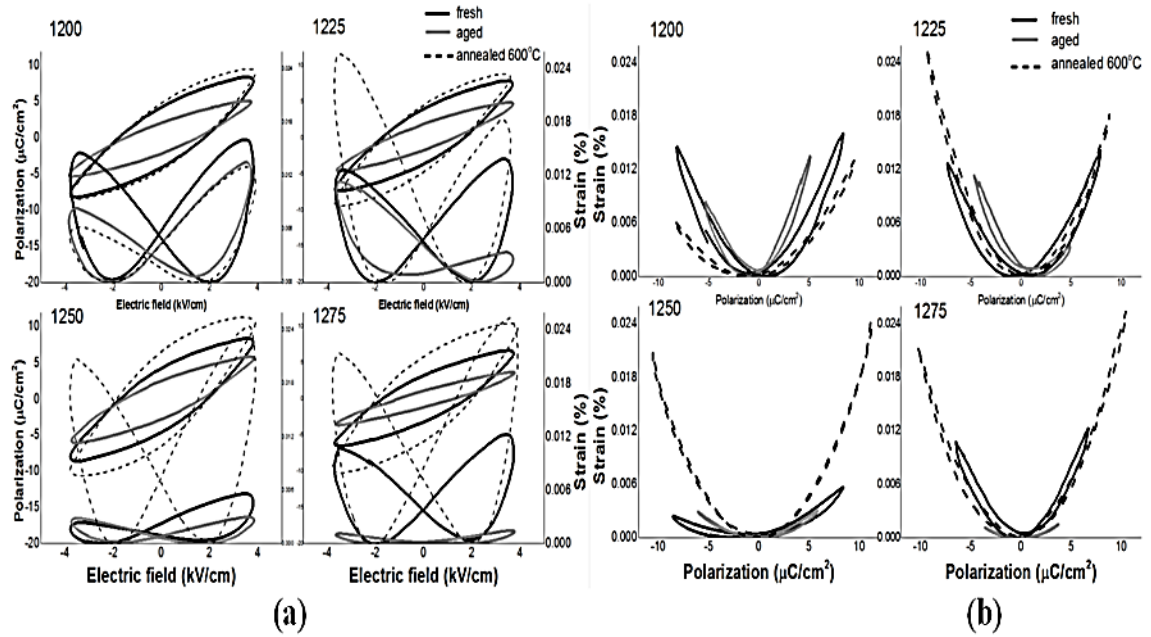


Figure 4.39 The induced-strain and polarization of PLZT (9/65/35) [52]

Figure 4.39 shows the fresh (black line), 19 days aged (gray line) and 600°C annealed (dash line) of induced strain and polarization as a function of applied electric field, and induced strain as a function of polarization of PLZT (9/65/35) samples which were sintered at 1200, 1225, 1250 and 1275°C. In Figure 4.39(a), the higher value of maximum and remnant in polarization and induced strain of fresh PLZT (9/65/35) was attributed to the coexistence of tetragonal and rhombohedral phases [53,54] which caused lattice distortion and high mobility of domains [56,57], and those values were decreased when PLZT (9/65/35) samples were left to aged 19 days due to the rearrangement of spontaneous polarization and crystal structure inside to reduce the potential energy in aging phenomena [45-51]. The induced strain of aged samples shows asymmetric butterfly shape at lower sintering temperature but less affected to high sintering samples at 1275°C due to preferred direction of domain from the residual mechanical stress after first fabrication where the samples were cooled from paraelectric phase to ferroelectric phase to minimize the elastic energy in the long  $c_T$ -axis of the tetragonal phase of PLZT (9/65/35) developed perpendicular to the stress (90° domain) [45]. A higher asymmetry at lower sintering temperature was due to less dense materials. After 600°C annealing, the PLZT (9/65/35) sample seems to be relaxed where the polarization and induced strain show higher values than fresh and aged samples

especially at high sintering temperature at 1250 and 1275°C. Dense materials due to elastic stress had to be released. In Figure 4.39(b), the induced strain was plotted as a function of polarization and demonstrated quadratic relation shape curve, implying the polarization dependence of induced strain, which the annealing process caused the induced strain to be in relaxation behavior and showed 90° domain orientation [1] especially at 1250 and 1275°C of sintering temperature. High elastic energy of aging phenomena as shown in Figure 4.23(b), the elastic energy was released.

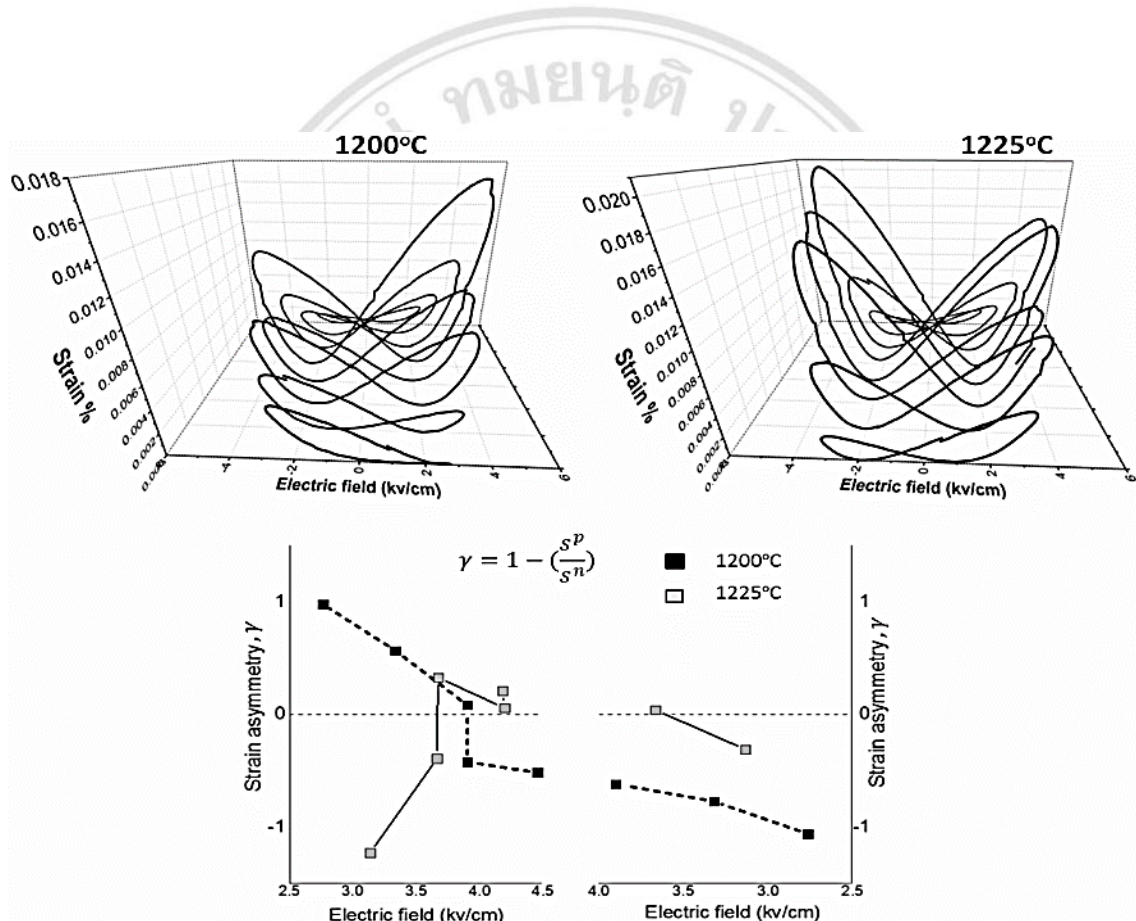


Figure 4.40 The strain asymmetry of PLZT (9/70/30) [52]

Figure 4.40 shows asymmetric behavior of induced strain of PLZT (9/70/30) which was fabricated by lower sintering temperature at 1200 and 1225°C, less dense materials. First, the samples was induced by unipolar electric field in the opposite direction of preferred induced strain direction, then the bipolar electric field was applied to observe the induced strain behavior which demonstrated that the asymmetric induced

strain was changed from unipolar electric field direction to preferred induced strain direction when the applied electric field was increased. For higher enough bipolar electric field the asymmetric induced strain direction was changed to prefer direction as 1200°C PLZT sample the strain changed asymmetrically from 1 to -1, but do not affect to 1225°C PLZT sample which needed higher electric field to change the asymmetric induced strain direction, as strain asymmetric was shown in Figure 4.40.

Table 4.1 The electrostrictive coefficient  $Q$  of PLZT (9/70/30) and PLZT (9/65/35), coercive fields  $E_c$  (kV/cm), remnant polarizations  $P_r$  ( $\mu\text{C}/\text{cm}^2$ ) and strains  $s_r$  (%) of PLZT at different sintering temperatures [52]

Sintering Temp (°C)	PLZT (9/70/30)						PLZT (9/65/35)								
	fresh			aged			fresh			aged			annealed		
	$E_c$	$P_r$	$s_r$	$E_c$	$P_r$	$s_r$	$E_c$	$P_r$	$s_r$	$E_c$	$P_r$	$s_r$	$E_c$	$P_r$	$s_r$
1200	0.53	0.70	0.00036	0.22	0.24	0.00007	1.78	4.17	0.0054	1.49	2.15	0.0034	1.75	4.65	0.0029
1225	0.52	0.63	0.00028	0.27	0.26	0.00008	1.72	3.81	0.0047	1.33	1.83	0.0026	1.64	4.61	0.0061
1250	0.52	0.69	0.00025	0.19	0.25	0.00007	1.80	4.39	0.0016	1.59	2.65	0.0008	1.89	6.51	0.0071
1275	0.45	0.62	0.00030	0.18	0.16	0.00008	1.74	3.22	0.0038	1.16	1.14	0.0001	2.00	5.86	0.0072

Table 4.1 shows coercive fields  $E_c$  (kV/cm), remnant polarizations  $P_r$  ( $\mu\text{C}/\text{cm}^2$ ) and strains  $s_r$  (%) of PLZT (9/70/30) and PLZT (9/65/35) at different sintering temperature, which was decreased when samples were left to 19 days aging.

Copyright© by Chiang Mai University  
All rights reserved

Table 4.2. The electrostrictive coefficient  $Q$  ( $(\text{cm}^2/\mu\text{C})^2$ ) for ceramics sintered at different temperatures [52]

Sintering Temp (°C)	PLZT (9/70/30)		PLZT (9/65/35)	
	fresh	aged	fresh	aged
1200	0.000220	0.000189	0.000222	0.000364
1225	0.000258	0.000242	0.000227	0.000253
1250	0.000158	0.000157	0.000050	0.000080
1275	0.000209	0.000273	0.000261	0.000097

Table 4.2 shows the electrostrictive coefficient  $Q$  (fitted from Figure 4.35), PLZT (9/70/30) samples demonstrated higher aging at lower sintering temperature samples but less affected to high sintering temperature, dense materials, due to reduce electrical energy was dominated. For PLZT (9/65/35) samples demonstrated higher asymmetry at lower sintering temperature and demonstrated higher effect at high sintering temperature samples, due to elastically energy was dominated, which annealing process was highly effected to release elastic stress.

### 4.1.3 Temperature dependence in induced-strain PLZT, PMN-PZT and PMN-PT

Temperature dependence of piezoelectric/electrostriction properties is the important character where the shape and size of ferroelectric materials change in response to temperature when piezoelectric/ electrostriction materials are selected in the commercial electronic equipment such as electroceramic, electrooptic and sensor/actuator applications. To observe temperature dependence behavior of ferroelectric samples, the attractive actuator ferroelectric ceramic material, the relaxor ferroelectric materials which the morphotropic phase boundary or the phase transition temperature was closed to room temperature,  $\text{Pb}_{0.91}\text{La}_{0.09}\text{Zr}_{0.65}\text{Ti}_{0.35}\text{O}_3$  PLZT (9/65/35),  $x\text{Pb}(\text{Mg}_{1/3}\text{Nb}_{2/3})\text{O}_3-(1-x)\text{Pb}(\text{Zr}_{0.52}\text{Ti}_{0.48})\text{O}_3$  or  $x\text{PMN}-(1-x)\text{PZT}$  samples where  $x = 0.9, 0.7$  and  $0.5$ , and  $x\text{Pb}(\text{Mg}_{1/3}\text{Nb}_{2/3})\text{O}_3-(1-x)\text{PbTiO}_3$  or  $x\text{PMN}-(1-x)\text{PT}$  samples where  $x = 0.9, 0.8$  and  $0.7$  were chosen and fabricated by solid mixing oxide method. To investigate the electric field induced strain and polarization behavior, modified Michelson interferometer technique was used at various temperatures from room temperature ( $30^\circ\text{C}$ ) to  $70^\circ\text{C}$ .

Figure 4.41 shows the temperature distribution profile of PLZT (9/65/35) sample when the sample temperature were changed in the range of  $30^\circ\text{C}$  to  $70^\circ\text{C}$  by heat transfer from ceramic heater. The temperature distribution profile was detected by infrared detector (FLIR) with  $\pm 2^\circ\text{C}$  temperature range resolution which detected deep distance position of sample inside sample holder. The area inside the rectangle, similar size to the sample side part, was used to average the sample temperature at  $28.4^\circ\text{C}, 37.4^\circ\text{C}, 48.9^\circ\text{C}, 60.1^\circ\text{C}$  and  $71.2^\circ\text{C}$ , corresponding to temperature measurement by the integral circuit temperature detector (AD592 CN; the temperature range  $0-120^\circ\text{C}$ ). This method is more accurate because the IC sensor was placed close to sample to observe the real time sample temperature, which showed  $30^\circ\text{C}, 40^\circ\text{C}, 50^\circ\text{C}, 60^\circ\text{C}$  and  $70^\circ\text{C}$ , respectively [58].

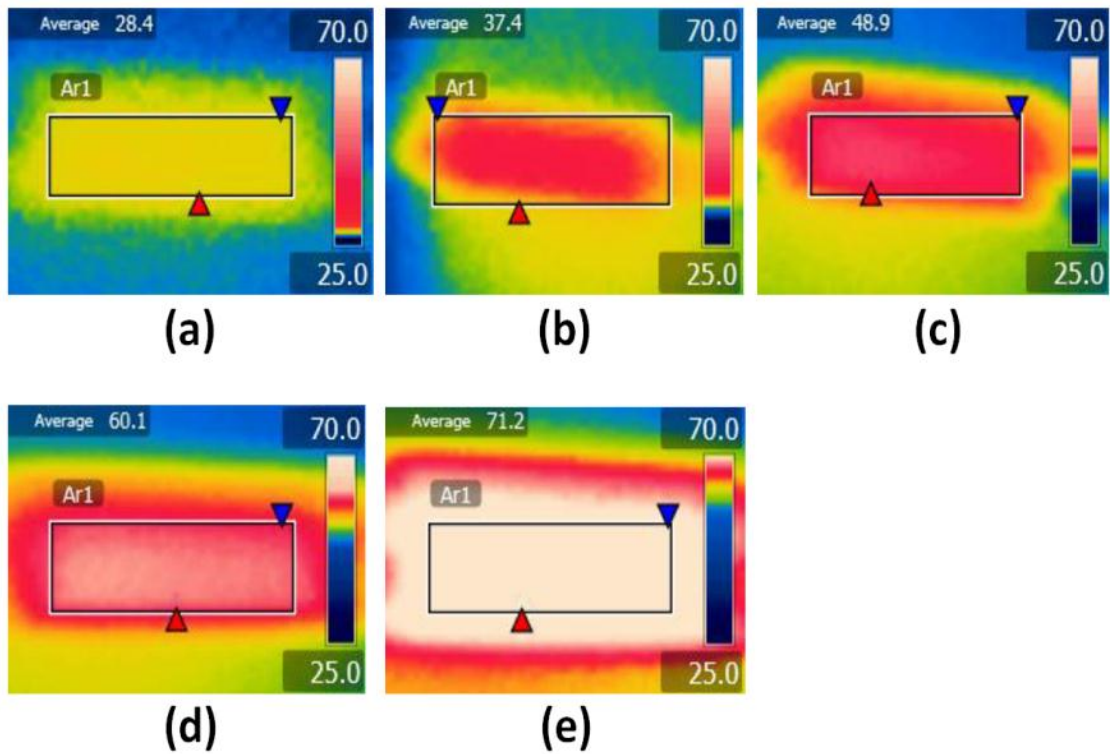


Figure 4.41 The sample temperature profile of PLZT (9/65/35) at (a) 28.4°C (b) 37.4°C (c) 48.9°C (d) 60.1°C and (e) 70°C [58]

Figure 4.42 shows dielectric constant and dielectric loss as a function of temperature of PLZT (9/65/35) sample, it can be seen that dielectric property of PLZT (9/65/35) sample was ferroelectric phase at room temperature which the maximum peak of dielectric constant  $T_m$ , phase transition temperature, was around at 90°C, and shows relaxor ferroelectric properties where the board maximum dielectric constant decreased and shifted to higher temperature when frequency was increased. And the dielectric loss demonstrated increases of maximum values at 50–60°C when higher frequency was applied. The higher hysteresis spontaneous polarization inside ferroelectric materials [44,58,59] was due to phase transition temperature from normal ferroelectric to relaxor ferroelectric closed to cubic paraelectric phase [60].

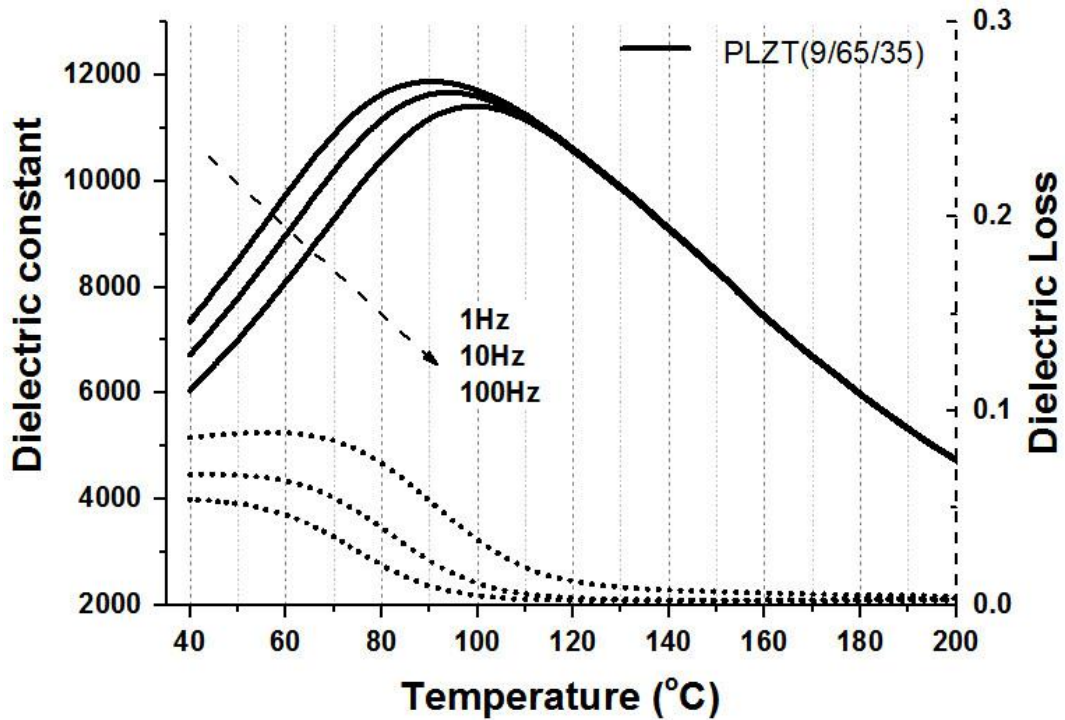


Figure 4.42 The dielectric constant and dielectric loss as a function of temperature of PLZT (9/65/35) [58]

Figure 4.43 shows electric field induced-strain and polarization at various temperatures of PLZT (9/65/35) sample. The sample shows hysteresis loop of polarization and butterfly shape curve of induced strain as a function of applied electric field, indicating spontaneous polarization inside in normal ferroelectric phase at 30°C. Then the induced strain and polarization was increased to a maximum value according to phase transition from normal to relaxor ferroelectric phase at 40°C, which asymmetric induced strain was observed due to different dominated domain and preferred direction of aging process [52]. After that the maximum induced strain and polarization was decreased and it showed slimmer loop polarization and quadratic induced strain as a function of electric field when the sample temperature was increased due to less spontaneous polarization and the phase transition from relaxor ferroelectric phase to cubic paraelectric phase at 50°C to 70°C, which is the same as dielectric constant and dielectric loss properties as shown in Figure 4.42. And the symmetric of induced strain according to the switching of microdomain in relaxor ferroelectric phase changed to cubic phase with non spontaneous polarization [58,61].

Figure 4.44 shows induced-strain as a function of polarization at various temperatures of PLZT (9/65/35) sample. The samples show polarization dependence of induced strain which the quadratic relation curve was shown for all sample temperatures from 30°C to 70°C. It also shows high hysteresis induced strain as a function of polarization referring to mixture of 90° and 180° dominated domain at 30°C to 40°C. Then the sample shows less hysteresis of induced strain when sample temperature increases to relaxor ferroelectric and paraelectric phase due to 90° rotation dominated domain and less spontaneous polarization, respectively [1,52].

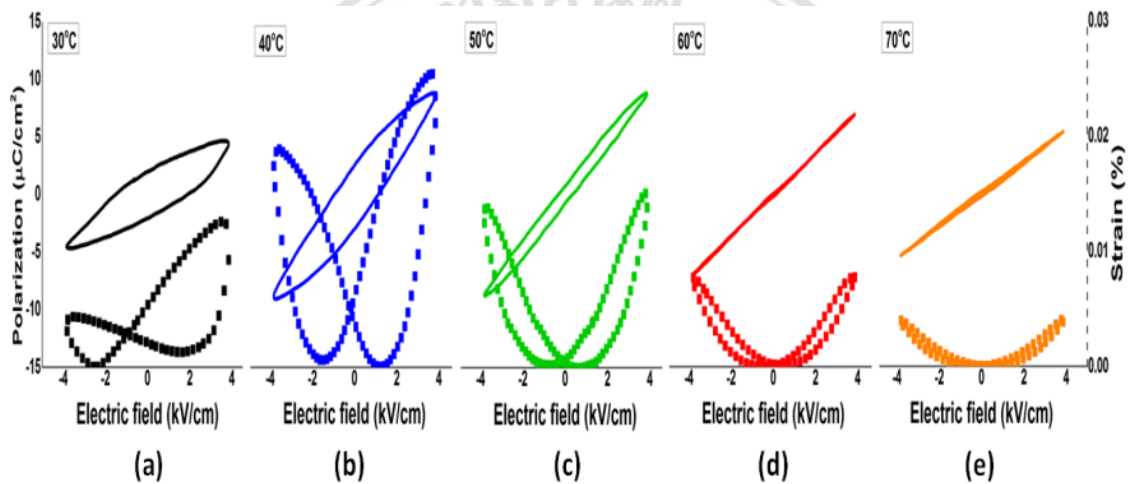


Figure 4.43 The electric field induced strain and polarization of PLZT (9/65/35) at various temperatures [58]

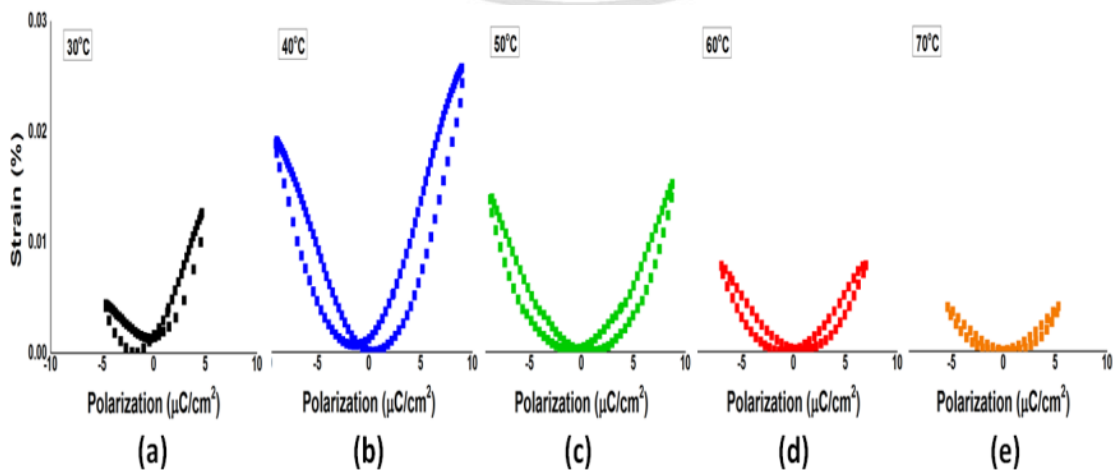


Figure 4.44 The induced strain as a function of polarization of PLZT(9/65/35) at various temperatures [58]

Figure 4.45 shows dielectric constant and dielectric loss as a function of temperature of  $x$ PMN– $(1-x)$ PZT samples where  $x = 0.9, 0.7$  and  $0.5$ . It can be seen that dielectric property of 0.9PMN–0.1PZT sample was paraelectric phase at room temperature where the maximum peak of dielectric constant  $T_m$ , phase transition temperature, was lower than room temperature. For 0.7PMN–0.3PZT and 0.5PMN–0.5PZT samples, the dielectric constant shows relaxor ferroelectric properties which the board maximum dielectric constant was decreased and changed to higher temperature when frequency was increased, which confirms the Curie-Weiss law of relaxor ferroelectric materials, and the maximum dielectric constant was around 60°C and 90°C, respectively. The dielectric loss of 0.7PMN–0.3PZT and 0.5PMN–0.5PZT samples had higher values when higher frequency measurement due to the higher hysteresis spontaneous polarization inside ferroelectric materials, and the maximum dielectric loss was around 40°C and 70°C, respectively [42,43,59].

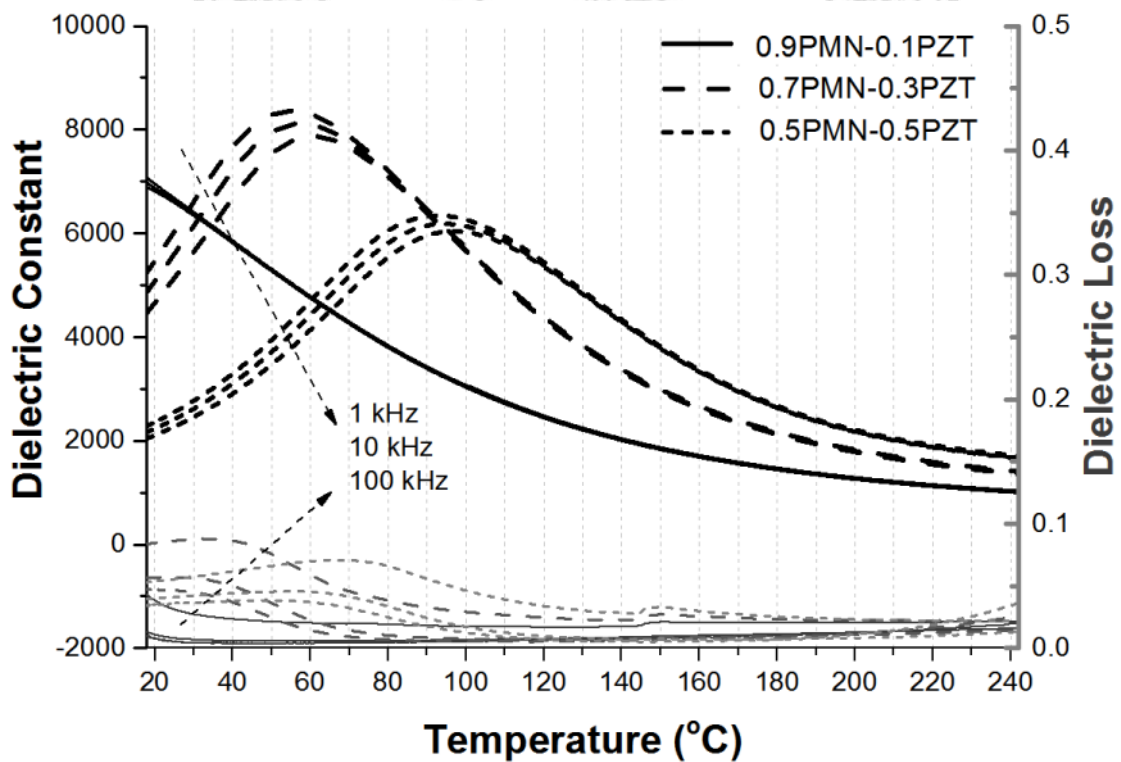


Figure 4.45 The dielectric constant and dielectric loss as a function of temperature of  $x$ PMN– $(1-x)$ PZT samples where  $x = 0.9, 0.7$  and  $0.5$

Figures 4.46, 4.47 and 4.48 show electric field induced-strain and polarization at various temperatures of  $x$ PMN– $(1-x)$ PZT samples where  $x = 0.9, 0.7$  and  $0.5$ . In Figure 4.46, 0.9PMN–0.1PZT sample shows slim loop of polarization and quadratic shape curve of induced strain as a function of applied electric field, indicating non spontaneous polarization inside in paraelectric phase. The maximum induced strain and polarization was decreased when the sample temperature was increased due to less spontaneous polarization and the phase transition from relaxor ferroelectric phase to cubic paraelectric phase from 30°C to 50°C. In Figure 4.47, 0.7PMN–0.3PZT sample shows hysteresis loop of polarization and butterfly shape curve of induced strain as a function of applied electric field, indicating spontaneous polarization inside in relaxor ferroelectric phase at 30°C. Then the maximum induced strain and polarization was decreased and showed slimmer loop polarization and quadratic induced strain as a function of electric field when the sample temperature was increased due to less spontaneous polarization and the phase transition from relaxor ferroelectric phase to cubic paraelectric phase from 30°C to 50°C, which was the same as dielectric constant and dielectric loss properties as shown in Figure 4.45. In Figure 4.48, 0.5PMN–0.5PZT sample shows hysteresis loop of polarization and butterfly shape curve of induced strain as a function of applied electric field, indicating spontaneous polarization in normal ferroelectric phase at 30°C. Then the induced strain and polarization was increased to a maximum values according to phase transition from normal to relaxor ferroelectric phase at 40°C. After that the maximum induced strain and polarization was decreased and demonstrated slimmer loop polarization and quadratic induced strain as a function of electric field when the sample temperature was increased due to less spontaneous polarization and the phase transition from relaxor ferroelectric phase to cubic paraelectric phase at 50°C to 70°C, same as dielectric constant and dielectric loss properties as shown in Figure 4.45.

Figures 4.49, 4.50 and 4.51 show induced-strain as a function of polarization at various temperatures of  $x$ PMN– $(1-x)$ PZT samples where  $x = 0.9, 0.7$  and  $0.5$  samples. The samples show polarization dependence of induced strain which the quadratic relation curve was observed for all sample temperature from 30°C to 70°C, referring to 90° domain rotation dominated.

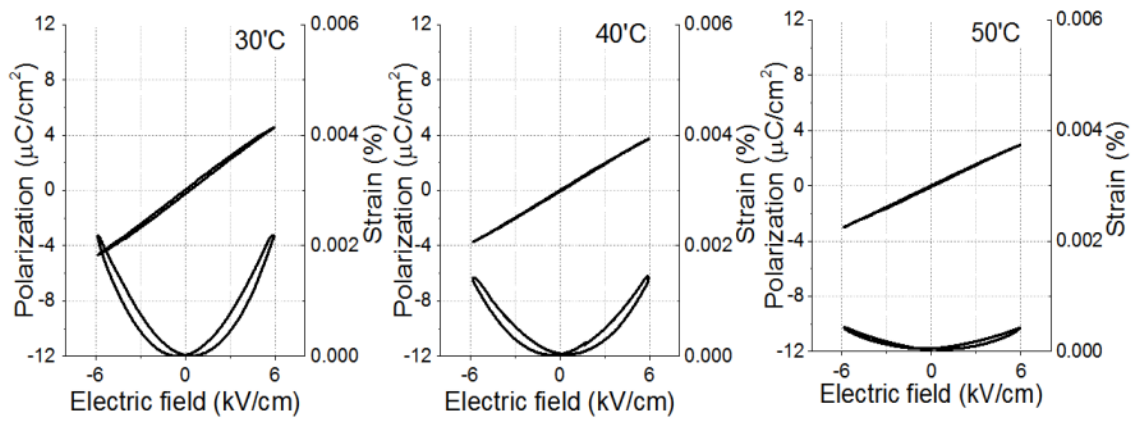


Figure 4.46 The electric field induced strain and polarization of 0.9PMN-0.1PZT at various temperatures

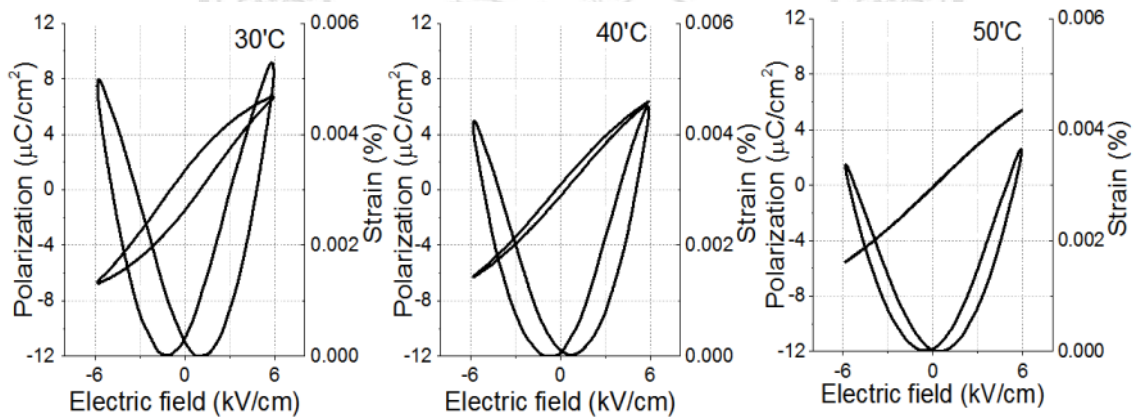


Figure 4.47 The electric field induced strain and polarization of 0.7PMN-0.3PZT at various temperatures

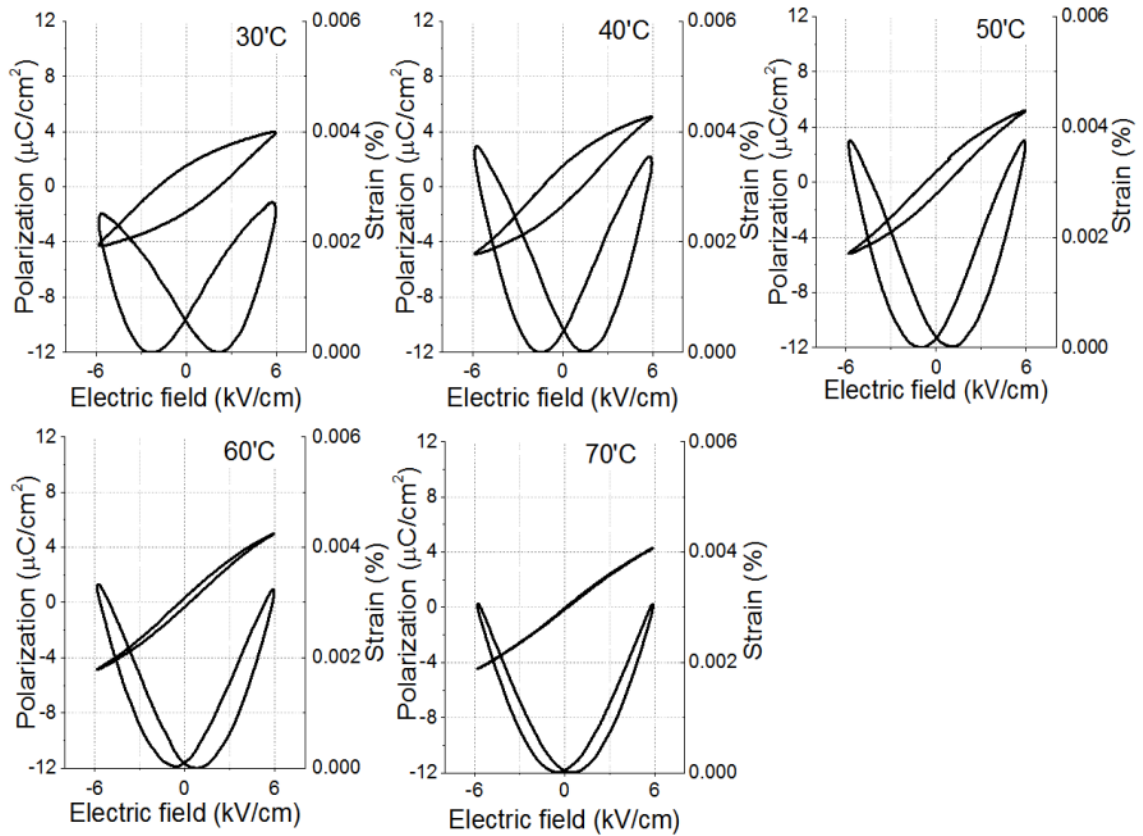


Figure 4.48 The electric field induced strain and polarization of 0.5PMN-0.5PZT at various temperatures

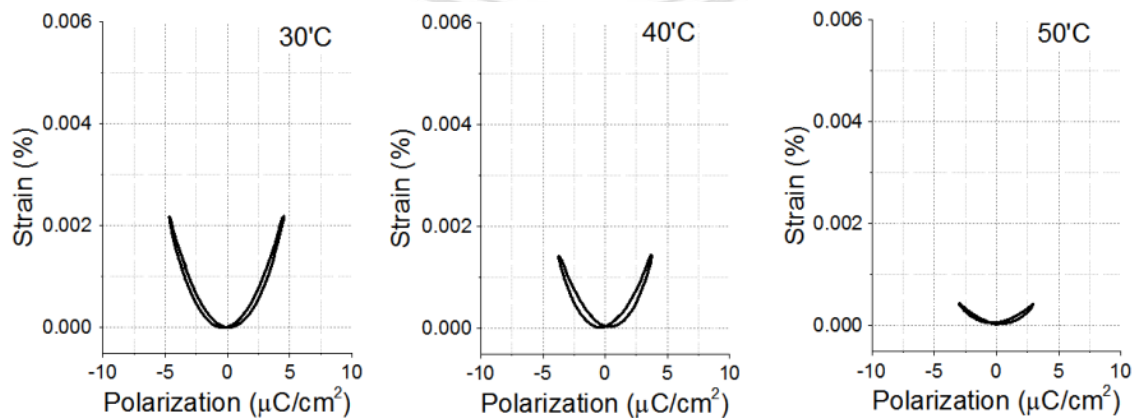


Figure 4.49 The induced strain as a function of polarization of 0.9PMN-0.1PZT at various temperatures

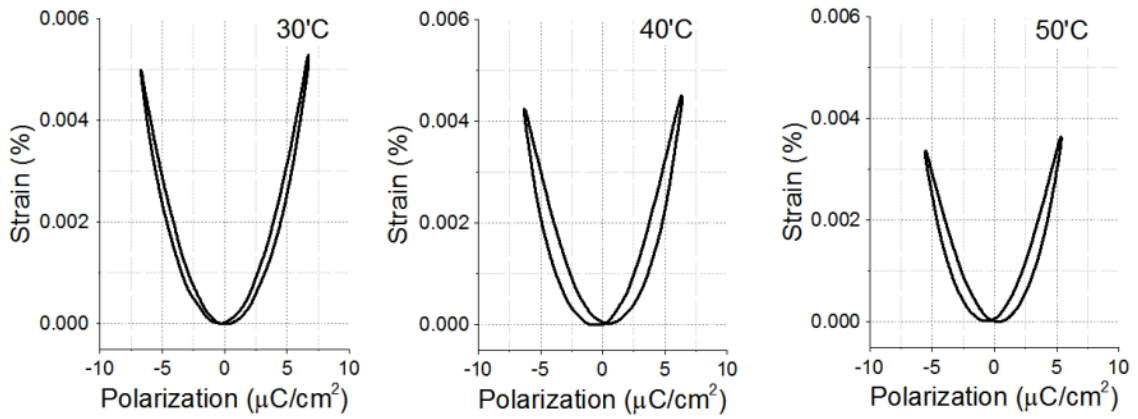


Figure 4.50 The induced strain as a function of polarization of 0.7PMN-0.3PZT at various temperatures

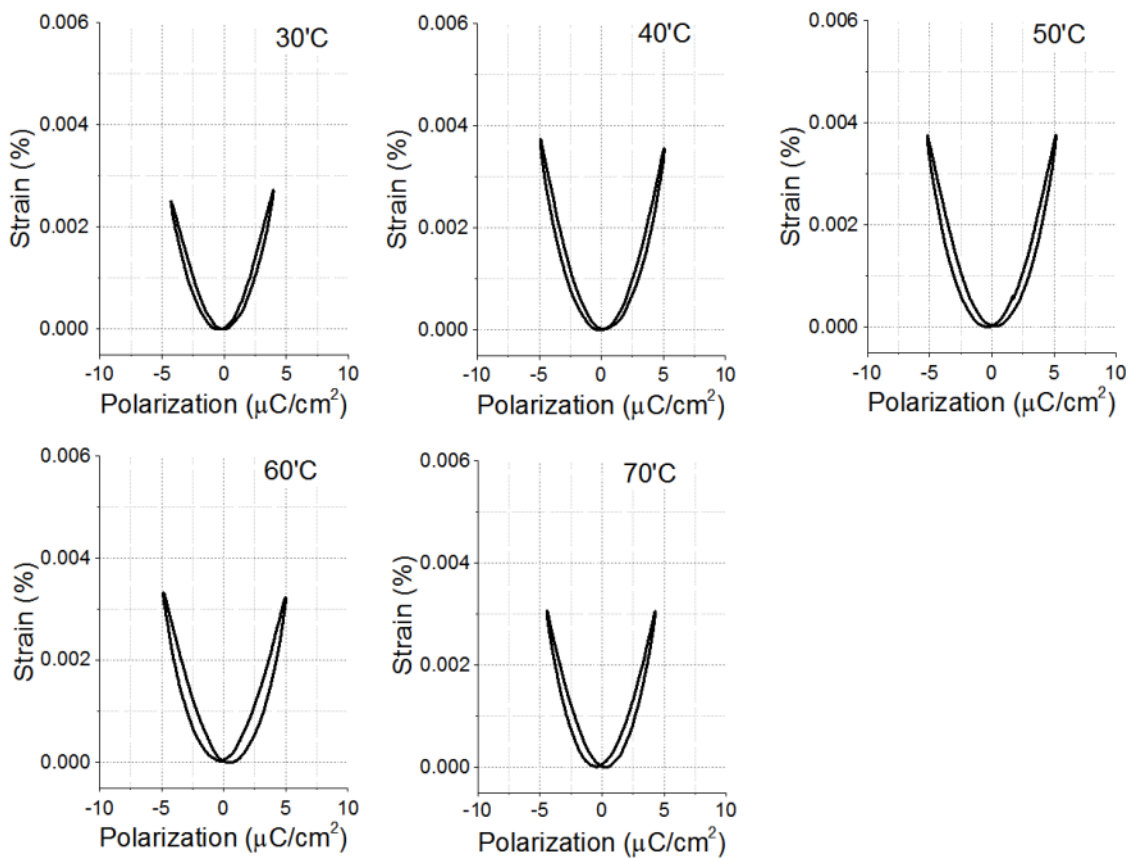


Figure 4.51 The induced strain as a function of polarization of 0.5PMN-0.5PZT at various temperatures

Figure 4.52 shows dielectric constant and dielectric loss as a function of temperature of  $x$ PMN–(1- $x$ )PT samples where  $x = 0.9, 0.8$  and  $0.7$ . It can be seen that dielectric behavior of 0.9PMN–0.1PT (high dielectric constant), 0.8PMN–0.2PT and 0.7PMN–0.3PT samples were relaxor ferroelectric where the maximum peak of dielectric constant  $T_m$ , phase transition temperature, was around 30°C, 90°C and 130°C, respectively [63-65]. MPB of (1- $x$ )PMN- $x$ PT is around  $x = 0.27$  to  $0.34$  [62]. The dielectric constant shows broad maximum dielectric constant peak which was decreased and shifted to higher temperature when frequency was increased, confirming the Curie-Weiss law of relaxor ferroelectric materials. The dielectric loss of 0.9PMN–0.1PT, 0.8PMN–0.2PT and 0.7PMN–0.3PT samples had higher values when higher frequency was applied. It was due to the higher hysteresis spontaneous polarization inside ferroelectric materials. The maximum dielectric loss was around 20°C, 80°C and 120°C respectively [63-65].

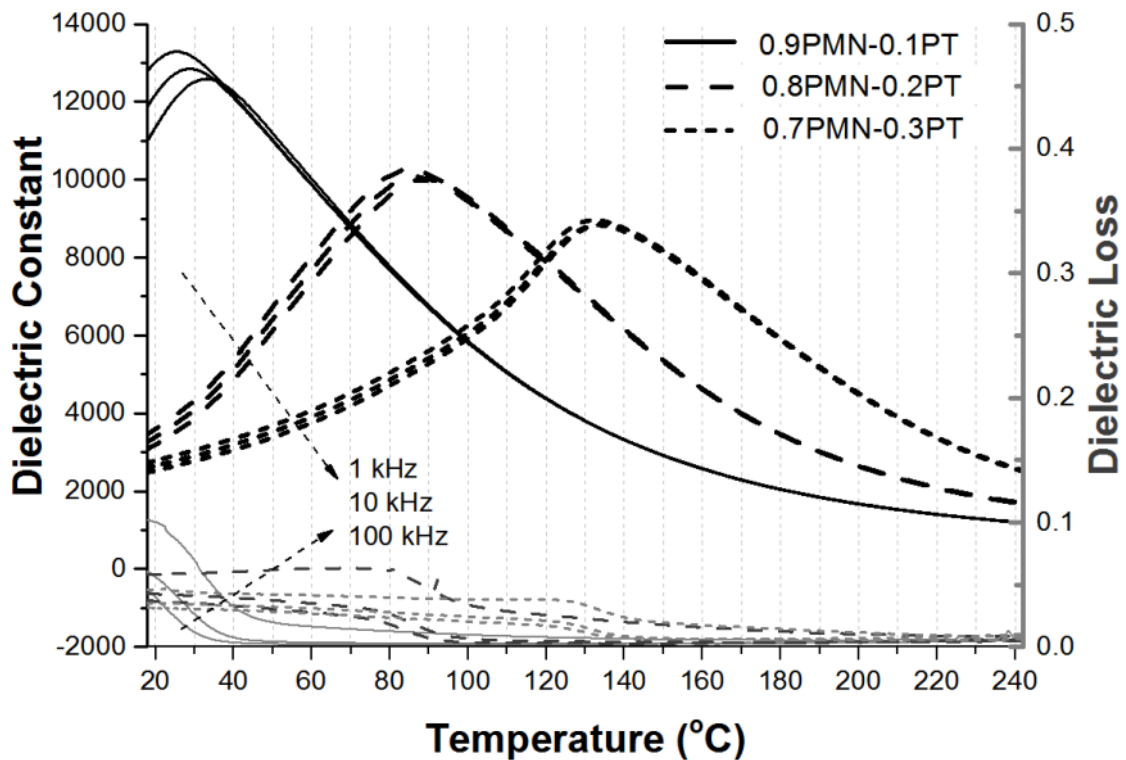


Figure 4.52 The dielectric constant and dielectric loss as a function of temperature  $x$ PMN–(1- $x$ )PT samples where  $x = 0.9, 0.8$  and  $0.7$

Figures 4.53, 4.54 and 4.55 show electric field induced-strain and polarization at various temperatures of  $x$ PMN–(1- $x$ )PT samples where  $x = 0.9, 0.8$  and  $0.7$ . In Figure 4.53, 0.9PMN–0.1PT sample shows hysteresis loop of polarization and butterfly shape curve of induced strain as a function of applied electric field, indicating spontaneous polarization in relaxor ferroelectric phase at 30°C. Then the maximum induced strain and polarization was decreased, and exhibited slimmer loop polarization and asymmetric induced strain as a function of electric field when the sample temperature was increased according to a decrease of high spontaneous polarization at the phase transition temperature of relaxor ferroelectric phase changed to cubic paraelectric phase but still higher spontaneous polarization around 30°C to 50°C. The same result was shown in the decrease of very high dielectric constant and dielectric loss as shown in Figure 4.52. In Figure 4.54, 0.8PMN–0.2PT sample shows hysteresis loop of polarization and butterfly shape curve of induced strain as a function of applied electric field, indicating spontaneous polarization inside like normal ferroelectric phase at 30°C. Then the induced strain and polarization was increased to a maximum value according to phase transition from tetragonal to rhombohedral phase, possibly monoclinic phase formation by another report, at 40°C and 50°C, respectively [63-65]. After that the maximum induced strain and polarization was decreased and exhibited slimmer loop polarization when the sample temperature was increased due to a decrease of spontaneous polarization and the phase transition from rhombohedral ferroelectric phase to relaxor ferroelectric phase, before paraelectric phase, at 50°C to 70°C, which is the same as dielectric constant and dielectric loss properties as shown in Figure 4.52. In Figure 4.55, 0.7PMN–0.3PT sample shows hysteresis loop of polarization and butterfly shape curve of induced strain as a function of applied electric field, indicating spontaneous polarization inside like normal ferroelectric phase at 30°C. Then the induced strain and polarization was increased to a maximum values according to phase transition from tetragonal to rhombohedral phase, possibly monoclinic phase formation by another report, at 60°C and 70°C respectively [63,64,66], before relaxor ferroelectric phase like dielectric constant and dielectric loss properties as shown in Figure 4.52.

Figures 4.56, 4.57 and 4.58 show induced-strain as a function of polarization at various temperatures of  $x$ PMN– $(1-x)$ PT samples where  $x = 0.9, 0.8$  and  $0.7$ . In Figure 4.56, 0.9PMN–0.1PT sample shows some hysteresis and asymmetric of quadratic shape curve of induced strain as a function of polarization for all sample temperatures, according to the mixture of  $90^\circ$  rotation and  $180^\circ$  reversal domain dominated in high spontaneous polarization relaxor ferroelectric of PMN with addition of PT. In Figure 4.57, 0.8PMN–0.2PT sample shows some hysteresis of induced strain as a function of polarization for all sample temperatures, according to the mixture of  $90^\circ$  rotation and  $180^\circ$  reversal domain dominated in phase transition from tetragonal to rhombohedral phase around  $40^\circ\text{C}$  and  $50^\circ\text{C}$  of PMN with addition of PT. In Figure 4.58, 0.7PMN–0.3PT sample shows slimmer loop induced strain as a function of polarization for all sample temperatures, according to the lower electric field to induced the switching of spontaneous polarization of  $180^\circ$  reversal domain but only  $90^\circ$  rotation was dominated in tetragonal phase developed to rhombohedral phase at  $30^\circ\text{C}$  to  $70^\circ$  of PMN with addition of PT.

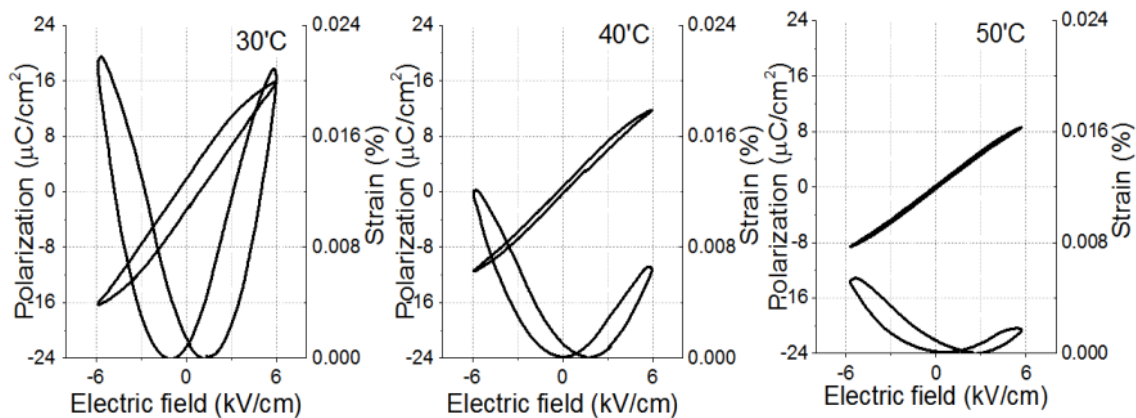


Figure 4.53 The electric field induced strain and polarization of 0.9PMN-0.1PT at various temperatures

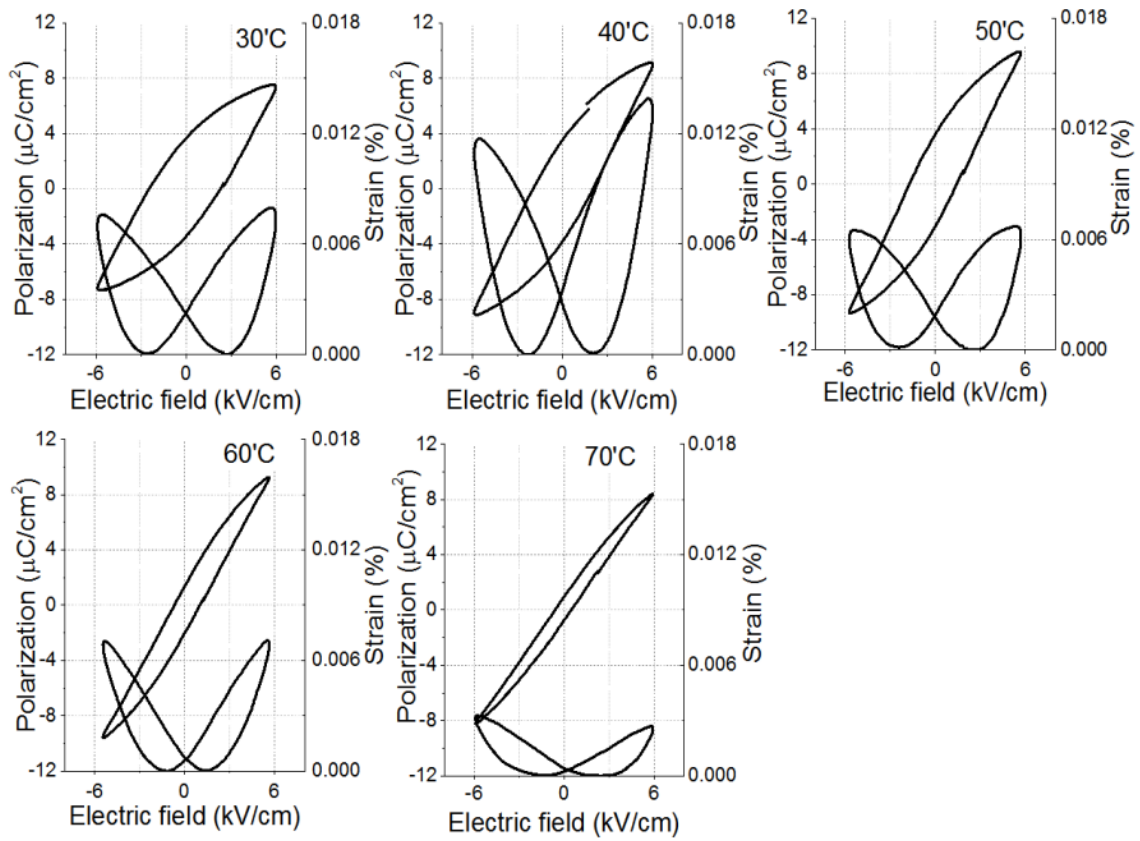


Figure 4.54 The electric field induced strain and polarization of 0.8PMN-0.2PZT at various temperatures

ลิขสิทธิ์มหาวิทยาลัยเชียงใหม่  
 Copyright© by Chiang Mai University  
 All rights reserved

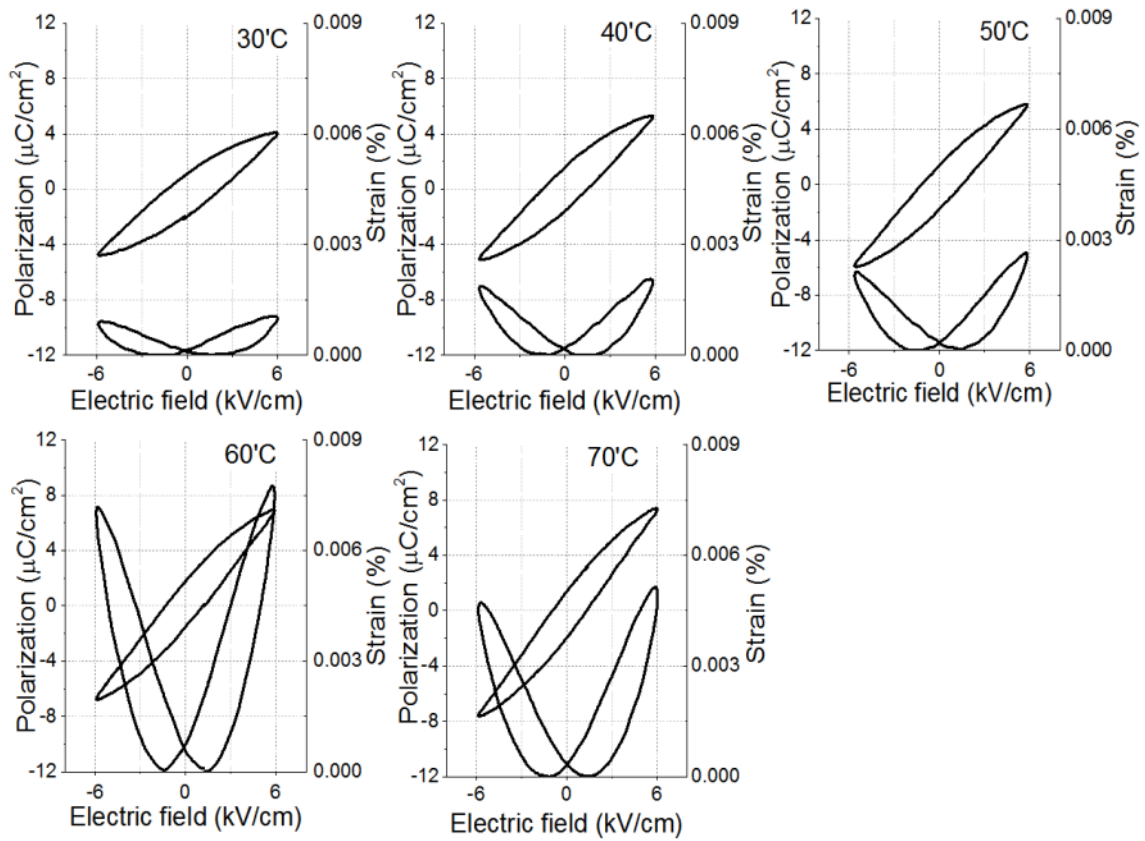


Figure 4.55 The electric field induced strain and polarization of 0.7PMN-0.3PZT at various temperatures

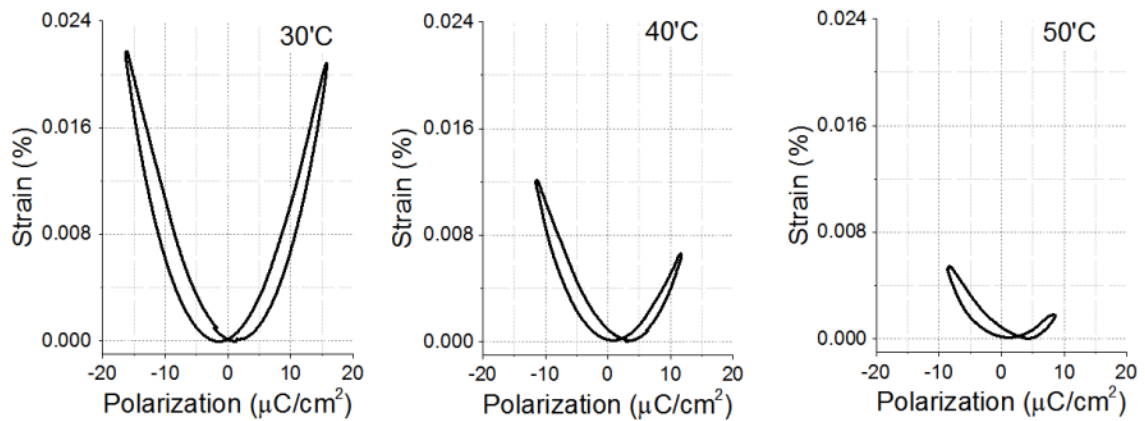


Figure 4.56 The induced strain as a function of polarization of 0.9PMN-0.1PT at various temperatures

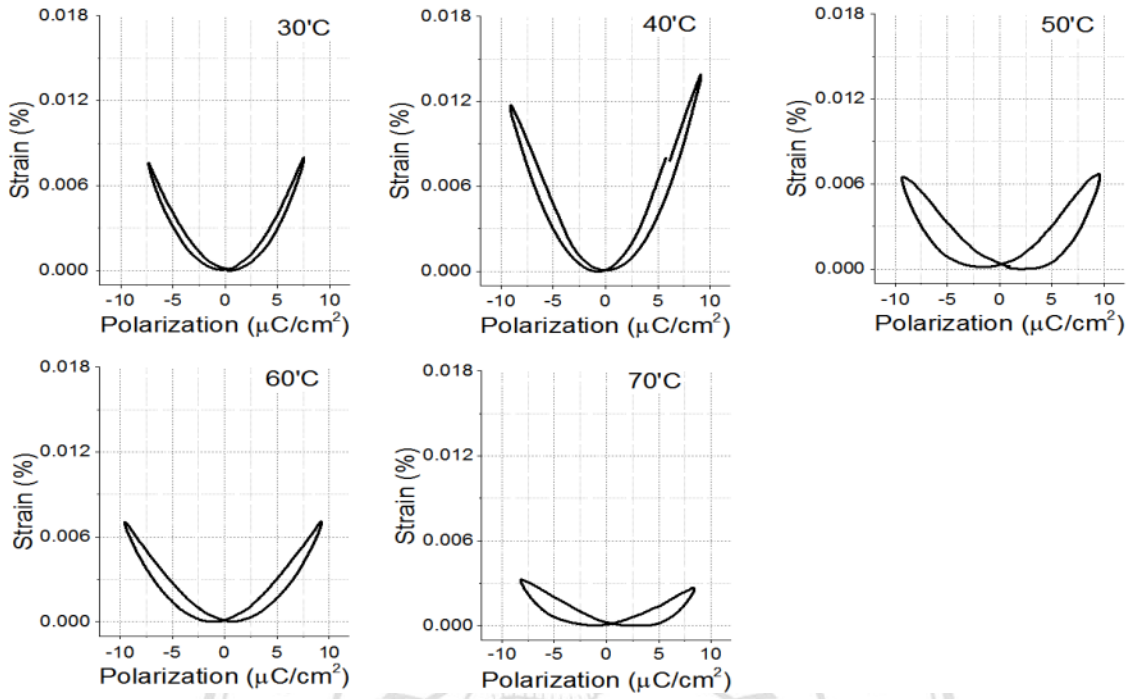


Figure 4.57 The induced strain as a function of polarization of 0.8PMN-0.2PT at various temperatures

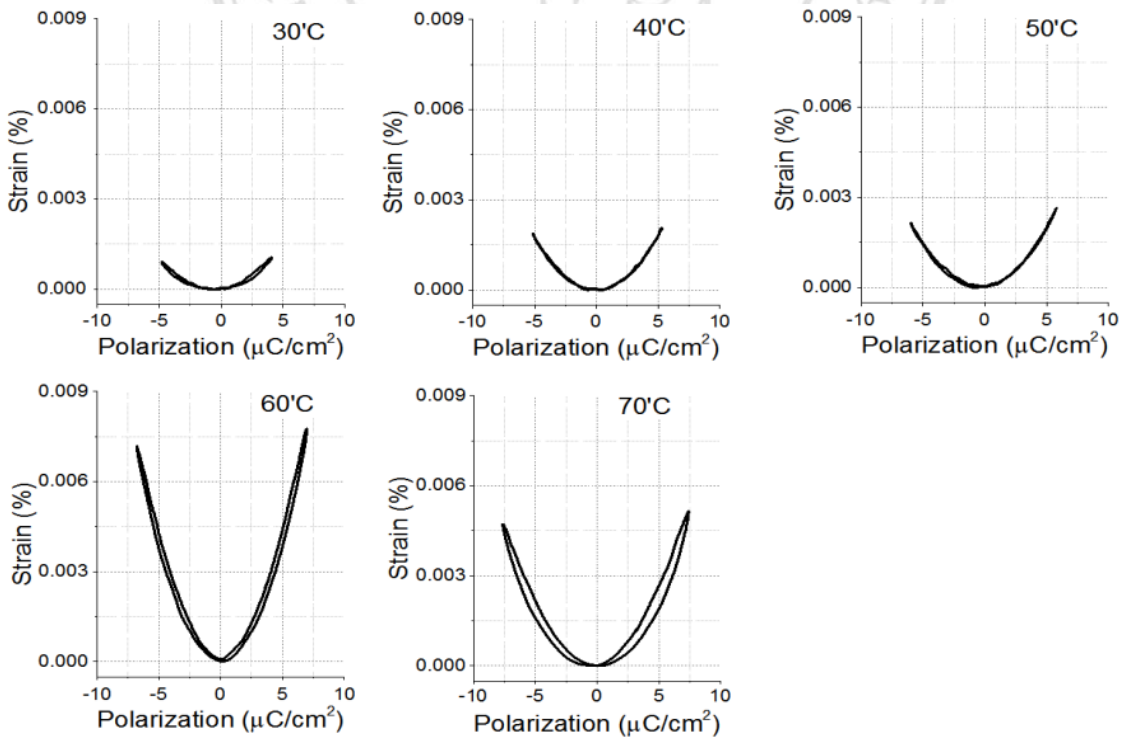


Figure 4.58 The induced strain as a function of polarization of 0.7PMN-0.3PT at various temperatures

Figures 4.59 and 4.60 show the polarization-electric field integrated area (int P-E) and strain-electric field integrated area (int s-E) of  $x$ PMN-( $1-x$ )PZT samples where  $x = 0.9, 0.7$  and  $0.5$  and  $x$ PMN-( $1-x$ )PT samples where  $x = 0.9, 0.8$  and  $0.7$ . For 0.9PMN-0.1PZT, 0.7PMN-0.3PZT and 0.9PMN-0.1PT samples, the int P-E or storage energy and int s-E demonstrated a non-linear decrease as temperature increased because the disappeared spontaneous polarization in ferroelectric to paraelectric phase transition, and that implied the diffuse phase transition of relaxor ferroelectric materials and  $T_m$  was in the range around 30°C to 50°C. For 0.5PMN-0.5PZT, the int s-E demonstrated non-linear decrease as temperature increased, referring to normal ferroelectric to relaxor ferroelectric phase transition at 40°C, and relaxor ferroelectric to paraelectric phase transition at 70°C. For 0.8PMN-0.2PT and 0.7PMN-0.3PT samples, the int P-E or storage energy and int s-E demonstrated normal ferroelectric to relaxor ferroelectric phase transition at 40°C and 60°C, and non-linear decreased as temperature increased because phase change in ferroelectric to paraelectric phase transition, and that implied the diffuse phase transition of relaxor ferroelectric materials and  $T_m$  was in the range around 50°C to 70°C and 60°C to 70°C, respectively.

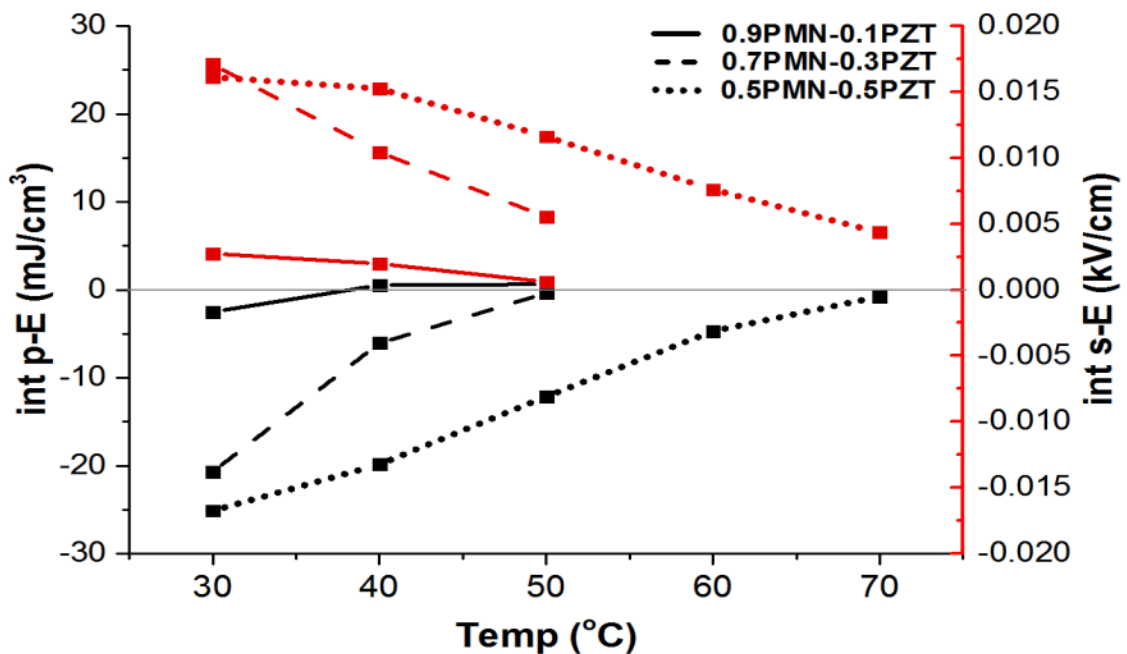


Figure 4.59 The integrated area of polarization and induced strain of  $x$ PMN-( $1-x$ )PZT samples where  $x = 0.9, 0.7$  and  $0.5$

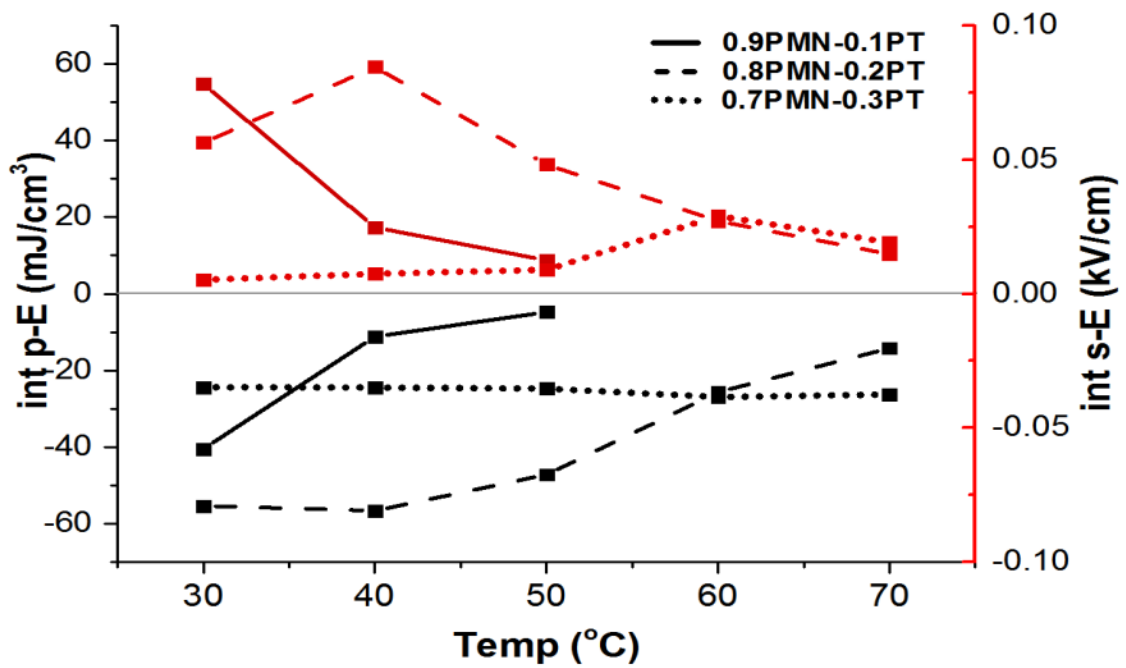


Figure 4.60 The integrated area of polarization and induced strain of  $x$ PMN-( $1-x$ )PT samples where  $x = 0.9, 0.8$  and  $0.7$

ลิขสิทธิ์มหาวิทยาลัยเชียงใหม่  
 Copyright© by Chiang Mai University  
 All rights reserved

## 4.2 Effect of magnetic field to piezoelectric and magnetoelectric properties

Magnetic field affected piezoelectric/electrostriction properties. This attracts attention in terms of character that means to magnetoelectric properties in multifunctional equipment such as sensor/actuator applications. To observe the effect of magnetic field to piezoelectric/electrostriction behavior of ferroelectric sample, the relaxor ferroelectric materials which have the morphotropic phase boundary or the phase transition temperature was closed to room temperature,  $\text{Pb}_{0.91}\text{La}_{0.09}\text{Zr}_{0.70}\text{Ti}_{0.30}\text{O}_3$  PLZT (9/70/30),  $\text{Pb}_{0.91}\text{La}_{0.09}\text{Zr}_{0.65}\text{Ti}_{0.35}\text{O}_3$  PLZT (9/65/35),  $\text{Pb}_{0.91}\text{La}_{0.09}\text{Zr}_{0.60}\text{Ti}_{0.40}\text{O}_3$  PLZT (9/60/40),  $x\text{Pb}(\text{Mg}_{1/3}\text{Nb}_{2/3})\text{O}_3-(1-x)\text{Pb}(\text{Zr}_{0.52}\text{Ti}_{0.48})\text{O}_3$   $x\text{PMN}-(1-x)\text{PZT}$  samples where  $x = 0.9, 0.7$  and  $0.5$ , and  $x\text{Pb}(\text{Mg}_{1/3}\text{Nb}_{2/3})\text{O}_3-(1-x)\text{PbTiO}_3$   $x\text{PMN}-(1-x)\text{PT}$  samples where  $x = 0.9, 0.8$  and  $0.7$  were chosen. To investigate the electric field induced strain and polarization behavior modified Michelson interferometer technique was used at various magnetic fields from 0 mT to 30.7 mT.

Figure 4.61 shows the magnetic field distribution along the solenoid coil length. The magnetic field was changed as a function of the electrical current from the programmable dc power supply (Rigol DP 1116A) at 0, 1, 2 and 3 A, and was detected by the gauss meter (ST probe; the magnetic range 0-30 kG) at 0, 10.5, 20.6 and 30.7 mT, which measured magnetic field along center position of solenoid coil where ferroic sample was placed to observe the actual real magnetic field at sample position as shown in Figure 3.6. The ferroelectric samples were placed at the middle of solenoid coil position between 3 and 4 cm, to measure the electric field induced strain and polarization in various magnetic field affect and the samples were subjected to a bipolar high extension voltage at 0.2 to 2 Hz of frequency from high voltage amplifier/controller supply (Trek 610D).

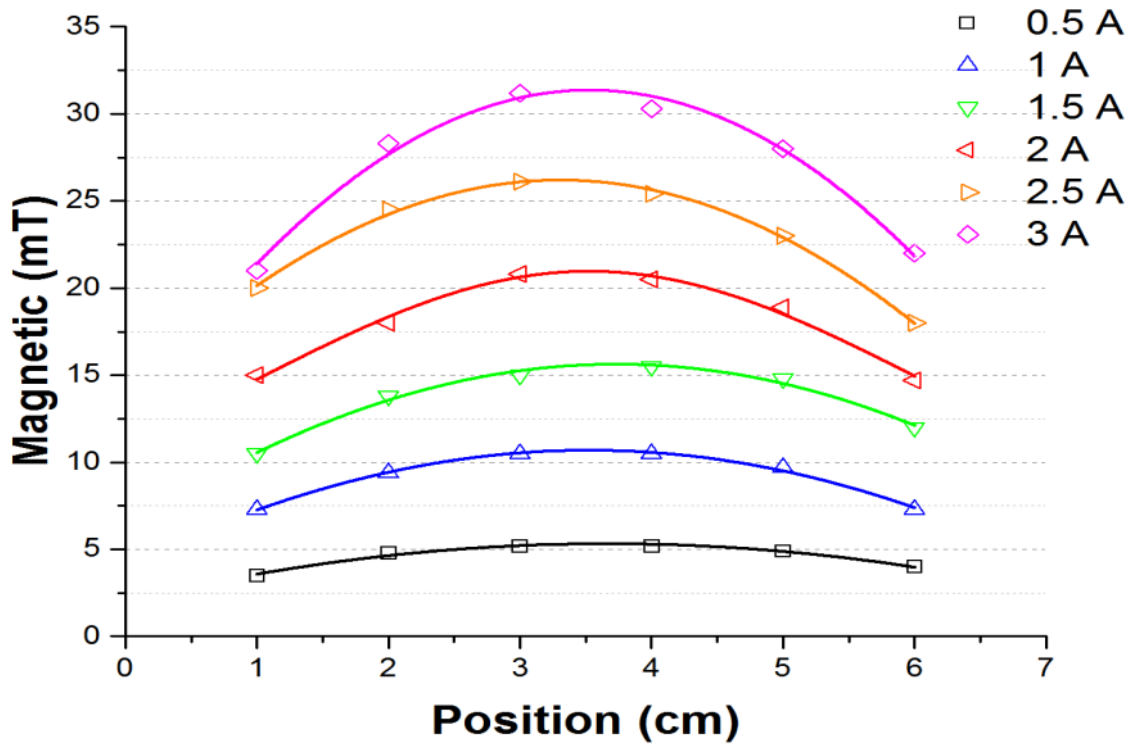


Figure 4.61 The magnetic field (flux density) as a function of solenoid coil length

Figures 4.62, 4.63 and 4.64 show electric field induced-strain and polarization at various magnetic fields of PLZT (9/70/30), PLZT (9/65/35) and PLZT (9/60/40) samples, respectively. In Figure 4.62, PLZT (9/70/30) sample shows pinched hysteresis loop of polarization and slimmer butterfly shape curve of induced strain as a function of applied electric field, indicating spontaneous polarization and depolarizing field inside of  $180^\circ$  domain like anti ferroelectric phase [52]. The pinch of polarization decreased when the frequency was increased due to frequency response of domain switching time, which was the same as the decreased of maximum polarization and induced strain. And the magnetic field showed no effect to polarization behavior, but fewer effect to induced strain which shows minimum values at 10.5 mT possibly due to microdomain of relaxor ferroelectric phase change to paraelectric, which was the same as dielectric constant as shown in Figure 4.20 of PLZT (9/70/30) sample at room temperature. In Figure 4.63, PLZT (9/65/35) sample shows more square hysteresis loop of polarization and asymmetric butterfly shape curve of induced strain as a function of applied electric field than PLZT (9/70/30) sample, indicating higher spontaneous polarization inside

ferroelectric phase which normal ferroelectric phase change to relaxor ferroelectric phase or near MPB at room temperature, which was the same as dielectric constant as shown in Figure 4.20. The decrease of maximum polarization and induced strain when the frequency increase was due to frequency response of domain switching time. For all frequency, PLZT (9/65/35) sample shows decrease both of polarization and induced strain when magnetic field was increased implying magnetic field suppressed domain switching behavior [24,28,35,67-72] where the sample are two structure composition like near MPB compositions. In Figure 4.64, PLZT (9/60/40) sample shows square hysteresis loop of polarization and asymmetric butterfly shape curve of induced strain as a function of applied electric field with the coercive field higher than PLZT (9/65/35) sample, indicating spontaneous polarization in normal ferroelectric far from MPB. The decrease of maximum polarization and induced strain when the frequency increased was due to frequency response of domain switching time. And show fewer effect from magnetic field to polarization and induced strain behavior possibly due to normal domain of PLZT (9/60/40) sample.

Figures 4.65, 4.66 and 4.67 show induced-strain as a function of polarization at various magnetic fields of PLZT (9/70/30), PLZT (9/65/35) and PLZT (9/60/40) samples, respectively. The samples show polarization dependence of induced strain which the quadratic relation curve was demonstrated for all samples. PLZT (9/70/30) sample shows 180° microdomain rotation dominated and PLZT (9/65/35) shows decrease of maximum values but more hysteresis when magnetic field was increased due to suppressed 180° domain near MPB composition, and PLZT (9/60/40) samples show more slimmer loop than PLZT (9/70/30) sample due to subswitching field of 90° domain at normal ferroelectric phase.

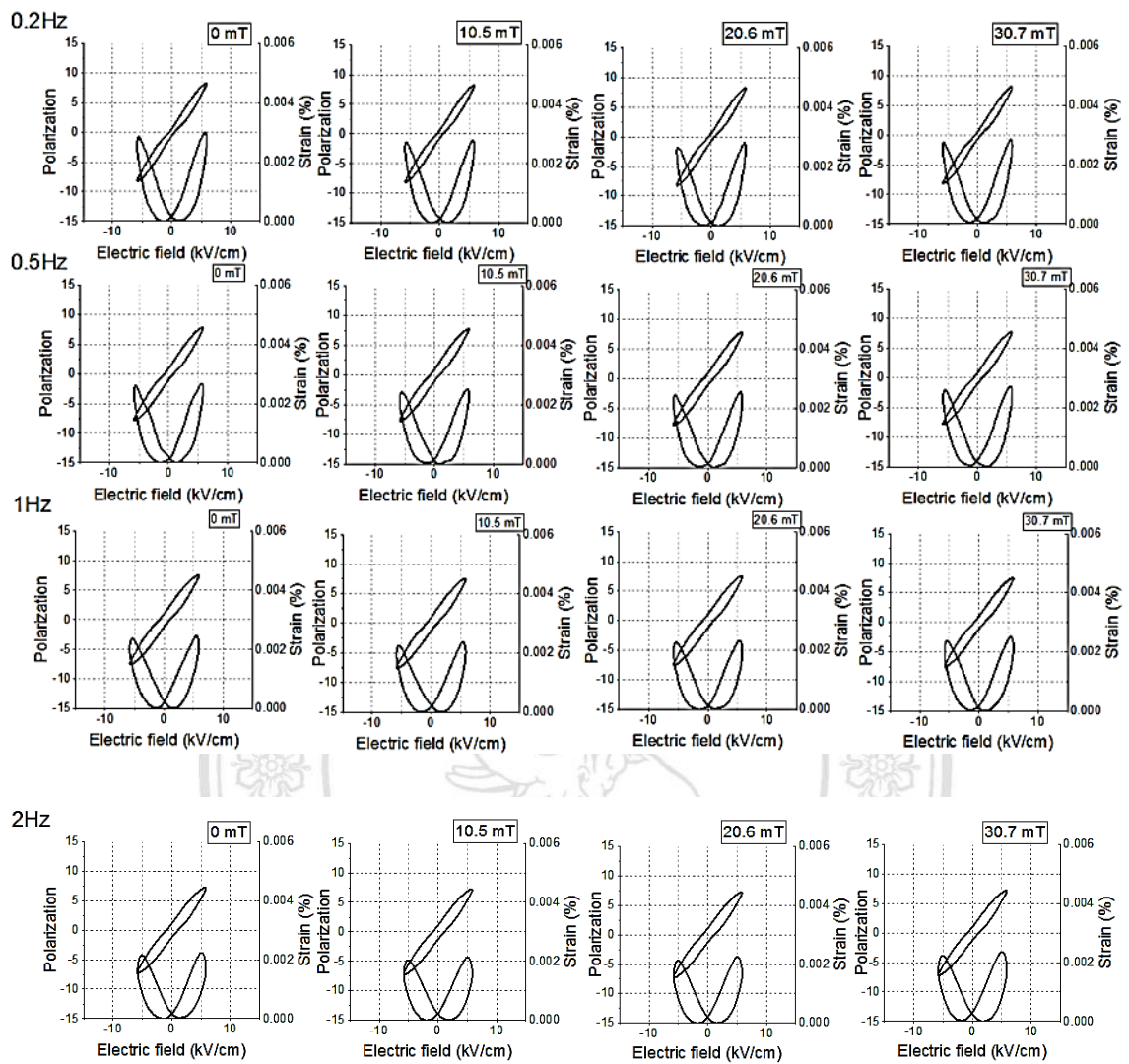


Figure 4.62 The electric field induced strain and polarization of PLZT (9/70/30) at various magnetic fields

ลิขสิทธิ์มหาวิทยาลัยเชียงใหม่  
Copyright© by Chiang Mai University  
All rights reserved

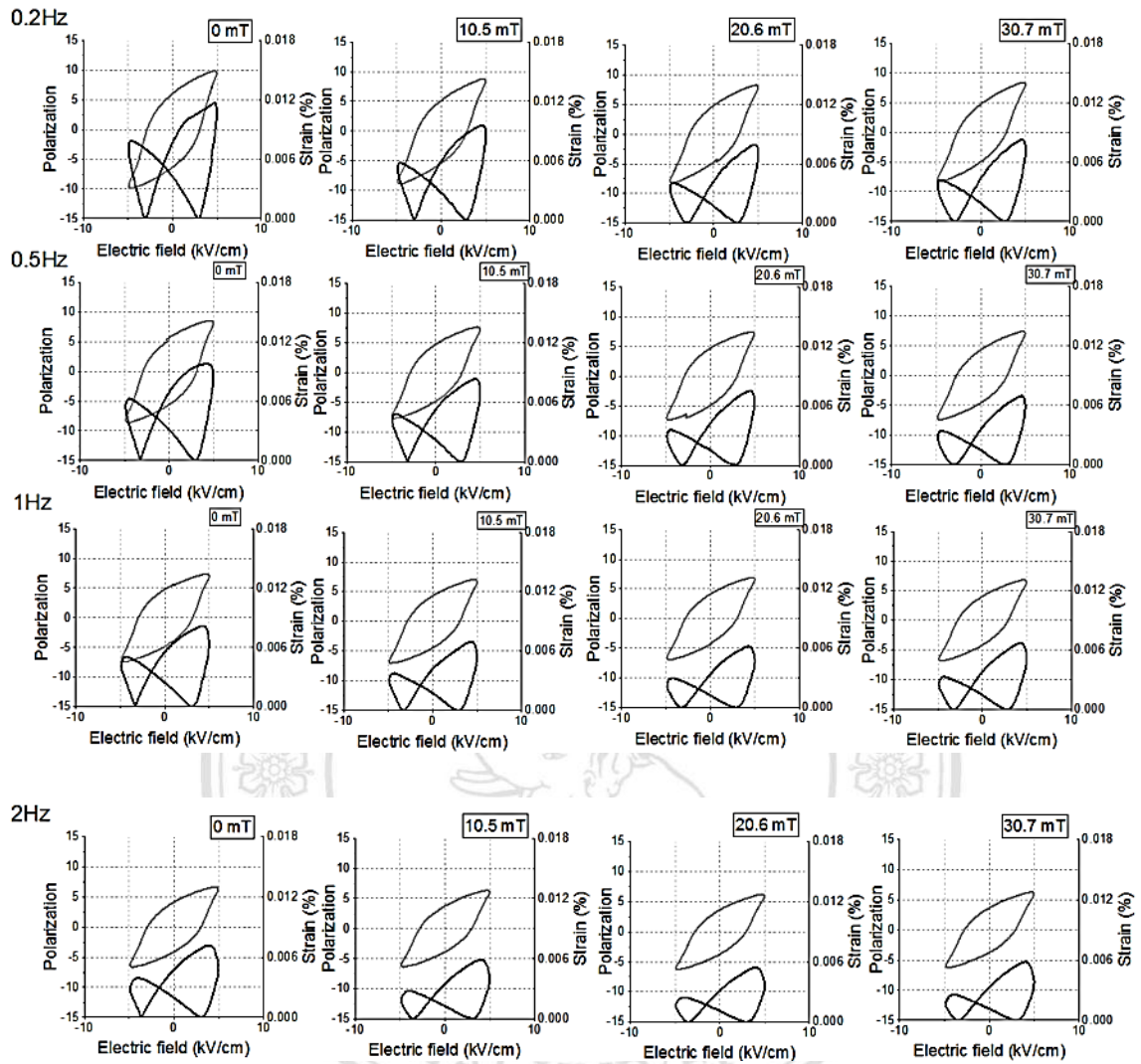


Figure 4.63 The electric field induced strain and polarization of PLZT (9/65/35) at various magnetic fields

ลิขสิทธิ์มหาวิทยาลัยเชียงใหม่  
Copyright© by Chiang Mai University  
All rights reserved

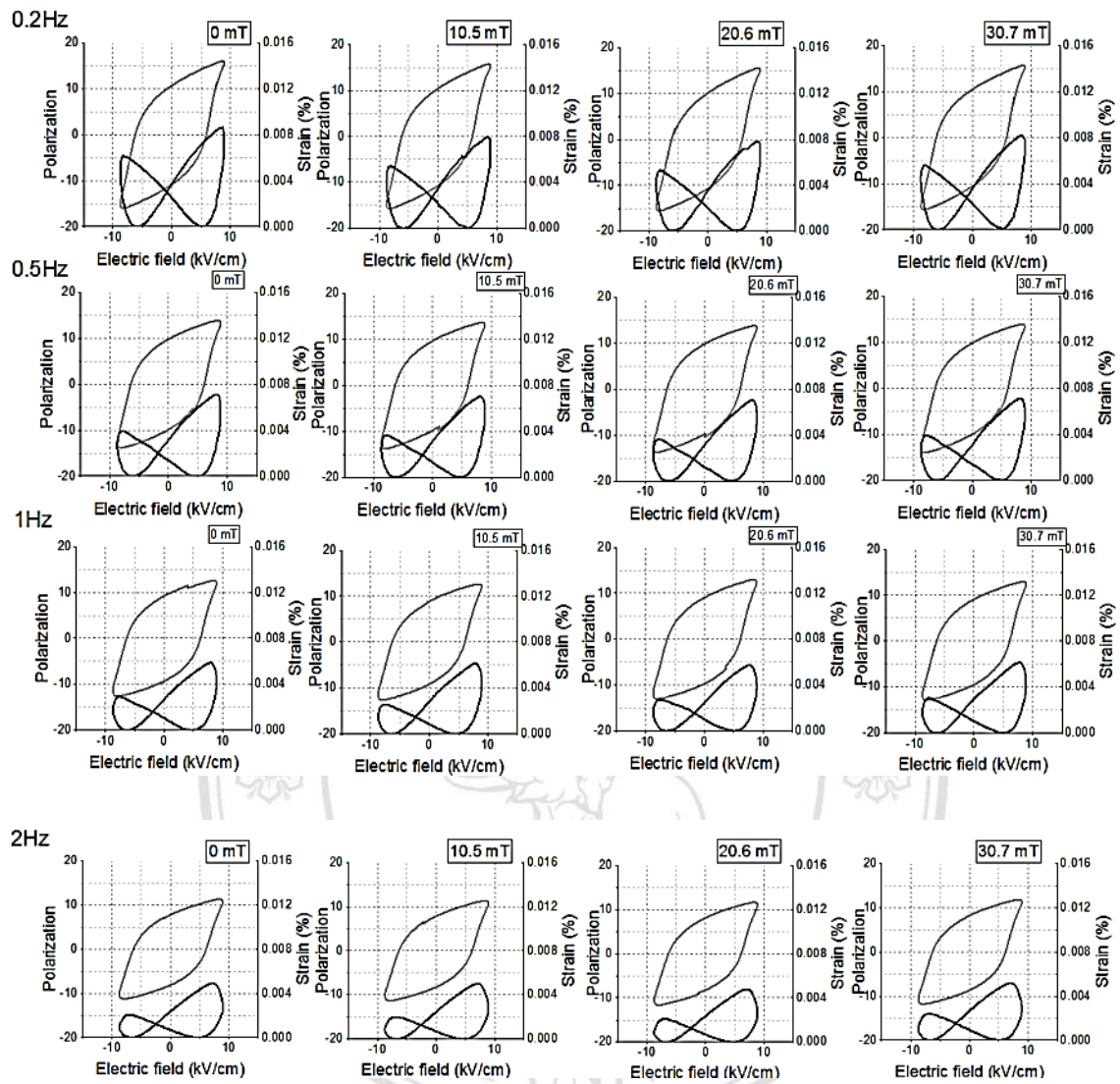


Figure 4.64 The electric field induced strain and polarization of PLZT (9/60/40) at various magnetic fields

ลิขสิทธิ์มหาวิทยาลัยเชียงใหม่  
Copyright© by Chiang Mai University  
All rights reserved

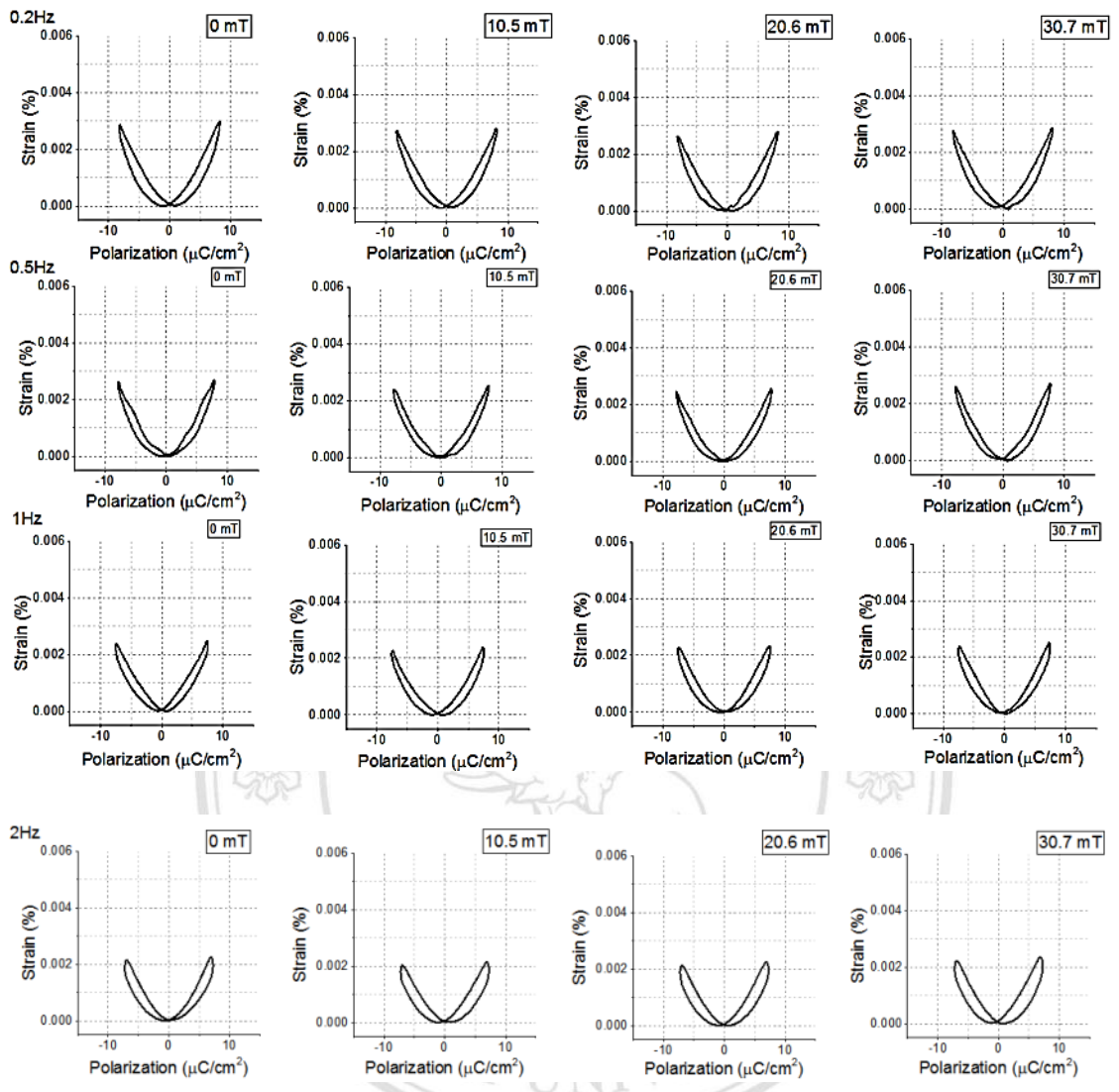


Figure 4.65 The induced strain as a function of polarization of PLZT (9/70/30) at various magnetic fields

ลิขสิทธิ์มหาวิทยาลัยเชียงใหม่  
 Copyright© by Chiang Mai University  
 All rights reserved

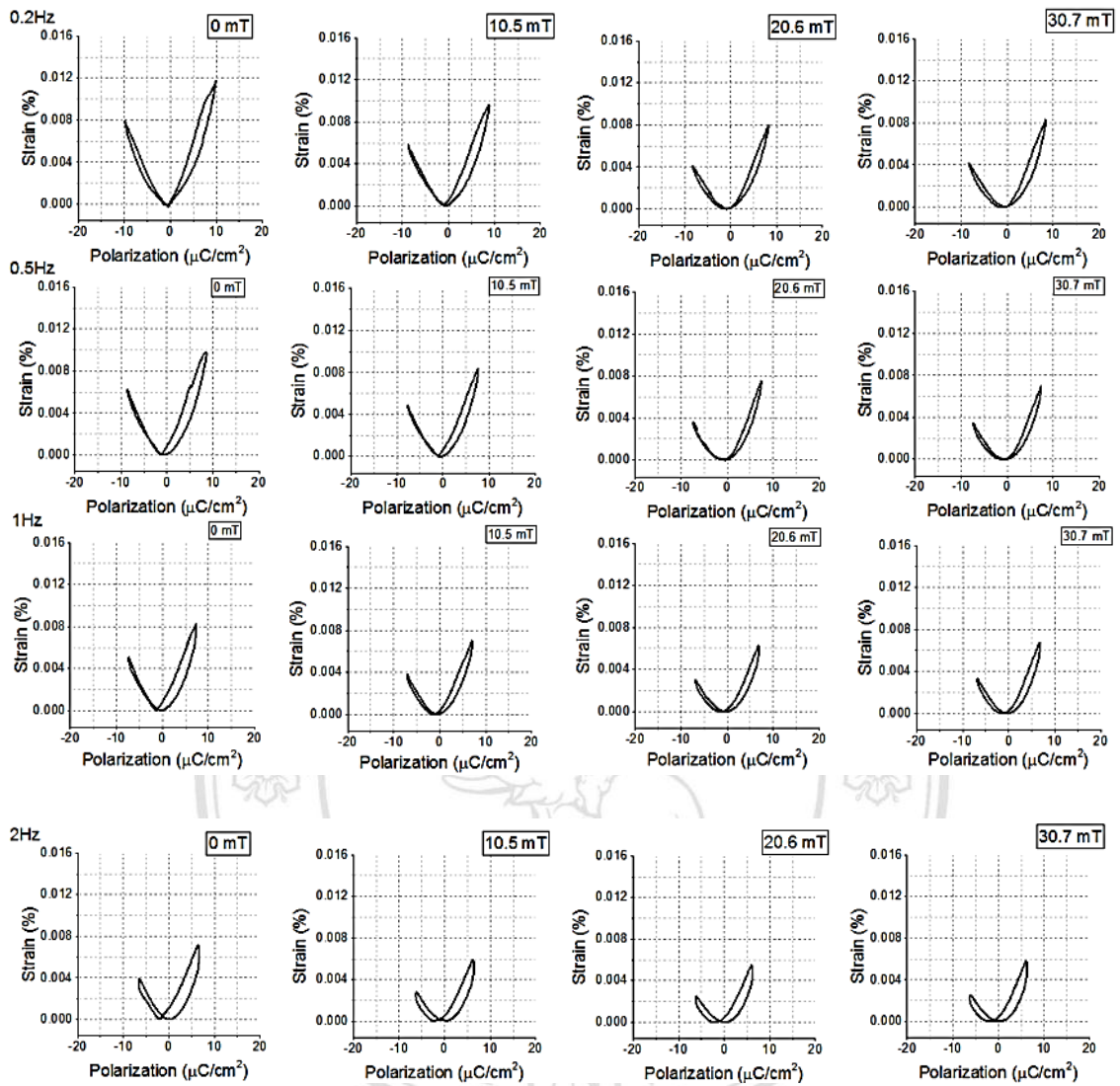


Figure 4.66 The induced strain as a function of polarization of PLZT (9/65/35) at various magnetic fields

ลิขสิทธิ์มหาวิทยาลัยเชียงใหม่  
Copyright© by Chiang Mai University  
All rights reserved

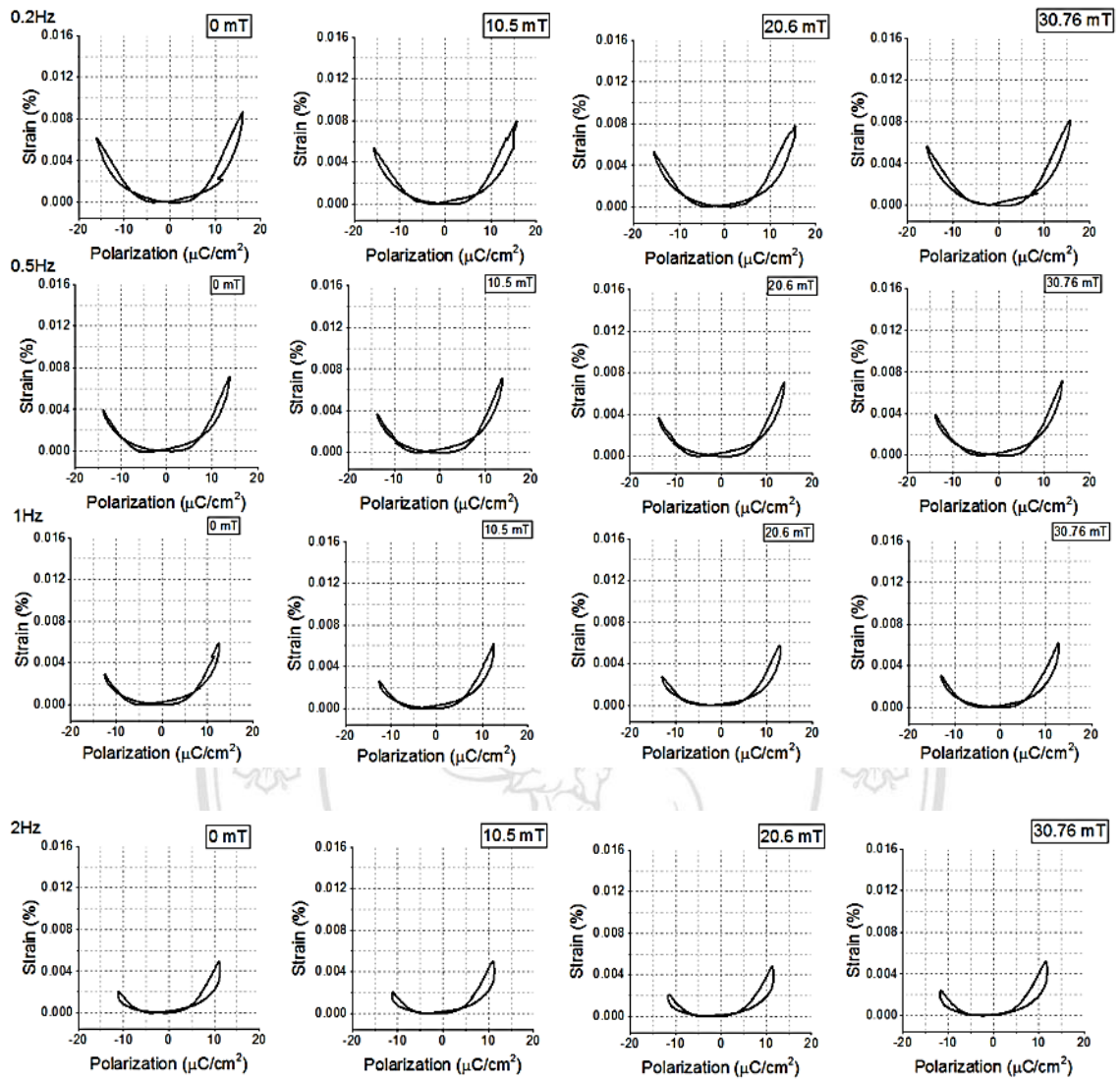


Figure 4.67 The induced strain as a function of polarization of PLZT (9/60/40) at various magnetic fields

ลิขสิทธิ์มหาวิทยาลัยเชียงใหม่  
Copyright © by Chiang Mai University  
All rights reserved

Figures 4.68, 4.69 and 4.70 show electric field induced-strain and polarization at various magnetic field of  $x$ PMN–(1- $x$ )PZT samples where  $x = 0.9, 0.7$  and  $0.5$ , respectively. In Figure 4.68, 0.9PMN–0.1PZT sample shows slim loop of polarization and quadratic shape curve of induced strain as a function of applied electric field indicating non spontaneous polarization inside sample. The effect of magnetic field to polarization and induced strain behavior was less due to less spontaneous polarization in paraelectric phase as dielectric constant shown in Figure 4.45 of 0.9PMN–0.1PZT sample at room temperature. In Figure 4.69, 0.7PMN–0.3PZT sample shows hysteresis loop of polarization and butterfly shape curve of induced strain as a function of applied electric field indicating spontaneous polarization inside sample in relaxor ferroelectric phase at room temperature. The sample shows more hysteresis loop of polarization and induced strain when the frequency was increased due to frequency response of domain switching behavior. And the magnetic field did not affect polarization behavior, but less affected to induced strain which shows minimum values at 20.6 mT for 0.2 to 0.5 Hz and at 10.5 mT for 1 to 2 Hz possible due to microdomain of relaxor ferroelectric phase change to paraelectric as dielectric constant shown in Figure 4.45 of 0.7PMN–0.3PZT sample at room temperature. In Figure 4.70, 0.5PMN–0.5PZT sample shows hysteresis loop of polarization and butterfly shape curve of induced strain as a function of applied electric field indicating spontaneous polarization inside in normal ferroelectric phase at room temperature. The sample shows more hysteresis loop of polarization and induced strain when the frequency was increased due to frequency response of domain switching behavior. And the magnetic field showed no effect to polarization behavior, but less affected to induced strain which shows increases the maximum values when the magnetic field was increased at 0 mT to 30.7 mT implying magnetic field suppressing domain switching behavior [24,28,35,67-72]. Normal ferroelectric phase changed to relaxor ferroelectric as dielectric constant shown in Figure 4.45 of 0.5PMN–0.5PZT sample at room temperature.

Figures 4.71, 4.72 and 4.73 show induced-strain as a function of polarization at various temperatures of  $x$ PMN–(1- $x$ )PZT samples where  $x = 0.9, 0.7$  and  $0.5$ , respectively. The samples show polarization dependence of induced strain where the quadratic relation curve was observed for all samples, which 0.9PMN–0.1PZT sample

shows non spontaneous polarization shape curve, 0.7PMN–0.3PZT sample shows more hysteresis when magnetic field was increased due to 180° microdomain rotation dominated of relaxor ferroelectric phase like PLZT (9/70/30) sample, and 0.5PMN–0.5PZT sample shows more slimmer loop than 0.7PMN–0.3PZT sample due to 90° domain orientation dominated near MPB of tetragonal to relaxor phase, and shows more hysteresis, indicating frequency dependence at 2Hz.

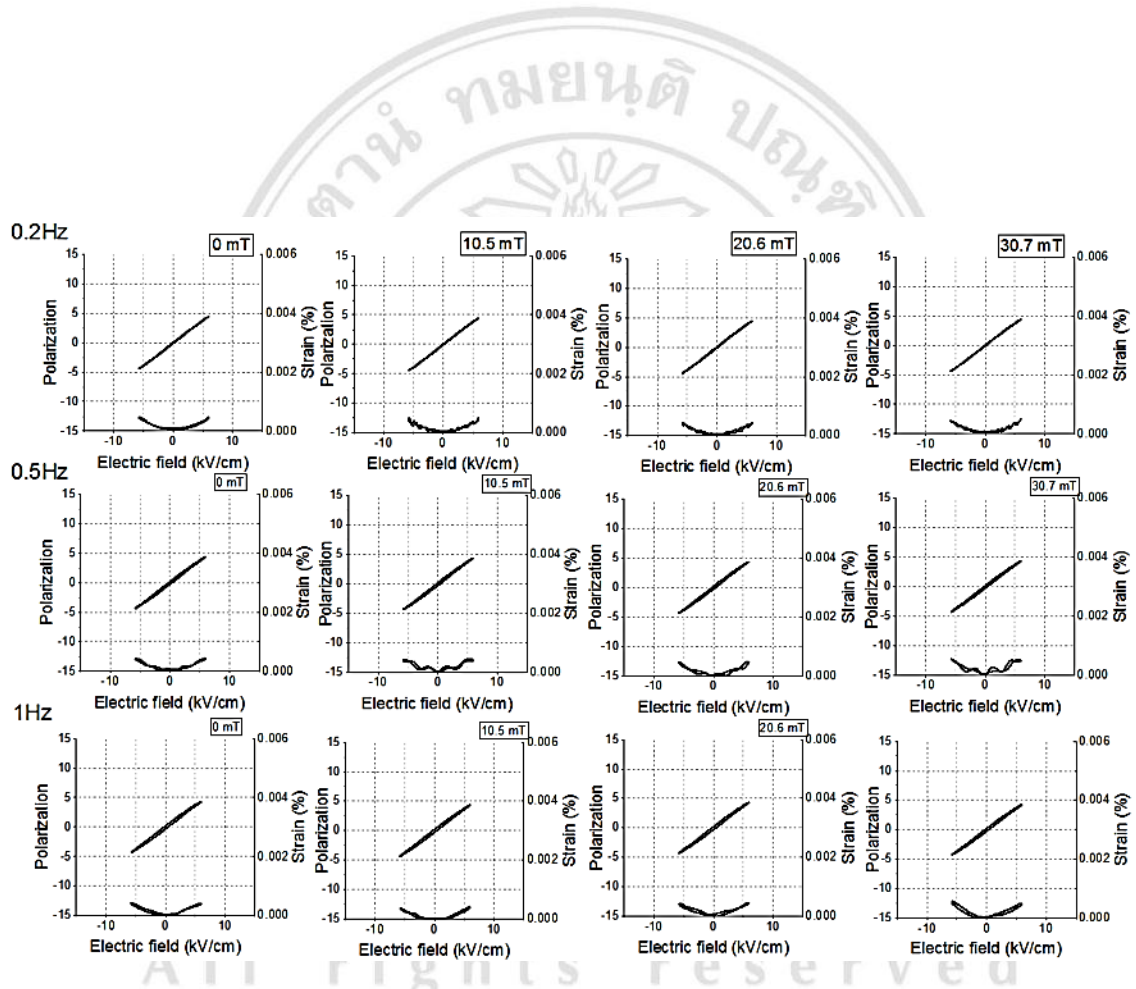


Figure 4.68 The electric field induced strain and polarization of 0.9PMN-0.1PZT at various magnetic fields

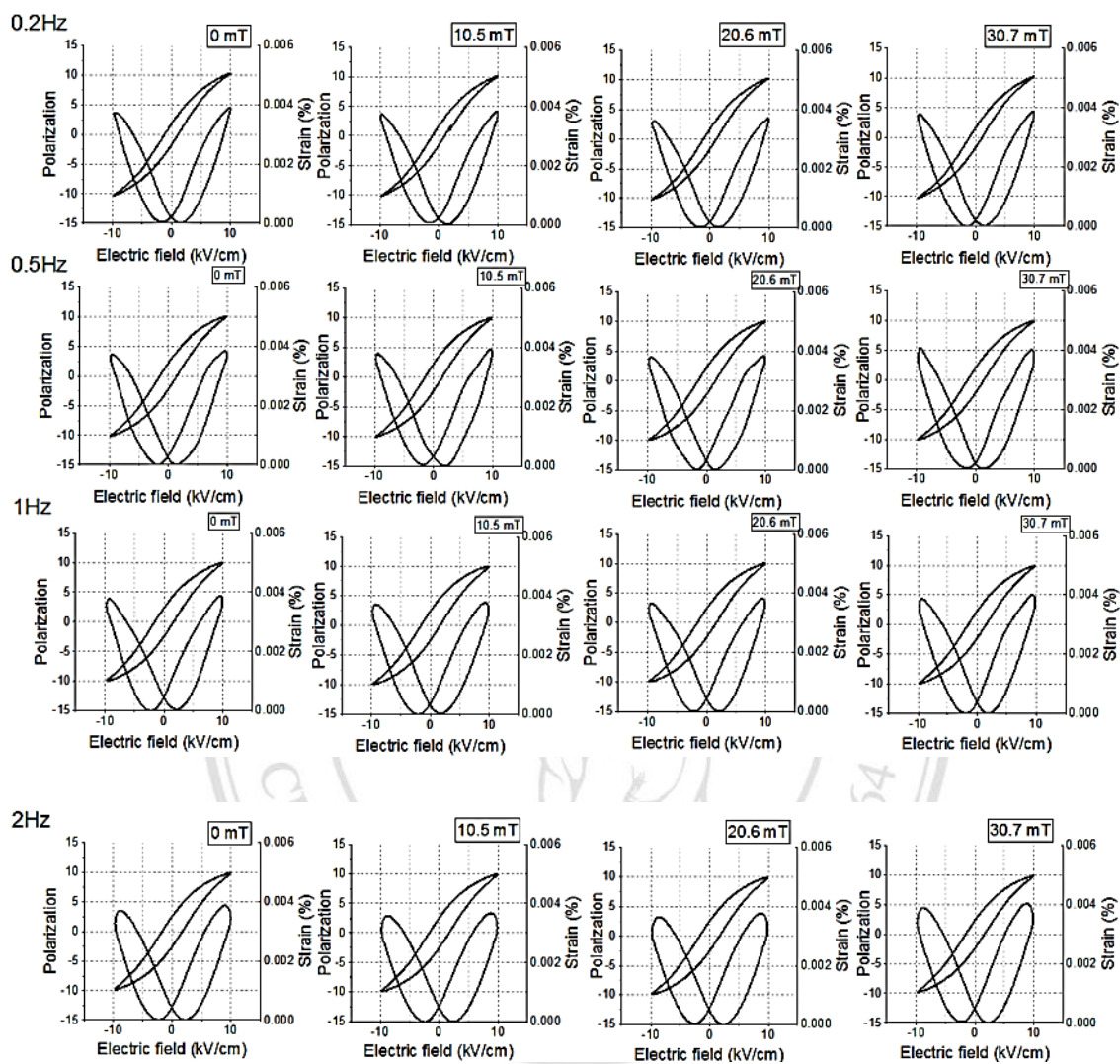


Figure 4.69 The electric field induced strain and polarization of 0.7PMN-0.3PZT at various magnetic fields

Copyright © by Chiang Mai University  
All rights reserved

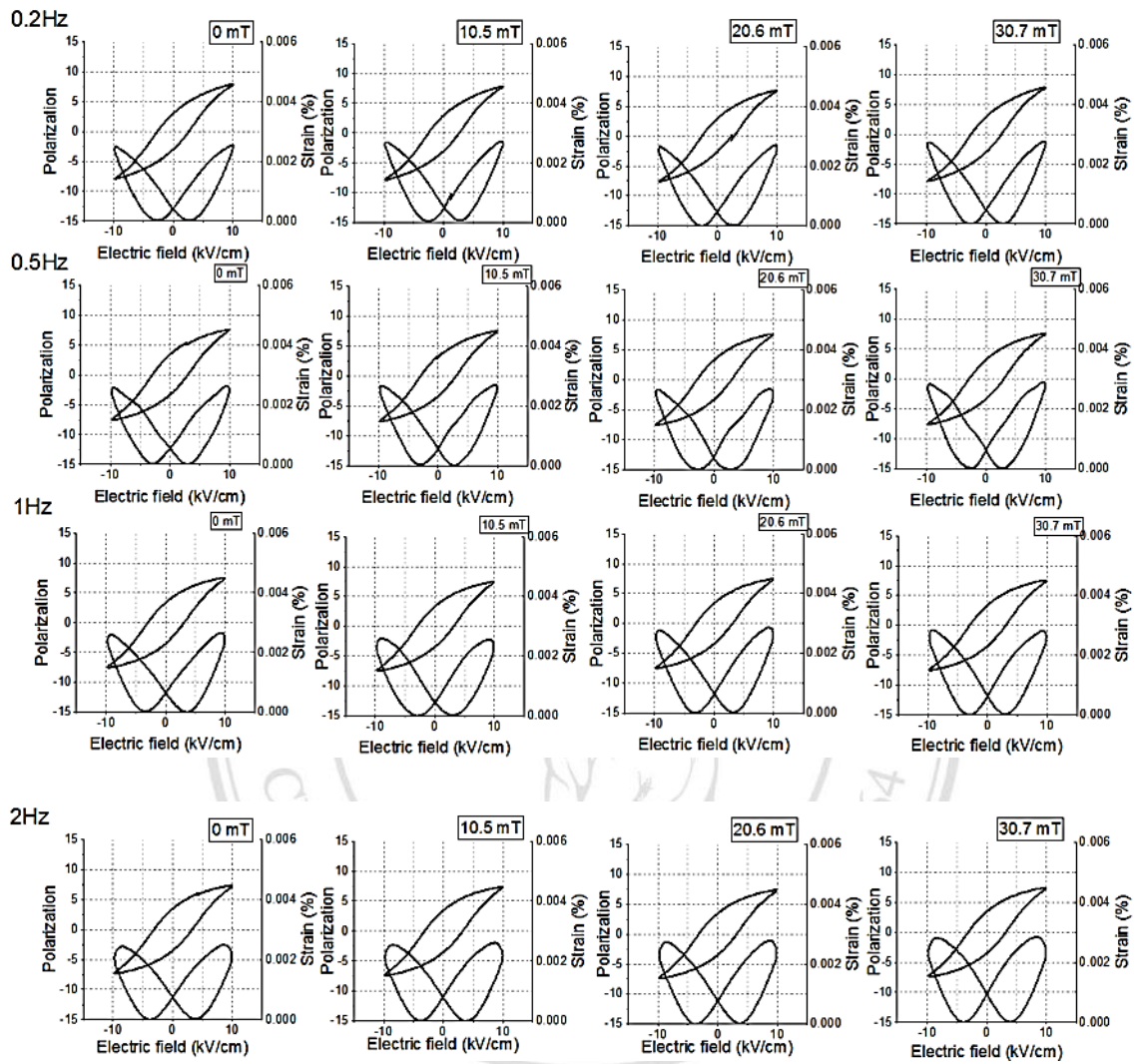


Figure 4.70 The electric field induced strain and polarization of 0.5PMN-0.5PZT at various magnetic fields

Copyright © by Chiang Mai University  
All rights reserved

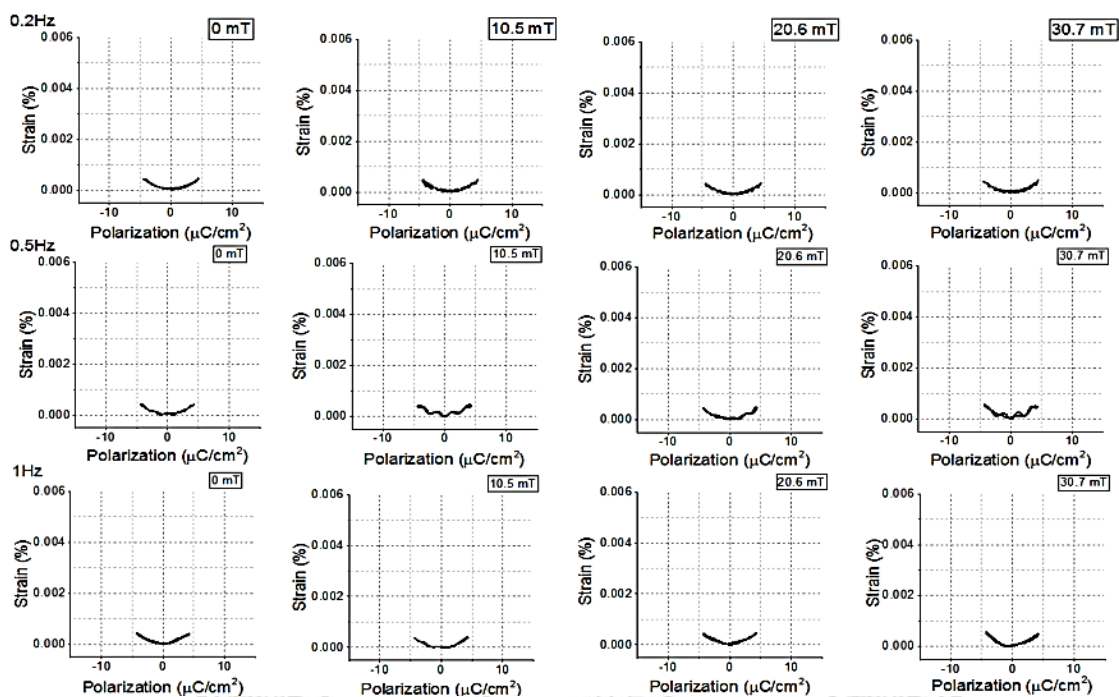


Figure 4.71 The induced strain as a function of polarization of 0.9PMN-0.1PZT at various magnetic fields

ลิขสิทธิ์มหาวิทยาลัยเชียงใหม่  
 Copyright© by Chiang Mai University  
 All rights reserved

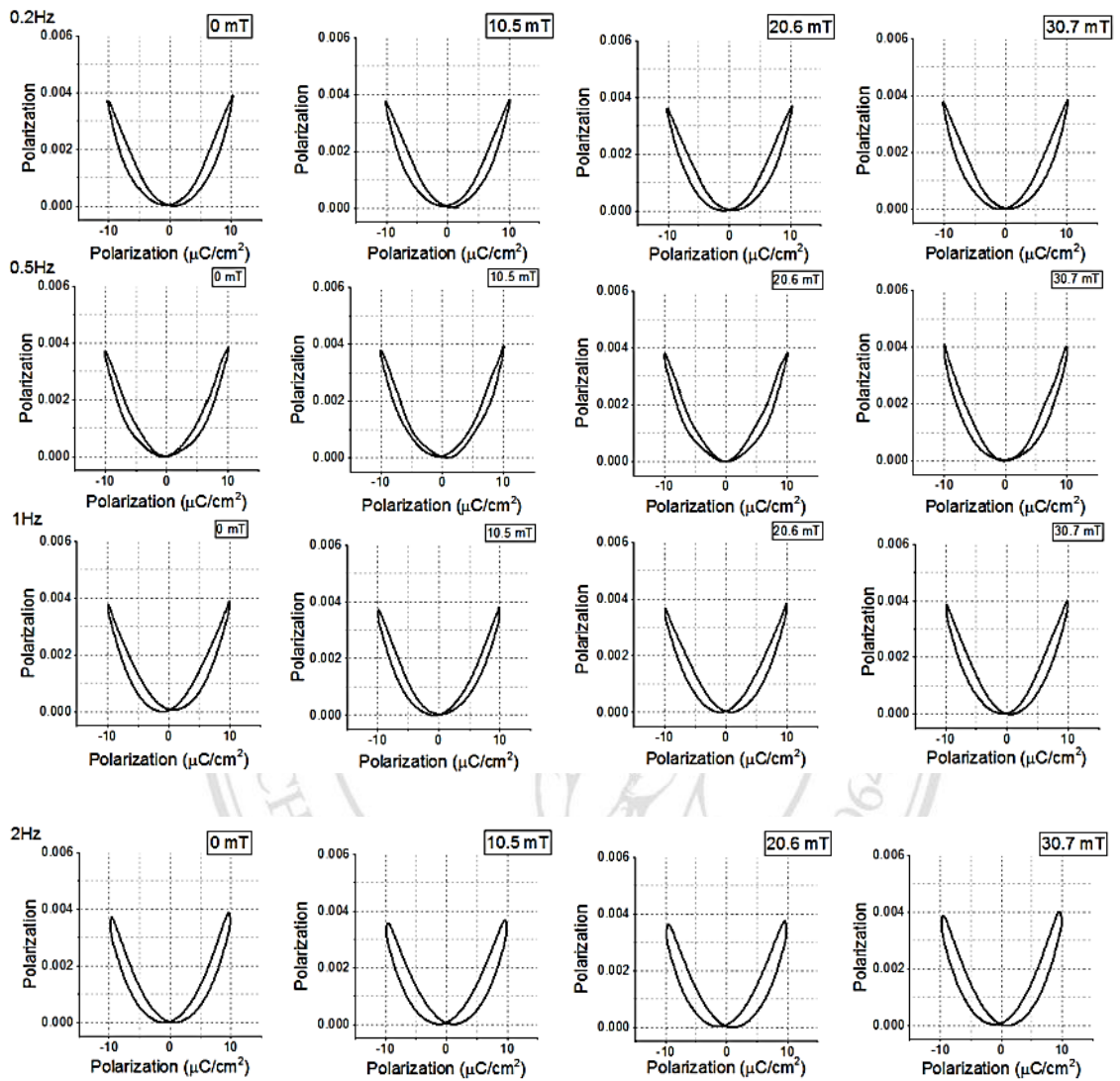


Figure 4.72 The induced strain as a function of polarization of 0.7PMN-0.3PZT at various magnetic fields

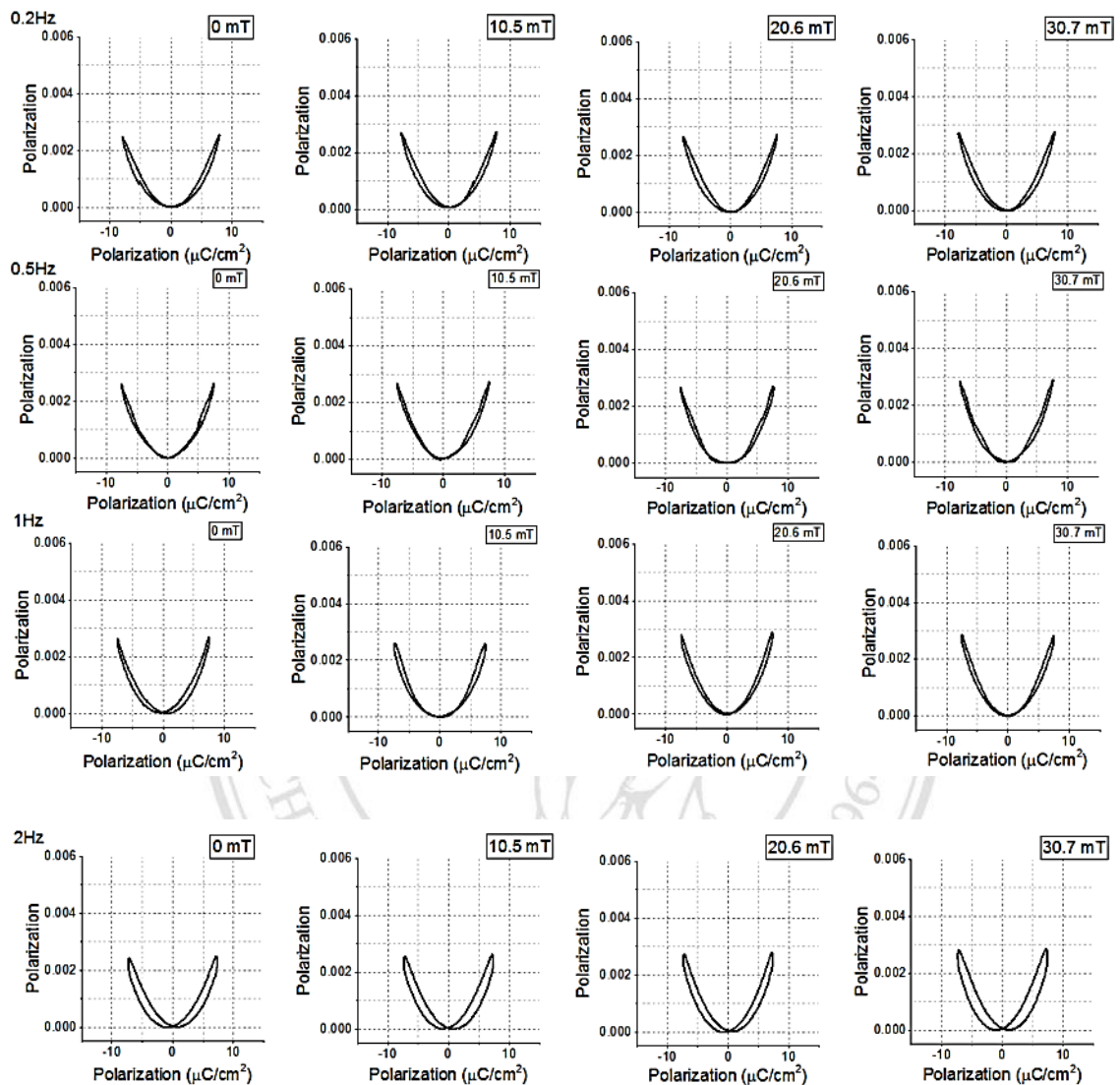


Figure 4.73 The induced strain as a function of polarization of 0.5PMN-0.5PZT at various magnetic fields

Figures 4.74, 4.75 and 4.76 show electric field induced-strain and polarization at various magnetic fields of  $x$ PMN-(1- $x$ )PT samples where  $x = 0.9, 0.8$  and  $0.7$ , respectively. In Figure 4.74, 0.9PMN-0.1PT sample shows hysteresis loop of polarization and butterfly shape curve of induced strain as a function of applied electric field indicating spontaneous polarization inside sample in relaxor ferroelectric phase at room temperature. The sample shows more hysteresis loop and decreases in maximum values of polarization and induced strain when the frequency was increased due to frequency response of domain switching behavior. And the magnetic field did not affect polarization behavior, but less affected to induced strain which shows maximum values at 10.5 mT for 0.2 Hz and at 20.6 mT for 0.5 to 1 Hz possibly due to microdomain of relaxor ferroelectric phase change to paraelectric as dielectric constant shown in Figure 4.52 of 0.9PMN-0.1PT sample at room temperature. In Figure 4.75, 0.8PMN-0.2PT sample shows hysteresis loop of polarization and asymmetric butterfly shape curve of induced strain as a function of applied electric field indicating spontaneous polarization inside sample in tetragonal ferroelectric phase transition to rhombohedral near room temperature [63-65]. The sample shows more hysteresis loop and decreases in maximum values of polarization and induced strain when the frequency was increased due to frequency response of domain switching behavior. And the magnetic field did not affect polarization behavior, but affected to induced strain which shows increases maximum values when magnetic field was increased, which means magnetic field suppressed domain switching behavior [24,28,35,67-72] for ferroelectric sample which composition near MPB, as dielectric constant shown in Figure 4.49 of 0.8PMN-0.2PZT sample at room temperature. In Figure 4.76, 0.7PMN-0.3PT sample shows hysteresis loop of polarization and butterfly shape curve of induced strain as a function of applied electric field indicating spontaneous polarization inside like normal ferroelectric phase at room temperature. The sample shows more hysteresis loop in induced strain and decreases in maximum values of polarization when the frequency was increased due to frequency response of domain switching behavior. And the magnetic field did not affect polarization behavior, but less affected to induced strain which shows increases maximum values when magnetic field was increased implying magnetic field suppressing domain switching behavior [24,28,35,67-72] for ferroelectric sample which

composition between MPB and normal ferroelectric phase as dielectric constant shown in Figure 4.52 of 0.7PMN–0.3PT sample at room temperature.

Figures 4.77, 4.78 and 4.79 show induced-strain as a function of polarization at various magnetic fields of  $x$ PMN–(1- $x$ )PT samples where  $x = 0.9, 0.8$  and  $0.7$ , respectively. The samples show polarization dependence of induced strain where the quadratic relation curve could be seen in all samples, which 0.9PMN–0.1PT sample  $180^\circ$  microdomain rotation dominated of relaxor ferroelectric phase like PLZT (9/70/30) and 0.7PMN–0.3PZT sample, and 0.8PMN–0.2PT and 0.7PMN–0.3PT sample shows more slimmer loop than 0.9PMN–0.1PT sample at lower frequency due to  $90^\circ$  domain rotation of composition near MPB [62-66] but shows hysteresis loop loss at high frequency due to frequency dependence like 0.5PMN-0.5PZT sample.

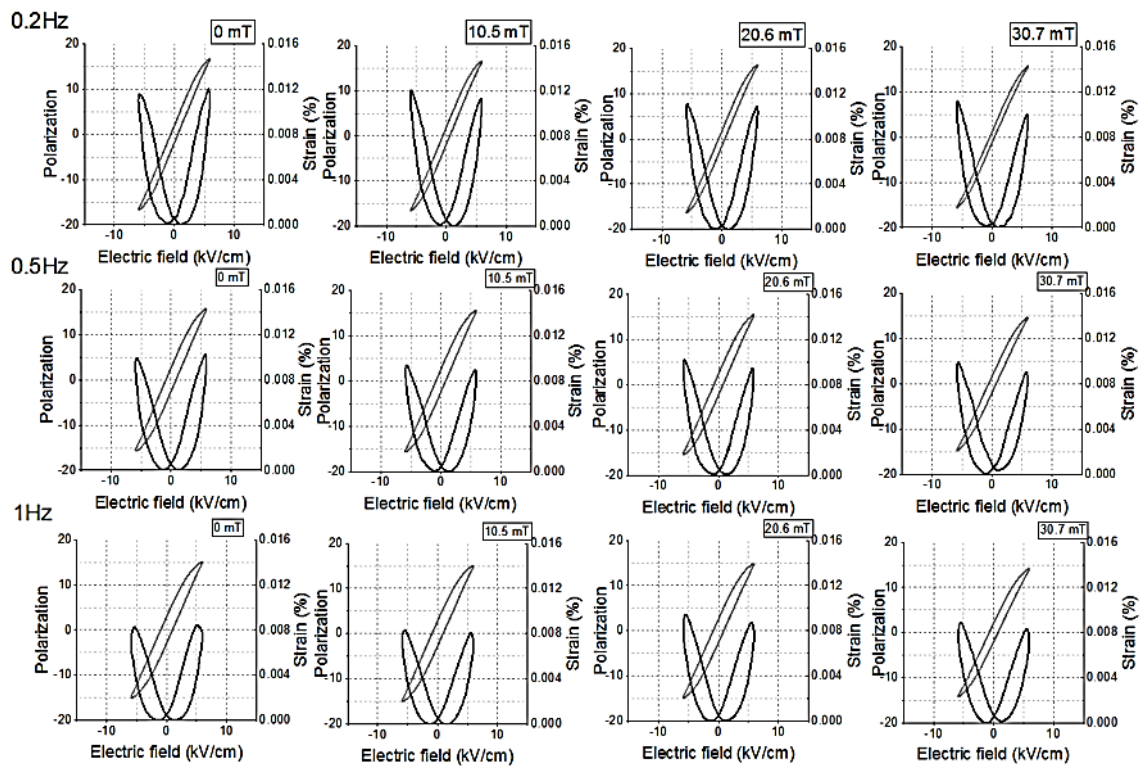


Figure 4.74 The electric field induced strain and polarization of 0.9PMN-0.1PT at various magnetic fields

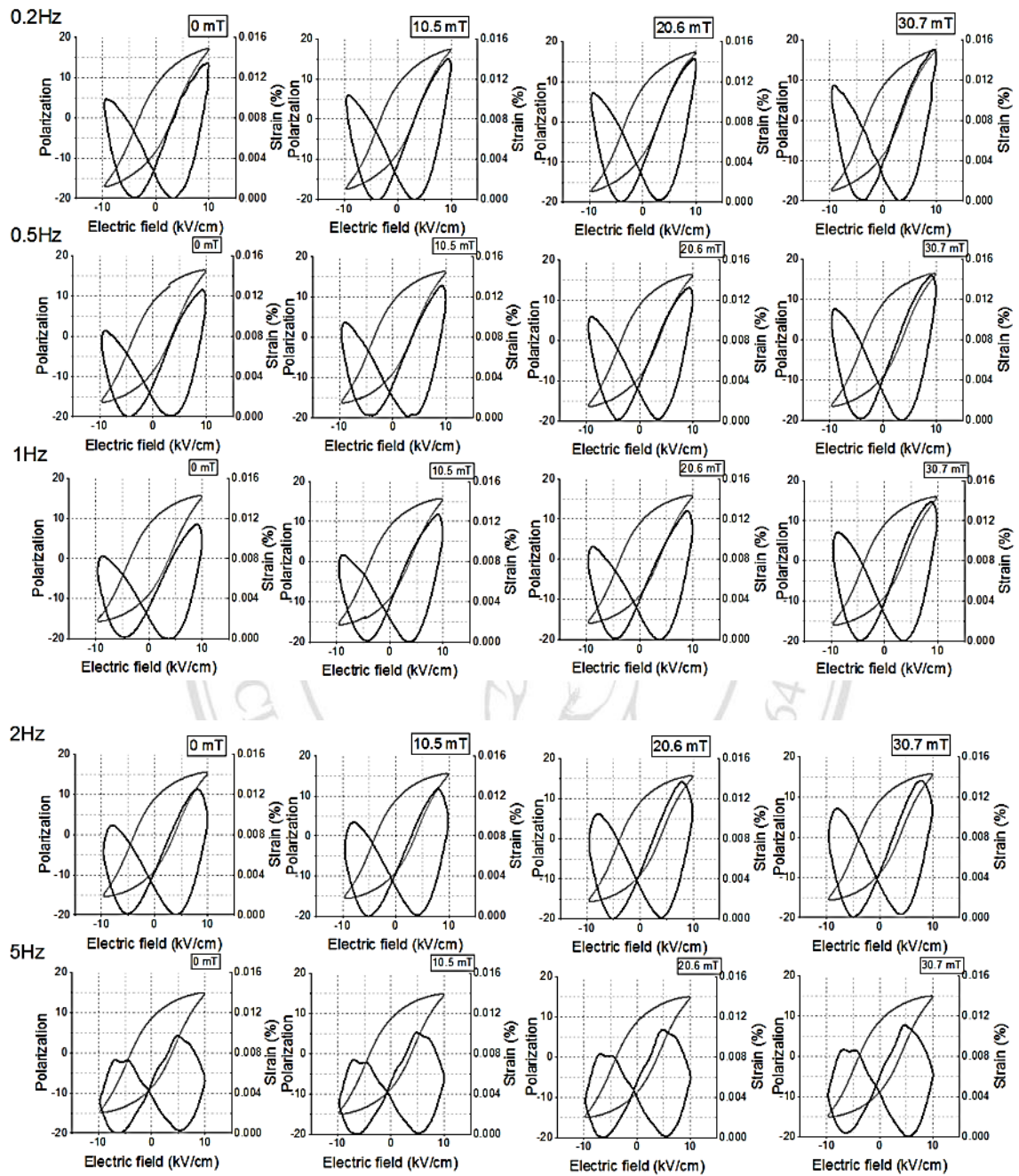


Figure 4.75 The electric field induced strain and polarization of 0.8PMN-0.2PT at various magnetic fields

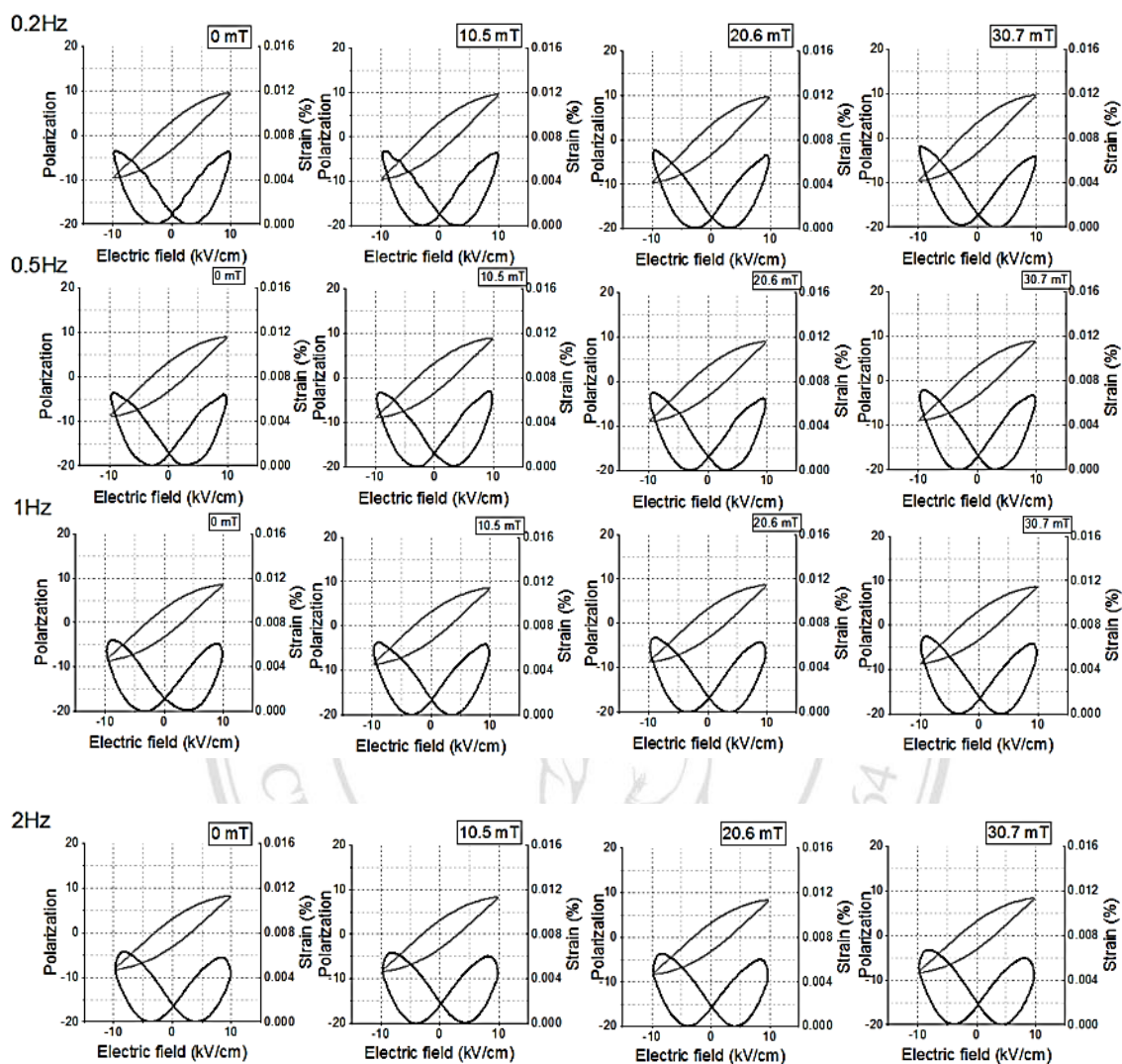


Figure 4.76 The electric field induced strain and polarization of 0.7PMN-0.3PT at various magnetic fields

Copyright © by Chiang Mai University  
All rights reserved

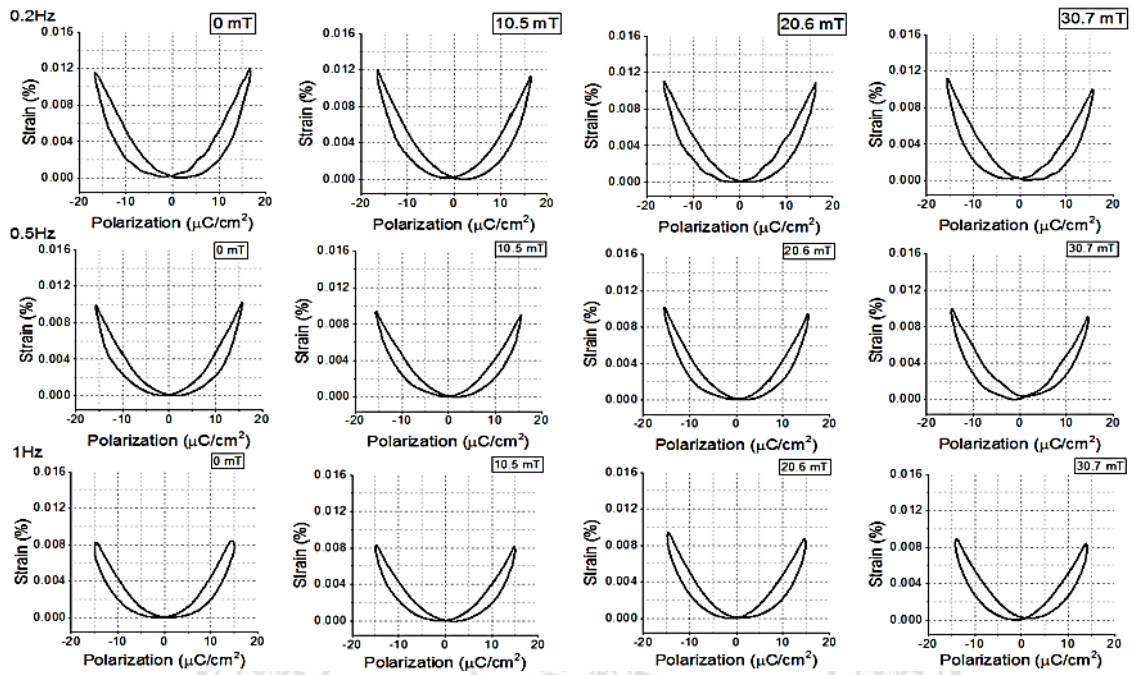


Figure 4.77 The induced strain as a function of polarization of 0.9PMN-0.1PT at various magnetic fields

ลิขสิทธิ์มหาวิทยาลัยเชียงใหม่  
 Copyright© by Chiang Mai University  
 All rights reserved

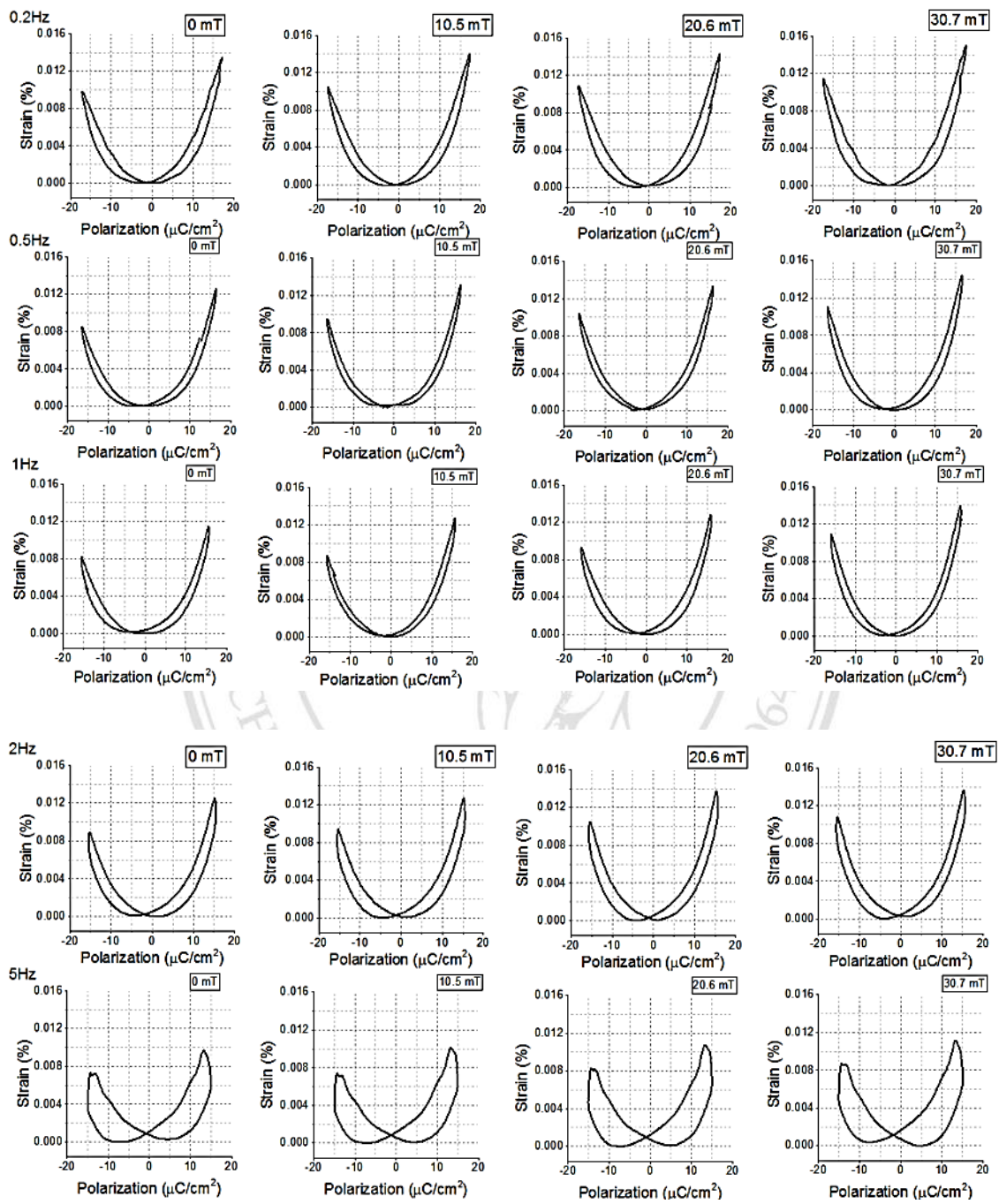


Figure 4.78 The induced strain as a function of polarization of 0.8PMN-0.2PT at various magnetic fields

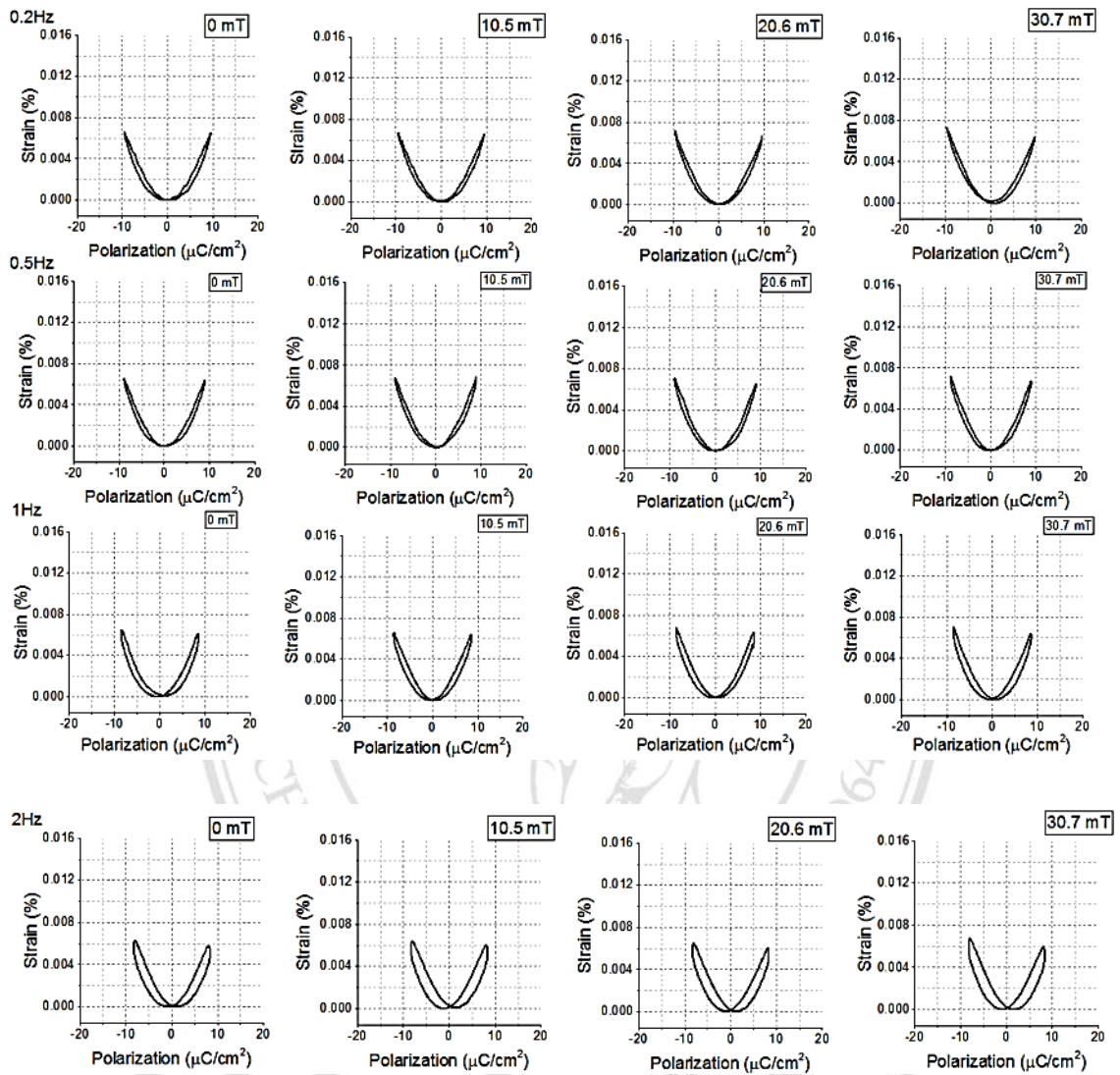


Figure 4.79 The induced strain as a function of polarization of 0.7PMN-0.3PT at various magnetic fields

Table 4.3 The magnetic field effect and frequency dependence of induced strain and polarization for PLZT, PMN-PZT and PMN-PT (S induced strain, P polarization, ↓ = decrease, ↑ = increase)

	Frequency dependence	Magnetic effect	Phase
PLZT (9/70/30)	S↓ P↓	-	relaxor
PLZT (9/65/35)	S↓ P↓	S↓ P↓	MPB
PLZT (9/60/40)	S↓ P↓	-	normal
0.9PMN-0.1PZT	-	-	Paraelectric
0.7PMN-0.3PZT	Loop loss	-	relaxor
0.5PMN-0.5PZT	Loop loss	S↑	MPB
0.9PMN-0.1PT	S↓ P↓	-	relaxor
0.8PMN-0.2PT	S↓ P↓	S↑	MPB
0.7PMN-0.3PT	S↓ P↓	S↑	MPB

Table 4.3 demonstrates the magnetic field effect and frequency dependence of induced strain and polarization in PLZT, PMN-PZT and PMN-PT, PLZT (9/70/30) samples. All samples show a decrease in the induced strain and polarization when frequency is increased according to loading rate, period time that materials need for full switched domain and response to exhibit a few loop loss in induced strain and polarization behaviors [67]. The magnetic field effect can only be observed at near morphotropic phase boundary MPB compositions. For 0.5PMN-0.5PZT, 0.8PMN-0.2PT and 0.7PMN-0.3PT samples show an increase of induced strain but no magnetic effect to the polarization according to mainly 90° domain switching was dominated. But in the case of PLZT (9/65/35), the induced strain and polarization exhibit a decrease affected by magnetic field according to some 90° and 180° domain response to switching and suppressed by magnetic field [1,67-72].